Tulips R
University of Tsukuba Repository

Three-dimensionally Designed π -Conjugated Polymers for Unique Optoelectronic Materials

著者	Pan Chengjun
year	2014
学位授与大学	筑波大学 (University of Tsukuba)
学位授与年度	2014
報告番号	12102甲第7099号
URL	http://hdl.handle.net/2241/00129580

Three-dimensionally Designed π-Conjugated Polymers for Unique Optoelectronic Materials

Chengjun Pan

June 2014

Three-dimensionally Designed π-Conjugated Polymers for Unique Optoelectronic Materials

Chengjun Pan
Doctoral Program in Materials Science and Engineering

Submitted to the Graduate School of
Pure and Applied Sciences
in Partial Fulfillment of the Requirements
for the Degree of Doctor of Philosophy in
Engineering

at the
University of Tsukuba

Contents

Abbreviations

IMWs	Insulated Molecular Wires
CPs	Conjugated polymers
CD	Cyclodextrin
GPC	Gel permeation chromatography
M_n	Number average molecular weight
M_w	Weight average molecular weight
PDI	Polydispersity index
ε	Molar absorption coefficient
E_m	Emission
E_x	Excitation
Φ	Fluorescence quantum yield
λ	Wavelength
d	Day
min	Minute
h	Hour
TLC	Thin layer chromatography
m.p.	Melting point
NMR	Nuclear magnetic resonance
TMS	Trimethylsilyl
δ	Chemical shift
J	Coupling constant
s	Singlet
d	Doublet
t	Triplet
m	Multiplet
MALDI-TOF-Mass	Matrix assisted laser desorption/ionization- Time of fright- Mass spectroscopy
Calcd.	Calculated
DFT	Density functional theory
HOMO	Highest occupied molecular orbital
LUMO	Lowest unoccupied molecular orbital
FRET	Föster resonance energy transfer

General Introduction

INTRODUCTION

Conjugated polymers (CPs) have been attracting significant interest for organic optoelectronic applications owing to their processability and tunable optical electrical properties. For example, organic light-emitting diodes (OLEDs), organic thin film transistors (OFETs), organic solar cells, plastic lasers, and organic sensors have been developed by using CPs.[1] The charge carrier mobility along individual conjugated polymer backbones can influence the performance of CPs based devices, thus CPs are often referred as molecular wires.[2] Those molecular wires are easy to interact with each other through π-π stacking, which alters the optical and electronic properties of CPs.[1-2] However, such a strong interpolymer interaction is not preferable for photoluminescence efficiency and limiting the application of CPs in luminescent devices.[3] Therefore, rational molecular designs are essential, and inevitably, the interpolymer interactions in the condensed phases that govern the properties of CPs need to be taken into consideration.

In the past decade, three-dimensional architecture has emerged as a design element for creating CPs with unprecedented properties and functions.[4] Such type of CPs is often referred as insulated molecular wires (IMWs), in which the conjugated backbone is molecularly covered by a protective sheath. IMWs are gaining increased attention owing to their unique properties (e.g., enhanced fluorescence, excellent hole mobility, chemical stability, and mechanical properties) as compared to the corresponding uninsulated CPs.[5]

Various kinds of molecular structures have been used to wrap CPs to form IMWs.[5a] In general, two approaches (supramolecular and synthetic) have been developed, wherein the polymer backbones are effectively isolated from each other. The advantage of supramolecular approach is the facile preparation procedure (i.e., just mixing two different components); since the supramolecular processes are governed by the thermodynamic equilibrium, thus the formation of structural defects are unavoidable.[5a] In order to address this issue, the synthetic approaches that can generate defect-free IMWs have been attracting great attention recently.[5c]

SUPRAMOLECULAR APPROACHES

One fascinating strategy to isolate CPs is to thread them to a series of macrocycles (such as cyclophanes, [6] cyclodextrins, [7] and cucurbiturils. [8]) to form conjugated polyrotaxanes. With the introduction of the insulating layers to the CPs backbones, the interchain π–π interactions can be prevented. Thus the fluorescence efficiency, solubility, and chemical stability of the encapsulated IMWs are enhanced compared to the corresponding uninsulated CPs. Figure I-1 describes the principle of threading a polymer backbone to a macrocycle.

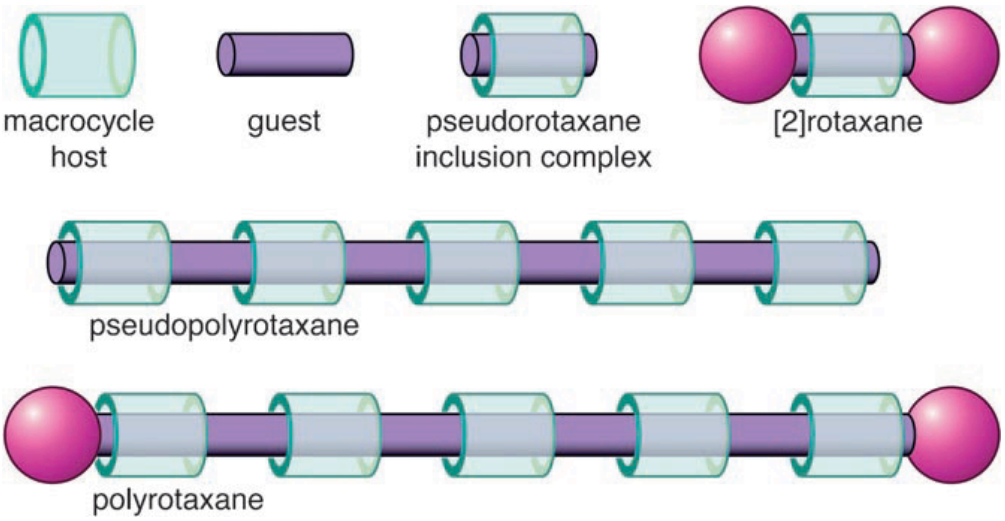

Figure I-1. The scheme of the formation of polyrotaxane. [5a] Figure reprinted from Ref. [5a].

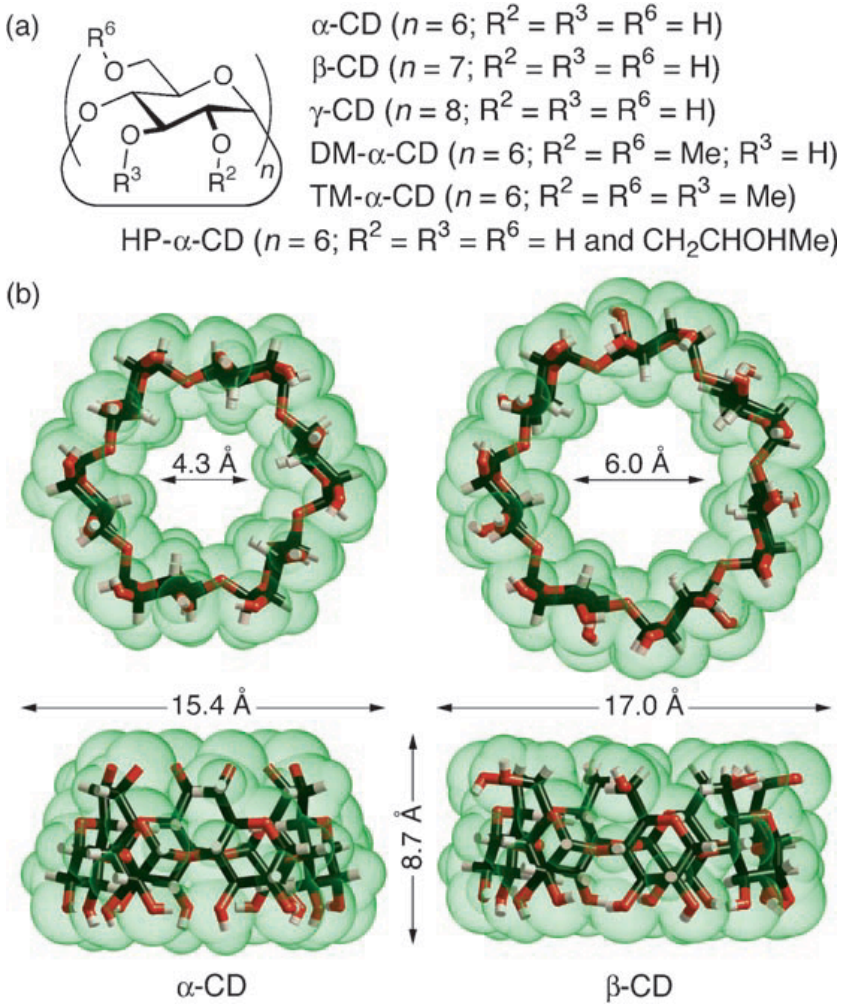

Figure I-2. Chemical structures of cyclodextrins (a) and crystallographic conformations of α- and β-cyclodextrin. [5a] Figure reprinted from Ref.[5a]

Cyclodextrin based IMWs.

Cyclodextrin (CD) is one of the most widely studied macrocycle motif for wrapping CPs, owing to it almost annular shape with a central void.[9-10] CD can be clarified as *α*–, *β*–, and *γ*–, CD which have 6, 7, and 8 saccharide units around the cyclic ring as shown in Figure I-2.[5a] Anderson and co-workers have synthesized a variety of CD based conjugated polyrotaxanes via Suzuki coupling starting from CD, a diboronic acid, water-soluble diiodide, and a bulky mono-iodo stopper: such as threaded poly(*para*-pheneylene) (*β*–CD-PPP), poly(4,4'-diphenylenevinylene) (*β*–CD-PDV and *α*–CD-PDV), threaded polyfluorene (*β*–CD-PF) have been successfully prepared. The inclusion of CP backbone into the cyclodextrin rings reduced the interpolymer interactions, enhanced the photoluminescence, and increased the stability of CPs, making such types of CPs have better performance of electroluminescence compared to the corresponding unthreaded CPs.[5a, 7e-h]

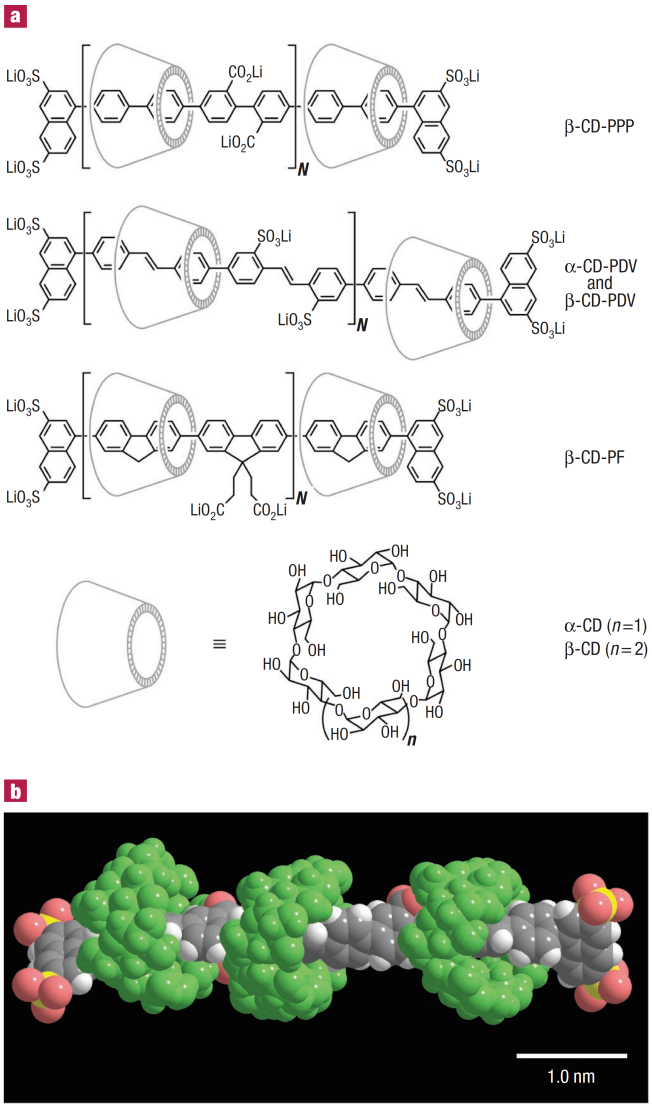

Figure I-3. Chemical structure of the cyclodextrin-threaded CPs.[11] Figure reprinted from Ref.[11].

Schizophyllan glucan (SPG) and Amylose based CPs

In addition to wrap CPs by using macrocycle molecules, helical polymers have been also used to encapsulate CPs, in which the CPs backbones are threaded inside the axial cavities of the helical polymers. [5a] Schizophyllan glucan (SPG) and amylose are most widely used helical polymers to afford IMWs (Figure I-4). [5a]

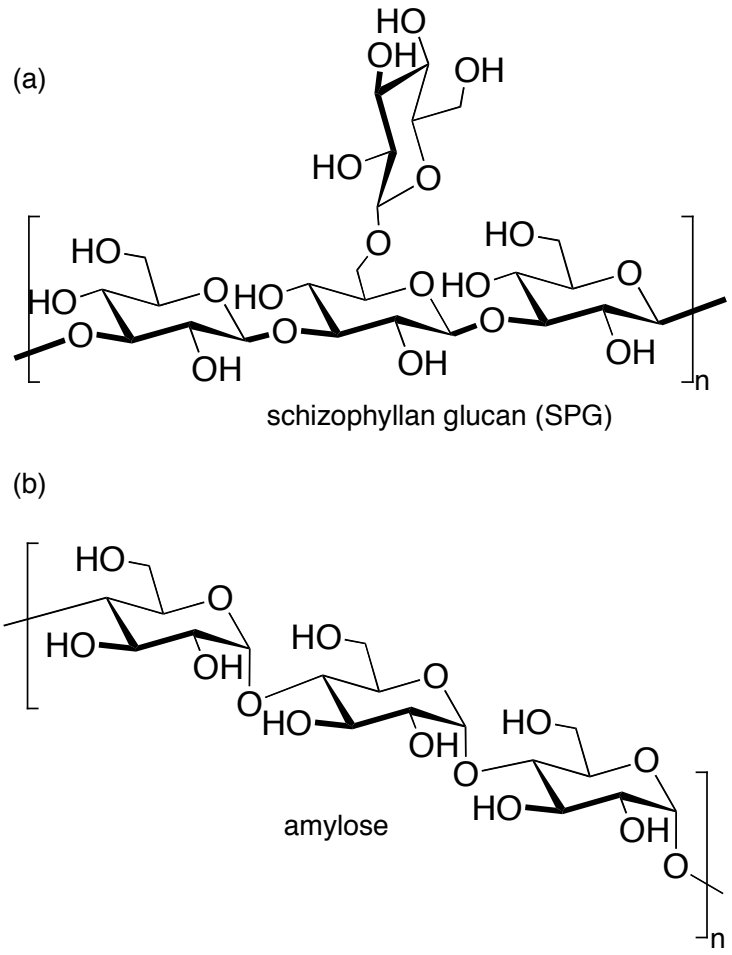

Figure I-4. Structures of schizophyllan glucan (SPG) (a) and amylose (b).[5a, 13]

Anderson, Cacialli, and coworkers have synthesized highly luminescent inclusion complexes comprising of poly(para-phenylene) (PPP) and poly(4,4'-diphenylene-vinylene) (PDV) and amylose.[12] The encapsulation processes of the CPs backbones to the amylose host were driven by hydrophobic interactions in aqueous, affording IMWs as shown in Figure I-5. The 2D ^{1}H NMR NOE spectra confirmed that the CPs are threaded inside the cavity of amylose and the obtained polymers (both PPP and PDV) have enhanced photoluminescence efficiencies compared to the cyclodextrins threaded CPs, the polymers can be also used to fabricate electroluminescent light-emitting diodes although the performances are slightly lower than those from the corresponding conjugated polyrotaxanes.

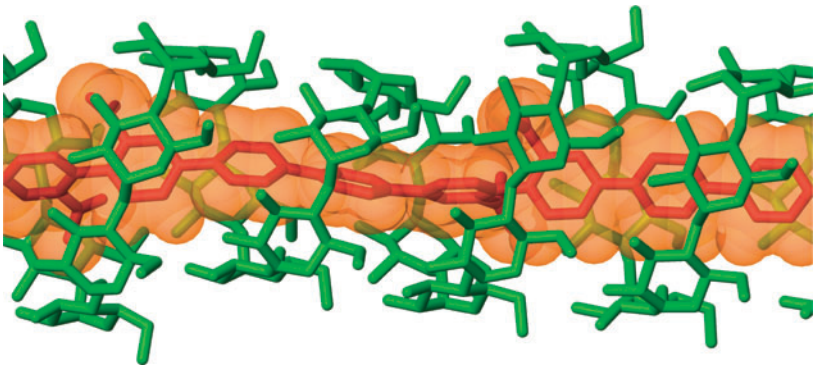

Figure I-5. A molecular mechanic model of a longer PPP/amylose complex.[12] Figure reprinted from Ref.[12].

Shinkai and co-workers have explored the use of SPG as a one-dimensional host to wrap a water-soluble polythiophene chain to form supramolecular chiral IMWs as shown in Figure I-6.[13] Upon addition of SPG to the polythiophene solution, the absorption spectral maximum is red-shifted from 403 nm to 454 nm, along with a solution color change from yellow to orange, indicating extended effective conjugation length of the polythiophene backbone after the formation of polythiophene-SPG complex. This result should be attributed to that the insulating layer–SPG could force the polythiophene backbone to adopt a more planar conformation. One more intriguing point of this work is that the results from circular dichroism (CD) spectrum showing that a right-handed helical conformation was induced by the SPG insulating layer. The almost no change of the absorption spectra of the solution and film state of the polythiophen/SPG complex indicated that the polythiophene backbone was well wrapped by the SPG host and thus the interchain interaction can be greatly reduced.

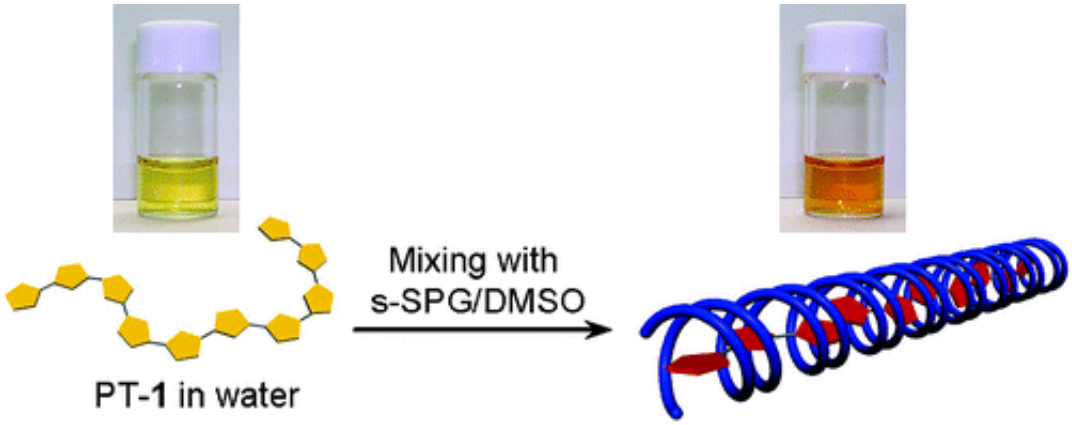

Figure I-6. The scheme of the formation of s-SPG and PT-1 complex.[13] Figure reprinted from Ref.[13].

SYNTHETIC APPROACHES

As aforementioned works, the formation of polyrotaxane and supramolecular complexes by wrapping CPs with insulating macrocycles (i.e. cyclophanes and cyclodextrins) and polysaccharides (amylose and schizophyllan) respectively is a facile approach to afford IMWs. All of these syntheses are governed by supramolecular noncovalent interactions, such as hydrophobic interaction in aqueous solution; thus most of the obtained IMWs were only dissolved in water (though there are several such types of IMWs also dissolved in organic solvents), which limit the structural characterizations and device fabrications.[5] The unavoidable defects of the formed IMWs, which mainly depend on the binding constants, are also detrimental to the better understanding of the structures and final application of these IMWs.[5c] Synthetic approach, in which the insulating layers are pre-attached to the monomer before polymerization, can address the above mentioned issues. The commonly used insulating layers are dendrimers, bulky substituents (i.e. iptycene,[22] *tert*-butyldiphenylsilyl (TBDPS)),[23] and self-threaded cyclic side-chains.[5c, d]

Dendronized CPs

Dendrimers which have highly branched three-dimensional structures have been widely used to encapsulate and site-isolation of molecular cores and CPs backbones.[14] The later one can be referred as IMWs because of the laterally attached dendrons can effectively isolate the CPs backbones. The three-dimensional cylindrical structure of dendronized CPs was proposed by Schlüter and Rabe as shown in Figure I-7.[15] The facile preparation of poly (benzyl ether)s which are the most widely studied dendrons developed by Fréchet and Hawker opened the door to develop dendronized CPs.[16]

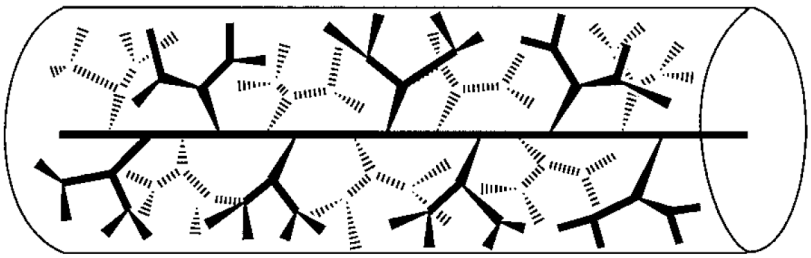

Figure I-7. A cartoon of dendronized CPs in which the CPs backbone was densely sheathed with the dendritic layer to form a molecular cylinder. [15] Figure reprinted from Ref.[15].

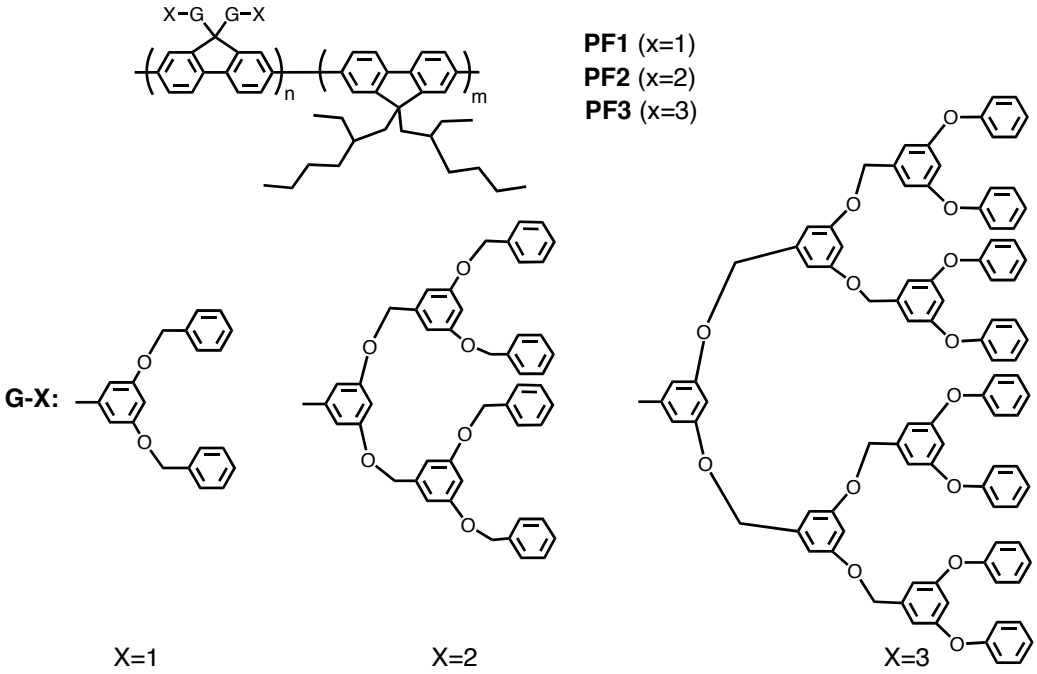

Figure I-8. Chemical structures of the dendronized polyfluorenes.[17]

By using dendrimers with well-predictable three-dimensional shape as insulating layers, various kinds of CPs have been developed. Cater and co-workers prepared dendronized polyfluorenes by using Fréchet-type dendrons as shown in Figure I-8.[17] The obtained CPs showed extensive conjugation along the polymer backbone and higher turn-on voltages of EL-devices then the corresponding conventional CPs. They found that the [G-2]-derivatives showed high reactivity with associated chain isolation, resulting high fluorescence quantum efficiencies.

Bao et al. have synthesized polyphenylenevinylene (PPV) with the first generation of Fréchet-type dendrons (3,4,5-tris(benzyloxy)benzyl ether through Heck polymerization starting from a 1,4-diiodobenzene-based macromonomer with 1,4-divinylbenzene.[18] The obtained polymers were found to self-order in the solid state and yield thermotropic nematic liquid crystal phases with a nematic-isotropic transition at 211 ^{o}C. Aida and co-workers investigated the luminescence properties of the light-emitting dendritic macromolecular rod having a rigid poly(phenyleneethylene)backbone wrapped with several generations of dendrimers. They found that the dendronized PPEs have significantly enhanced luminescence activity.

Malenfant and Fréchet have prepared insulated polythiophene with aliphatic polyether dendrons through Stille coupling reaction. The obtained polymers show high solubility in organic solvents.[19]

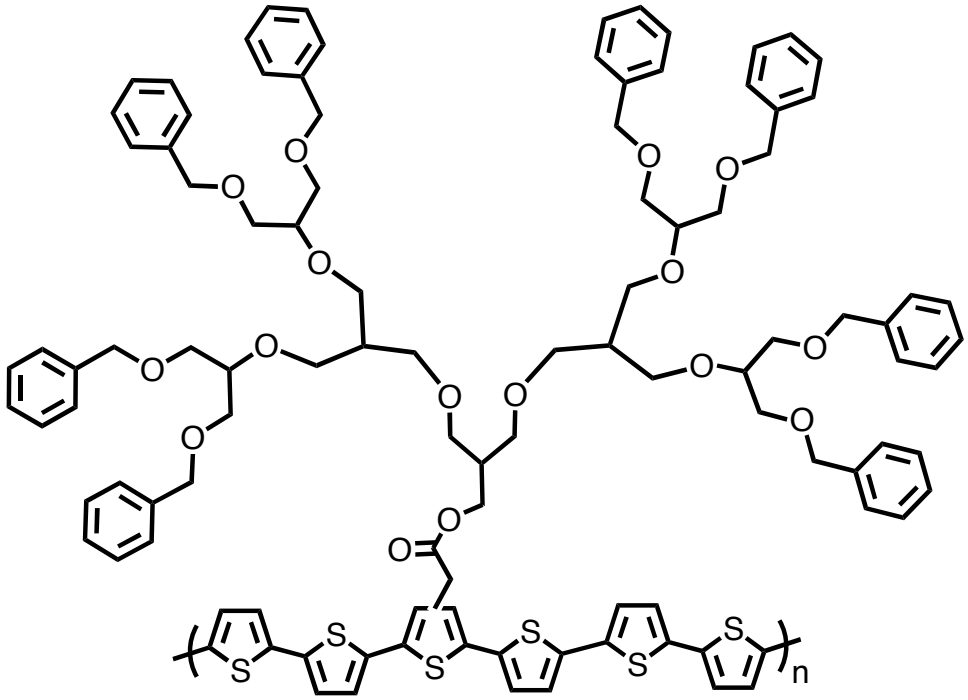

Figure I-9. Chemical structures of the dendronized polythiophene.[19]

The Müllen-type dendrimers (Figure I-10) also attracted a lot of attention owing to their shape persistency compared to the flexible Fréchet-type poly(benzyl ether) dendrons.[20] Therefore the three-dimensional shielding ability of the polyphenylene dendrimers can exclude the interpolymer interaction at lower dendritic generation than the Fréchet-type.

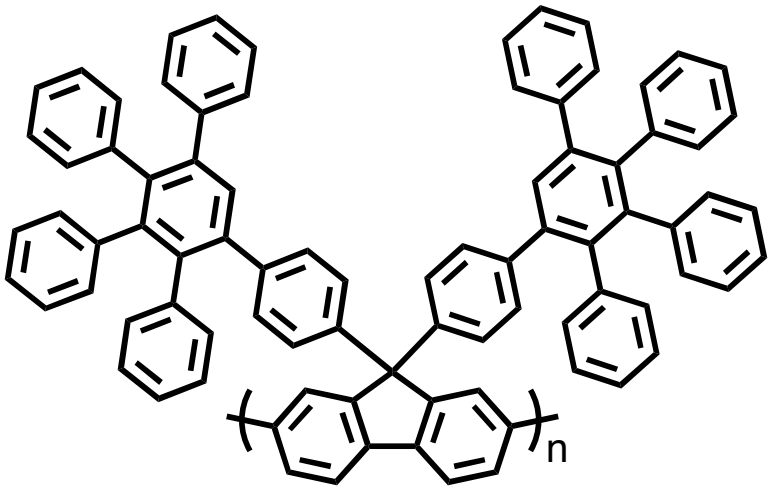

Figure I-10. Chemical structures of the dendronized polyfluorenes. [20]

Cyclodextrin based IMWs through Self-inclusion Method

Terao and co-workers developed a unique method to form cyclodextrin based IMWs, involving the self-inclusion of the rotaxane precursors containing π-conjugated molecules as a guest and permethylated cyclodextrin (PMCD) as an insulating layer (Figure I-11).[21] The obtained IMWs have good solubility in common organic solvents, enhanced fluorescence intensity in solid state, high covering ratio, and high rigidity of the backbone. IMWs with such unique feature can generate various kinds of properties, for example, a cholesteric LC phase was observed for polyrotaxanes due to the high rigidity of the polymer backbones threaded through chiral macrocycles (Figure I-12).[5b]

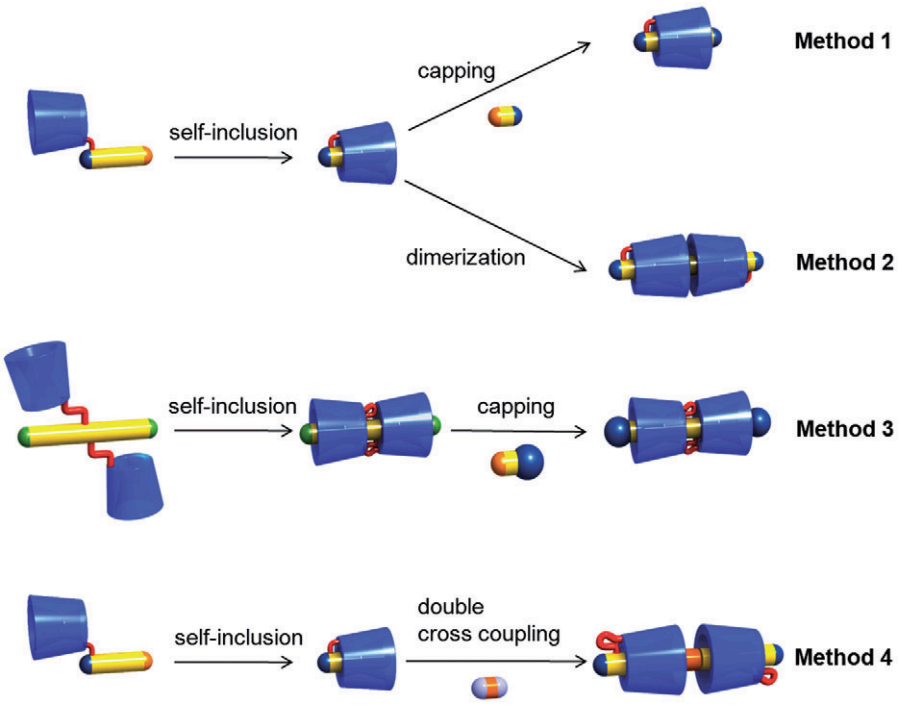

Figure I-11. Synthetic route towards cyclodextrin-based IMW.[21c] Figure reprinted from Ref. [21c].

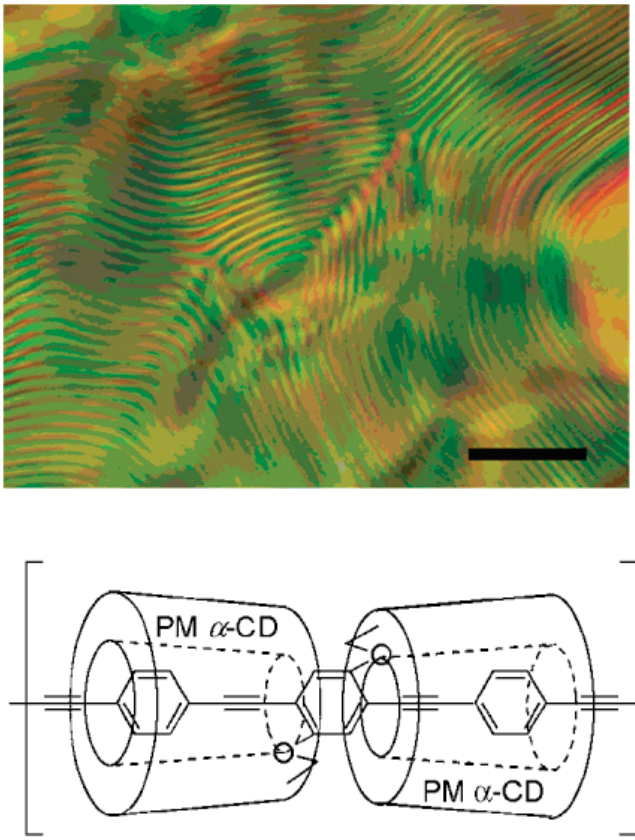

Figure I-12. Polarized optical micrograph (upper) of the IMWs (bottom) in chloroform solution (about 15 wt %) sealed in a glass capillary tube at 25 °C. Scale bar: 50 μm.[5b] Figure reprinted from Ref.[5b].

The collaborated work of Terao, Taniguchi, Seki and co-workers found that the IMWs having a poly(phenylene ethynylene) backbone show extremely high hole mobility along the π-conjugated polymer core.[21a] The intramolecular charge mobility of the CPs can be further enhanced by rational molecular design, such as through regularly localizing the molecular orbitals of CPs that realize an ideal orbital alignment for charge hopping.[21f] They found that IMWs containing *meta*-junctioned poly(phenylene-ethynylene) as the conjugated backbones have high intramolecular charge mobility to about 8.5 $cm^2V^{-1}s^{-1}$, because such a molecular structure provides the most effective pathways for the hopping of charge carriers.[21f]

Bulky Substituents contained IMWs

In addition to the elegant structure of dendronized CPs, CPs bearing bulky substituents also behave as IMWs. Swager and coworkers have investigated iptycene-containing poly(aryleneethylene)s in detail.[22] They found that the introduction of the iptycene to conjugated polymer backbone could prevent the interchain interactions without isolating the polymer chains. It is worth to mention that the photoluminescence efficiency of the thin films is not affected by heating and / or repeated exposure to

organic vapors. As shown in Figure I-13, the pentiptycene containing PPE can host planar electron-acceptor molecules like nitroaromatics.[22a, 22c]

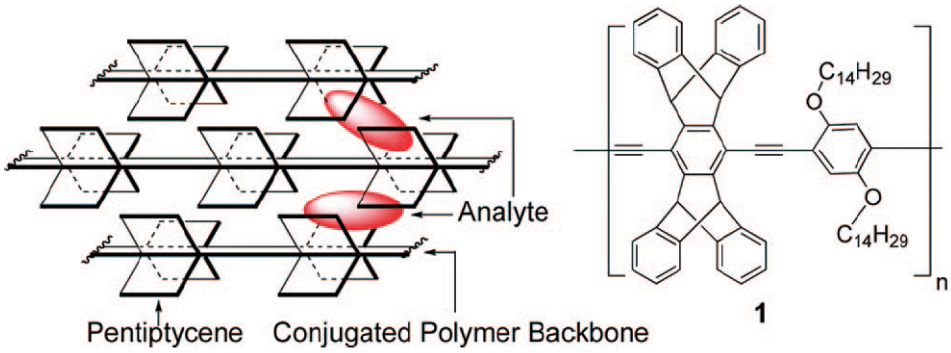

Figure I-13. Schematic representation of galleries defined between polymer chains that can host analytes.[22a, 22c] Figure reprinted from Ref. [22a, 22c].

Aso and co-workers have succeeded in the creation of a series of encapsulated oligothiophenes bearing bulky substituents (*tert*-butyldiphenylsilyl (TBDPS) (Fgiure I-14),[23a] bis(di-*t*-butylphenyl),[23b] and fluorene unit (Figure I-14).[23d]) as insulating layers. All the encapsulated oligothiophenes are highly conjugated despite the introduction of bulky insulating layers. They found that the formation of interchain radical-cation (π-dimer), which is often observed in conjugated system, is perfectly prohibited in the 6-mer of TBDPS based oligomer. Polaron, bipolaron, and multi-charged species of the TBDPS contained 12-mer have been clearly observed as individual nearly single cationic species. Introducing a fluorene unit as a insulating layer to the oligothiophene backbone through rational molecular design let the successfully introduction of anchoring functional groups at the terminal α positions of the oligothiophenes, thus the single-molecular conductivity can be measured by using this IMWs.[23]

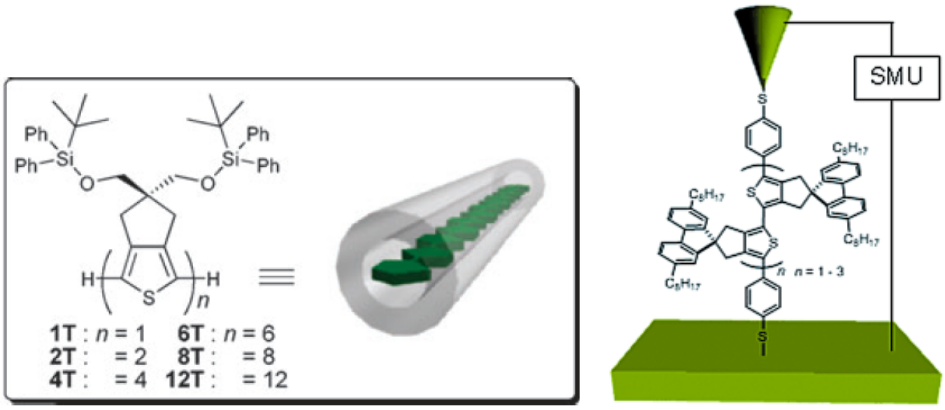

Figure I-14. Chemical structures of the oligothiophenes and the cartoon of the encapsulated molecular wire (left) and the schematic presentation of the single molecular conductance measurement (right).[23] Figure reprinted from Ref[23a and 23 c].

Sugiyasu and Takeuchi, et al. have reported a unique method to wrap CPs: a self-threading polythiophene whose backbone is encapsulated within its own cyclic side chains (Figure I-15).[5c] The three-dimensional architecture of the encapsulated polythiophene has limited electronic-communication between the adjacent polyhiophene backbones and extended effective conjugation length, thus the obtained polythiophene has excellent *intrawire* hole mobility of 0.9 $cm^2V^{-1}s^{-1}$. In the unique three-dimensional structure of the monomer, the dihedral angle of the bithiophene part can be defined by changing the cyclic side-chain ring size.[24]

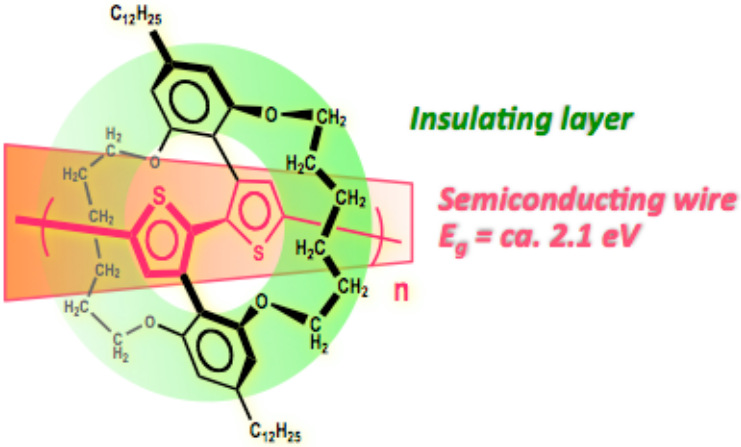

Figure I-15. The three-dimensional structure of the self-threading polythiophene.[5c] Figure reprinted from Ref.[5c]

In order to unveil the conducting mechanism of a single polythiophene, a sterically isolated polythiophene – poly(**1EDOT**) was designed by using the same molecular design concept (Figure I-16).[5d] Poly(**1EDOT**) was electrochemically deposited on the electrodes. Because the *interwire* interaction of the polythiophene wire of the poly(**1EDOT**) is effectively prevented, the electrochemistry of poly(**1EDOT**) reflects the p-doping process of a single polythiophene backbone, which is recognized as the essential phenomenon to understand polythiophene-based materials. It was found that the polaron pair plays an important role in elucidating the conduction mechanism.[5d]

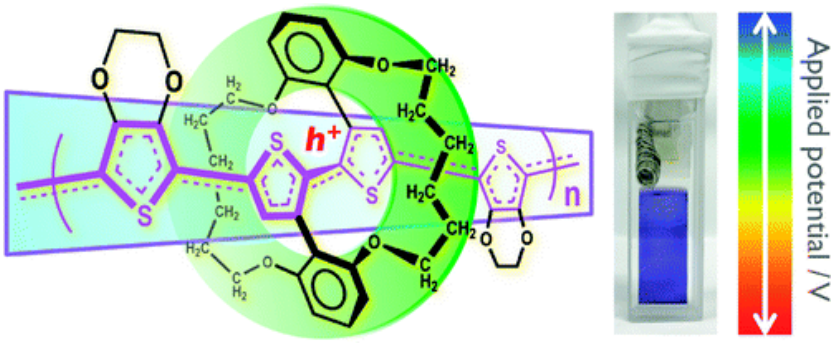

Figure I-16. Chemical structure of the poly(**1EDOT**) with an isolated, planar geometry.[5d] Figure reprinted from Ref. 5d].

Applications of IMWs

One of the most important applications of CPs is to fabricate organic light-emitting diodes (OLEDs).[1] The enhanced photoluminescence and chemical stability of IMWs suggest they should be good candidates to be used as emitting layers in OLEDs.[5a] Anderson and Cacialli, et al.[11] have shown that polyrotaxanes exhibited enhanced electroluminescence efficiency in the EL devices compared to the corresponding uninsulated CPs. They also found that the polyrotaxane based OLEDs have higher turn-on voltages than the corresponding uninsulated CPs, but can produce more light for a given current.[25] Although the external electroluminescence quantum yields of the polyrotaxane OLEDs were very low, it can be significantly increased after blending the polyrotaxane with poly(ethylene oxide), which indicated that IMWs should be promising materials for OLED applications.[26]

Müllen and co-workers have constructed electroluminescence devices by using pentaphenylene dendrons shielded polyfluorenes as electroluminescent materials. They found that the luminance and electrical characteristics of the dendronized CPs are comparable to the uninsulated polyfluorenes. This indicated that the introduction of bulky substituents has no dramatic influence of the desirable properties of polyfluorenes with enhanced chemical stability, solubility, and photoluminescence.[27] Cater and co-workers have also fabricated EL device by using polyfluorenes encapsulated by benzyl ether dendrons without optimizing the devices.[17]

Structure of this Thesis

This thesis describes herein a series of CPs with three-dimensionally designed architectures, focusing on the development of unexploited topics in the field of IMWs.

1) Synthesis of isolated CPs through catalyst transfer polycondensation (CTP)

Catalyst transfer polycondensation (CTP) is developing extremely fast since the first discovery of its chain-growth feature for the synthesis of head-to-tail poly(3-hexylthiophene) a decade ago. Although more and more monomers with different structures can be polymerized by CTP, this approach is still at an earlier stage of development. Understanding the chain-growth mechanism and expanding the monomers scope would be the key points for the further development of CTP. Particular interest is extending CTP to more complex monomers, which have been mainly polymerized by step-growth polymerization.

In Chapter 1, we attempted to apply CTP to polymerize a ‘fenced’ thiophene monomer to afford IMWs. We unexpectedly found that CTP can be even used to synthesize steric-hindered monomer, which have been supposed to be not suitable for CTP. This finding will stimulate this field to deep understand the mechanism of the catalyst transfer, chain termination, and chain propagation.

2) First example of microphase separation of all-conjugated block copolymers comprising 'stacked' polythiophene and 'isolated' polythiophene.

Fully conjugated block copolymers (BCPs) are a new class of organic materials that comprised two covalently linked conjugated polymer backbones. Such type of block copolymers is promising material for organic electronic devices owing to the combination of the optoelectronic properties of CPs and microphase segregated nanostructure of BCPs.

In Chapter 2, we synthesized all-conjugated block copolymers comprising 'stacked' polythiophene and 'isolated' polythiophene ensemble. Because π–π stacking determines the functions and properties of polythiophenes, this novel microphase separation allows for the synergy of the contrasting properties. Importantly, we found that the "hybrid" film shows both the characteristics of stacked and isolated polythiophenes, while exhibiting homogeneous microphase-separated morphology. Thus, we expect that our material design will extend the use of these organic materials into various unprecedented applications.

3) Synthesis of thermoplastic fluorescent conjugated polymers

Organic materials that can emit in condensed phases are of great importance for the further developments of organic optoelectronic applications. To this end, sophisticated molecular designs and well-established organic syntheses are essential. Among the fluorescent organic materials, CPs are attractive for such applications owing to their distinguished mechanical properties, processability, lower production costs, and electronic conductivity.

In Chapter 3-5, we developed new CPs that are enveloped within their own cyclic sidechains; such polymers are referred to as IMWs and have recently attracted much attention. Our IMWs have several remarkable features in comparison with other IMWs and fluorescent organic materials (crystals, glasses, liquid crystals, liquid) as briefly summarized below.

1) Molecular design and synthetic approach of the monomer have been established very well, which could lead to a variety of CPs with violet, green, red, and yellow fluorescence. Importantly, they are emissive even in the solid-state (Chapter 3).
2) Since all the polymers are wrapped by the same cyclic sidechains, they do not undergo phase separation in polymer blends, which allows us to combine the above-mentioned four colors and provide various fluorescence colors (Chapters 3–4).
3) Because of the unique three-dimensional architecture, our IMWs are thermoplastic unlike common conjugated polymers. Flexible self-standing films and periodic micro patterns have been prepared by taking advantage of the mechanical stability and processablity (Chapter 3 and Chapter 5).

REFERENCES

[1] a) J. H. Burroughes, D. D. C. Bradley, A. R. Brown, R. N. Marks, K. Mackay, R. H. Friend, P. L. Burn, A. B. Holmes, *Nature* **1990**, *347*, 539; b) S. R. Forrest, *Nature* **2004**, *428*, 911; c) R. H. Friend, R. W. Gymer, A. B. Holmes, J. H. Burroughes, R. N. Marks, C. Taliani, D. D. C. Bradley, D. A. Dos Santos, J. L. BrRdas, M. LWgdlund, W. R. Salaneck, Nature **1999**, *397*, 121; d) A. Kraft, A. C. Grimsdale, A. B. Holmes, *Angew. Chem.* **1998**, *110*, 416; *Angew. Chem. Int. Ed.* **1998**, *37*, 402; e) H. Sirringhaus, N. Tessler, R. H. Friend, *Science* **1998**, *280*, 1741; f) C. D. Dimitrakopoulos, P. R. L. Malenfant, *Adv. Mater.* **2002**, *14*, 100; g) K. M. Coakley, M. D. McGehee, *Chem. Mater.* **2004**, *16*, 4533; h) M. GranstrWm, K. Petritsch, A. C. Arias, A. Lux, M. R. Andersson, R. H. Friend, *Nature* **1998**, *395*, 257; i) A. Rose, Z. G. Zhu, C. F. Madigan, T. M. Swager, V. Bulovic, *Nature* **2005**, 434, 876; j)J. H. Wosnick, T. M. Swager, *Curr. Opin. Chem. Biol.* **2000**, *4*, 715.

[2] a) R. L. Carroll, C. B. Gorman, *Angew. Chem. Int. Ed.* **2002**, *41*, 4378; b) R. E. Martin, F. Diederich, *Angew. Chem. Int. Ed.* **1999**, *38*, 1350; c) T. M. Swager, Acc. Chem. Res. **1998**, *31*, 201.

[3] a) Y. -J. Jin, J.-E. Bae, K.-S. Cho, W.-E. Lee, D.-Y. Hwang, G. Kwak, *Adv. Funct. Mater.* **2014**, *24*, 1928; b) I. F. Perepichka, D. F. Perepichka, H. Meng, F. Wudl, *Adv. Mater.* **2005**, *17*, 2281.

[4] S.-C. Lo, P. L. Burn, *Chem. Rev.* **2007**, *107*, 1097.

[5] a) M. J. Frampton, H. L. Anderson, *Angew. Chem. Int. Ed.* **2007**, *46*, 1028; b) J. Terao, S. Tsuda, Y. Tanaka, K. Okoshi, T. Fujihara, Y. Tsuji, N. Kambe, *J. Am. Chem. Soc.* **2009**, *131*, 16004; c) K. Sugiyasu, Y. Honsho, R. M. Harrison, A. Sato, T. Yasuda, S. Seki, M. Takeuchi, *J. Am. Chem. Soc.* **2010**, *132*, 14754; d) R. Shomura, K. Sugiyasu, T. Yasuda, A. Sato, M. Takeuchi, *Macromolecules* **2012**, *45*, 3759.

[6] a) P. N. W. Baxter, H. Sleiman, J. -M. Lehn, K. Rissanen, *Angew. Chem. Int. Ed. Engl.* **1997**, *36*, 1294; b) H. Sleiman, P. N. W. Baxter, J. -M. Lehn, K. Airola, K. Rissanen, *Inorg. Chem.* **1997**, *36*, 4734. c) S. S. Zhu, P. J. Caroll, T. M. Swager, *J. Am. Chem. Soc.* **1996**, *118*, 8713; d) J. Buey, T. M. Swager, *Angew. Chem. Int. Ed.* **2000**, *39*, 608.

[7] a) A. Harada, M. Kamachi, *Macromolecules* **1990**, *23*, 2823; b) A. Harada, J. Li, M. Kamachi, *Nature* **1992**, *356*, 325; c) A. Harada, J. Li, M. Kamachi, *Macromolecules* **1993**, *26*, 5698; d) G. Wenz, B. Keller, *Angew. Chem. Int. Ed. Engl.* **1992**, *31*, 197; e) C. A. Stanier, M. J. O'Connell, W. Clegg, H. L. Anderson, *Chem. Commun.* **2001**, 493; f) C. A. Stanier, M. J. O'Connell, W. Clegg, H. L. Anderson, *Chem. Commun.* **2001**, 787; g) J. Terao, A. Tang, J. J. Michels, A. Krivokapic, H. L. Anderson, *Chem. Commun.* **2004**, 56; h) H. Onagi, B. Carrozzini, G. L. Cascarano, C. J. Easton, A. J. Edwards, S. F. Lincoln, A. D. Rae, *Chem. Eur. J.* **2003**, *9*, 5971.

[8] D. Tuncel, J. H. G. Steinke, *Macromolecules* **2004**, *37*, 288.

[9] D. J. Cardin, *Adv. Mater.* **2002**, *14*, 553.

[10] G. Wenz, *Angew. Chem. Int. Ed.* **1994,** *33,* 803.

[11] F. Caciall, J. S. Wilson, J. J. Michels, C. Daniel, C. Silva, R. H. Friend, N. Severin, P. Samorì, J. P. Rabe, M. J. O'Connell, P. N. Taylor, H. L. Anderson, *Nat. Mater.* **2002**, *1*, 160.

[12] M. J. Frampton, T. D. W. Claridge, G. Latini, S. Brovelli, F. Cacialli, H. L. Anderson, *Chem. Commun.* **2008**, 2797.

[13] C. Li, M. Numata, A. -H. Bae, K. Sakurai, S. Shinkai, *J. Am. Chem. Soc.* **2005**, *127*, 4548.

[14] H. Frey, *Angew. Chem. Int. Ed.* **1998**, *37*, 2193.

[15] A. D. Schlüter, J. P. Rabe, *Angew. Chem. Int. Ed.* **2000**, *39*, 864.

[16] C. J. Hawker, J. M. J. Fréchet, *J. Am. Chem. Soc.* **1990**, *112*, 7638.

[17] D. Marsitzky, R. Vestberg, P. Blainey, B. T. Tang, C. J. Hawker, K. R. Carter, *J. Am. Chem. Soc.* **2001**, *123*, 6965.

[18] Z. Bao, K. R. Amundson, A. J. Lovinger, *Macromolecules* **1998**, *31*, 8647.

[19] P. R. L. Malenfant, J. M. J. Fréchet, *Macromolecules* **2000**, *33*, 3634.

[20] J. Berresheim, M. Müller, K. Müllen, *Chem. Rev.* **1999**, *99*,1747.

[21] a) J. Terao, Y. Tanaka, S. Tsuda, N. Kambe, M. Taniguchi, T. Kawai, A. Saeki, S. Seki, *J. Am. Chem. Soc.* **2009**, *131*, 18046; b) J. Terao, *Polym. Chem.* **2011**, *2*, 2444; c) J. Terao, *The Chemical Record*, **2011**, *11*, 269. d) J. Terao, K. Ikai, N. Kambe, S. Seki, A. Saeki, K. Ohkoshi, T. Fujihara, Y. Tsuji, *Chem. Commun.* **2011**, *47*, 6816; e) J. Terao, H. Masai, T. Fujihara, Y. Tsuji, *Chem. Lett.* **2012**, 41, 652. f) J. Terao, A. Wadahama, A. Matono, T. Tada, S. Watanabe, S. Seki, T. Fujihara, Y. Tsuji, *Nat. Commun.* **2013**, *4*, 1691.

[22] a) T. M. Swager, *Acc. Chem. Res.* **2008**, *41*, 1181; b) Z. Chen, J. Bouffard, S. E. Kooi, T. M. Swager, *Macromolecules* **2008**, *41*, 6672; c) Y. -S. Yang, T. M. Swager, *J. Am. Chem. Soc.* 1998, 120, 11864.

[23] a) Y. Ie, A. Han, T. Otsubo, Y. Aso, *Chem. Commun.* **2009**, 3020; b) M. Endou, Y. Ie, Y. Aso, *Chem. Commun.* **2012**, *48*, 540; c) Y. Ie, M. Endou, S. K. Lee, R. Yamada, H. Tada, Y. Aso, *Angew. Chem., Int. Ed.* **2011**, *50*, 11980.

[24] Y. Ouchi, K. Sugiyasu, S. Ogi, A. Sato, M. Takeuchi, *Chem. Asian J.* **2012**, *7*,75.

[25] a) S. Brovelli , F. Meinardi , G. Winroth , O. Fenwick , G. Sforazzini , M. J. Frampton , L. Zalewski , J. A. Levitt , F. Marinello , P. Schiavuta , K. Suhling , H. L. Anderson , F. Cacialli , *Adv. Funct. Mater.* 2010, 20, 272; b) S. Brovelli, G. Sforazzini, M. Serri, G. Winroth, K. Suzuki, F. Meinardi, H. L. Anderson, F. Cacialli, *Adv. Funct. Mater.* **2012**, *22*, 4284; c) review, see: S. Brovelli, F. Cacialli, *Small* **2010**, 6, 2796.

[26] J. S. Wilson, M. J. Frampton, J. J. Michels, L. Sardone, G. Marletta, R. H. Friend, P. Samorì, H. L. Anderson, F. Cacialli, *Adv. Mater.* **2005**, *17*, 5365.

[27] S. Setayesh, A. C. Grimsdale, T. Weil, V. Enkelmann, K. Müllen, F. Meghdadi, E. J. W. List, G. Leising, *J. Am. Chem. Soc.* **2001**, *123*, 946.

Chapter 1

Synthesis of 'Picket-Fenced' Polythiophene through Catalyst Transfer Polycondensation (CTP)

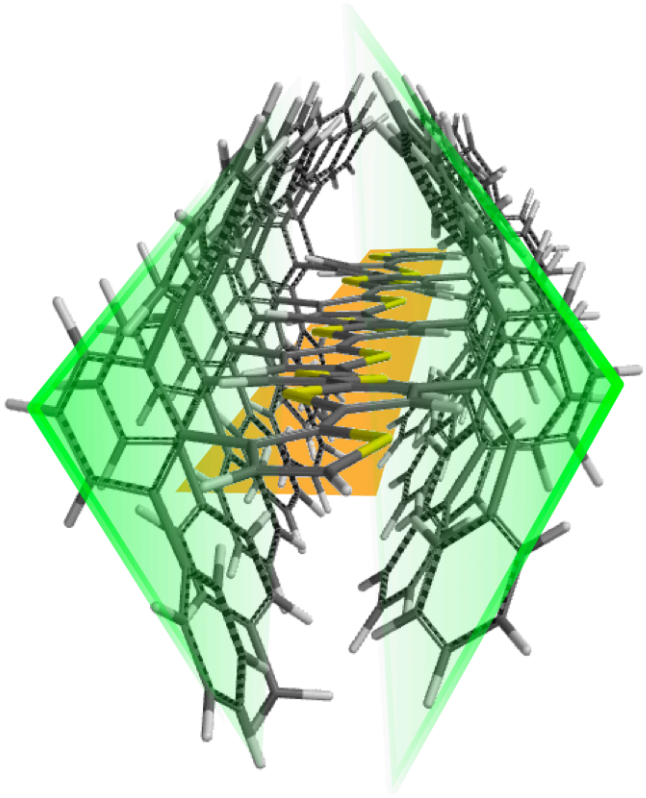

ABSTRACT: *Regioregular poly (3-'fenced'thiophene) (**P3FT**) with relatively high molecular weight and narrow polydispersity were successfully prepared by the catalyst transfer polycondesation (CTP). The obtained **P3FT** showed high conjugation and intense emission in the solid state (fluorescence quantum yield (Φ): 7 %).*

INTRODUCTION

Among the recent developed CPs, polythiophenes are one of the most studied *CPs* with widely applications in a variety of optoelectronic devices,[1] such as field-effect transistors,[2] light-emitting diodes,[3] and organic solar cells.[4] It is well known that the regioregularity, molecular weight, and polydispersity index of polythiophenes determine the properties of PTs,[5] thus influencing the performance of devices fabricated from PTs. The conventional condensation polymerization for synthesizing PTs generally proceeds in a step-growth manner, in which the synthesized PTs posses a broad molecular weight distribution, and also the length (molecular weight) and end group of the polymers are not controlled.[6] The recently developed catalyst transfer polycondensation (CTP), which was developed by Yokozawa, et al and McCullough, et al, has been attracted great attention to synthesize poly(3-hexylthiophene) (P3HT) with controlled molecular weight (M_n) and narrow molecular distribution (PDI).[7] Such a living, chain-growth method greatly advances the research activities in this field.[8]

IMWs with three-dimensional structure show distinct properties compared with the conventional uninsulated CPs. Especially IMWs can be a very good motif to study the conduction mechanism of conjugated polymers due to the fact that the pathway of charge carrier was confined in a single polymer chain.[9] Therefore, if we can control the length (molecular weight) of IMWs (such as isolated polythiophene), the relationship between charge carrier mobility and polymer length can be elucidated. However, as recently reviewed by Bryan and McNeil, the monomers that can be efficiently polymerized by CTP are still limited and as yet unestablished.[10] As such, our interest in this chapter stems from whether isolated CPs, which have unique three-dimensional structures, can be synthesized through quasi-living CTP. The main concern, in this context, is the proposed CTP mechanism that involves the formation of a Ni-complex (Ni–π complex[7a] or associated pair[7b]) at the propagating terminal. Accordingly, CTP is assumed to be unfavorable for processing sterically hindered monomers that are designed for the isolated block. Remarkably though, our initial attempt demonstrated that the CTP method has unexplored potential even for the synthesis of CPs with such distinctive three-dimensional structures. Herein, we report on the synthesis through CTP of a new isolated CP, which we call picket-fence polythiophene (poly(3-'fenced'thiophene) (**P3FT**)).[11]

RESULTS AND DISCUSSION

Synthesis of the Monomers and Polymers. 2,5-Dibromo-3-'fenced'thiophene monomers (i.e., 1.1 and 1.2 shown in Scheme 1-1) were readily synthesized through well-established reactions and characterized by using routine methods. X-ray crystal structure of 1.2 revealed the steric protection of the thiophene monomer by the terphenyl "picket" (Figure 1-1).

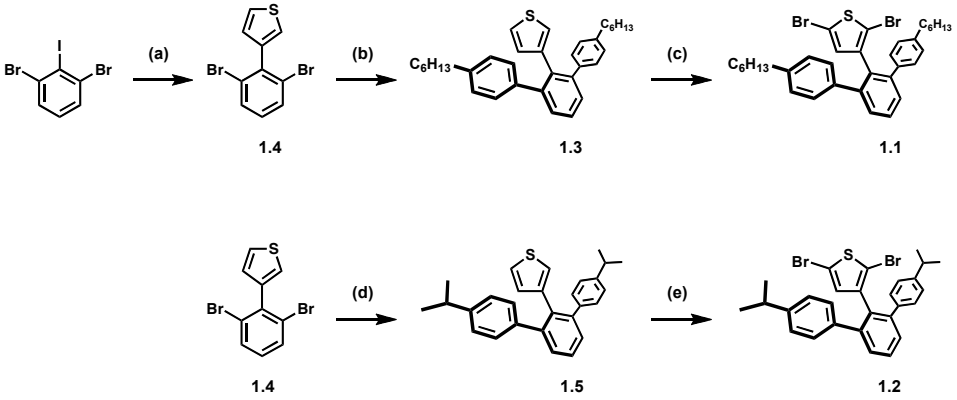

Scheme 1-1. Synthetic scheme toward monomers **1.1** and **1.2.**[18] (a) 3-thienylboronic acid, $Pd(PPh_3)_4$, Na_2CO_3, toluene, EtOH, H_2O, reflux, 3 days; (b) 4-hexylphenylboronic acid, $Pd(PPh_3)_4$, Na_2CO_3, toluene, EtOH, H_2O, reflux, 3 days; (c) Br_2, DCM, 0 °C ~r.t., 6 h; (d) 4-isopropylphenylboronic acid, $Pd(PPh_3)_4$, Na_2CO_3, toluene, EtOH, H_2O, reflux, 3 days; (e) Br_2, DCM, 0 °C ~ r.t., 6 h.

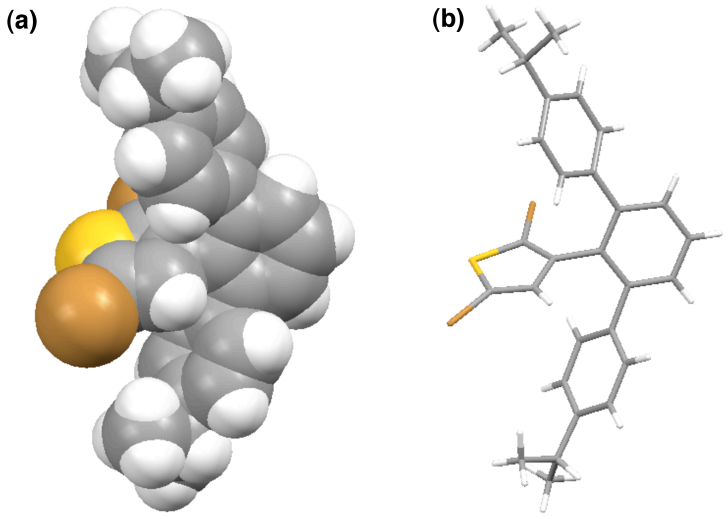

Figure 1-1. Monomer **1.2** in the crystalized form.

To test the magnesium-halogen exchange (Scheme 1-2),[19] a small vial was charged with monomer **1.1** (151 mg, 0.24 mmol) and the atmosphere was replaced with argon. Into the vial was added dry THF (5.0 ml) with LiCl (0.5 M) via a syringe, and the mixture was stirred at 0 °C. To the mixture was added isopropylmagnesium chloride (2.0 M solution in THF, 0.14 ml, 0.28 mmol) via a syringe, and the mixture was stirred at 0 °C for 30 min and then at room temperature for 1 h. An

aliquot (0.3 ml) was taken out and quenched with methanol, washed with H_2O, extracted with EtOAc, the organic layer was dried with $MgSO_4$ and filtered through silica gel. The solvent was removed under reduced pressure and the resulting colorless oil was dried under vacuum for ^{1}H-NMR spectral measurement (Figure 1-2).

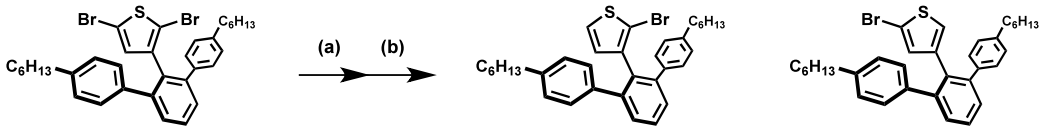

Scheme 1-2. (a) LiCl, *i*-PrMgCl, THF, (b) MeOH quench.

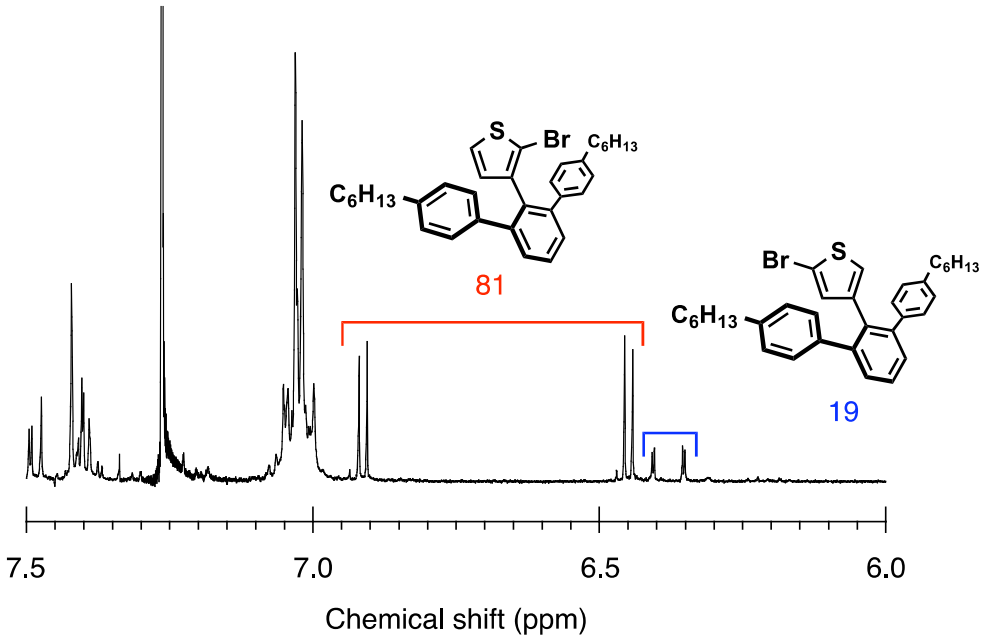

Figure 1-2. ^{1}H NMR (400 MHz, $CDCl_3$, 298 K) spectrum of the product obtained after Grignard metathesis of monomer **1.1** taken without purification.

The polymerization scheme was shown in Scheme 1-3, **1.1** was first treated with isopropylmagnesium chloride in the presence of LiCl. The transmetalation selectivity of desired 5-position bromide group in preference to the inverted 2-position bromide group was 81:19 (Scheme 1-2 and Figure 1-2). Subsequent addition of Ni(dppp)Cl_2 to the reaction mixture initiated the polymerization, as briefly confirmed by the solution color change from pale yellow to red. It should be noted that the polymerization required slightly elevated temperature (65 °C) owing to steric hindrance. The reaction mixture was treated through the common work-up procedure, yielding a red powder.[12]

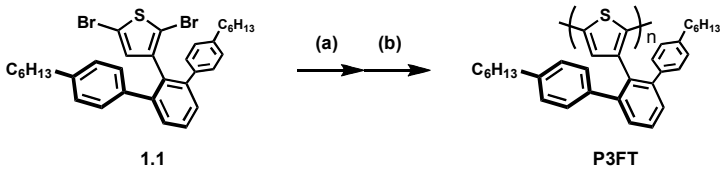

1.1 P3FT

Scheme 4-3. Polymerization of **1.1** to synthesize **P3FT**: (a) LiCl, *i*-PrMgCl, THF, (b) Ni(dppp)Cl_2, 65°C.

The obtained polymer was highly soluble in common organic solvents and had a moderate molecular weight (M_n = up to 15 K vs. polystyrene standard, which corresponds to about 32 repeating units). ^{1}H-NMR spectrum of the obtained **P3FT** confirmed a regioregular head-to-tail structure, suggesting that the 'inverted' monomer was not involved in the polymerization (Figure 1-3). Importantly, the polydispersity index (PDI) of the **P3FT** was lower than 1.2 (Figure 1-4). All these results indicate that **P3FT** was polymerized in a chain-growth manner. As shown in Figure 1-5, the MALDI-TOF Mass spectrum contained one series of major peaks attributable to the Br/H terminals together with concomitant series of minor peaks due to the Br/Br terminals (as can be seen the magnified spectrum): both of the species were observed with sodium ion [Na^+]. The former (Br/H) is derived from the magnesiochloride end group and/or Ni complex end group by quenching, and the latter (Br/Br) is due to the disproportionation. This observation is consistent with the previous results of CTP for other CPs.[7-8]

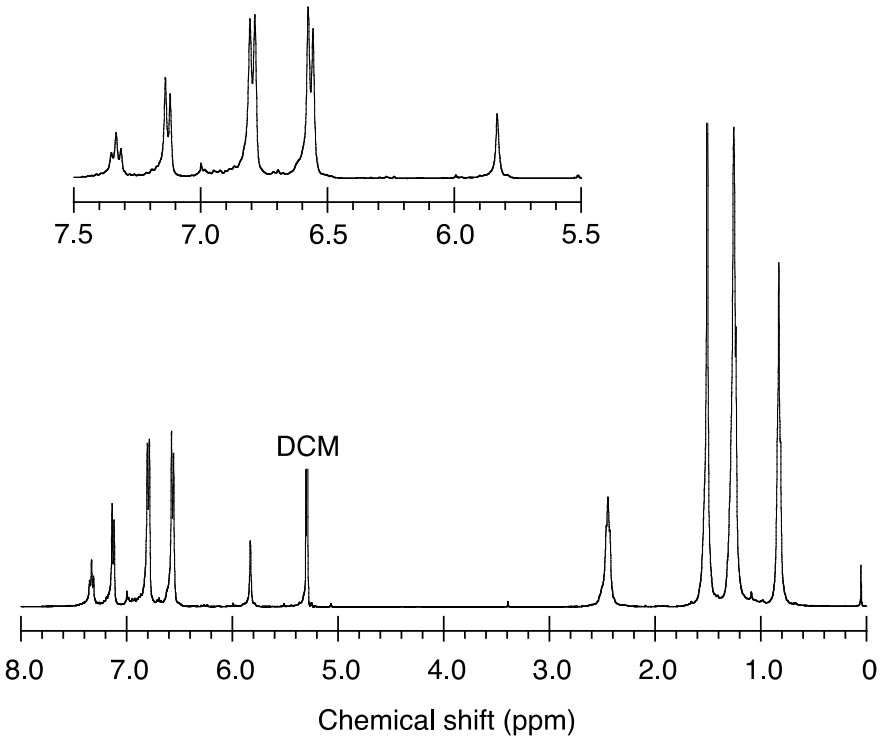

Figure 1-3. ^{1}H NMR spectrum of **P3FT** homopolymer (400 MHz in CD_2Cl_2 at 298 K).

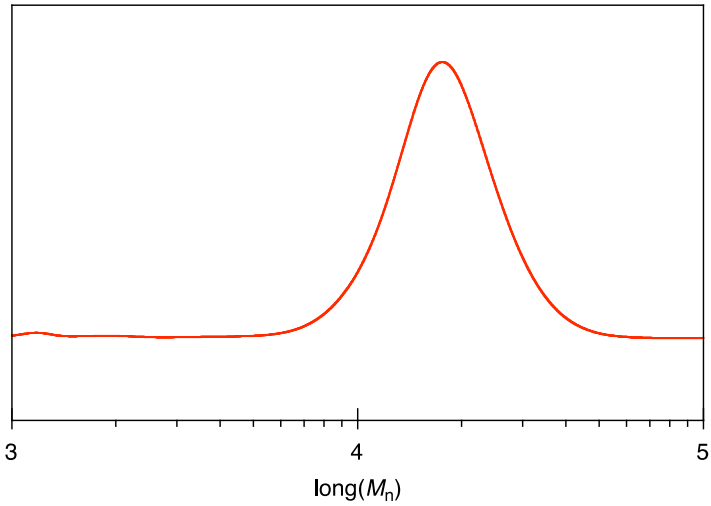

Figure 1-4. GPC elution curve of **P3FT** homopolymer: M_n = 15 K, PDI = 1.15.

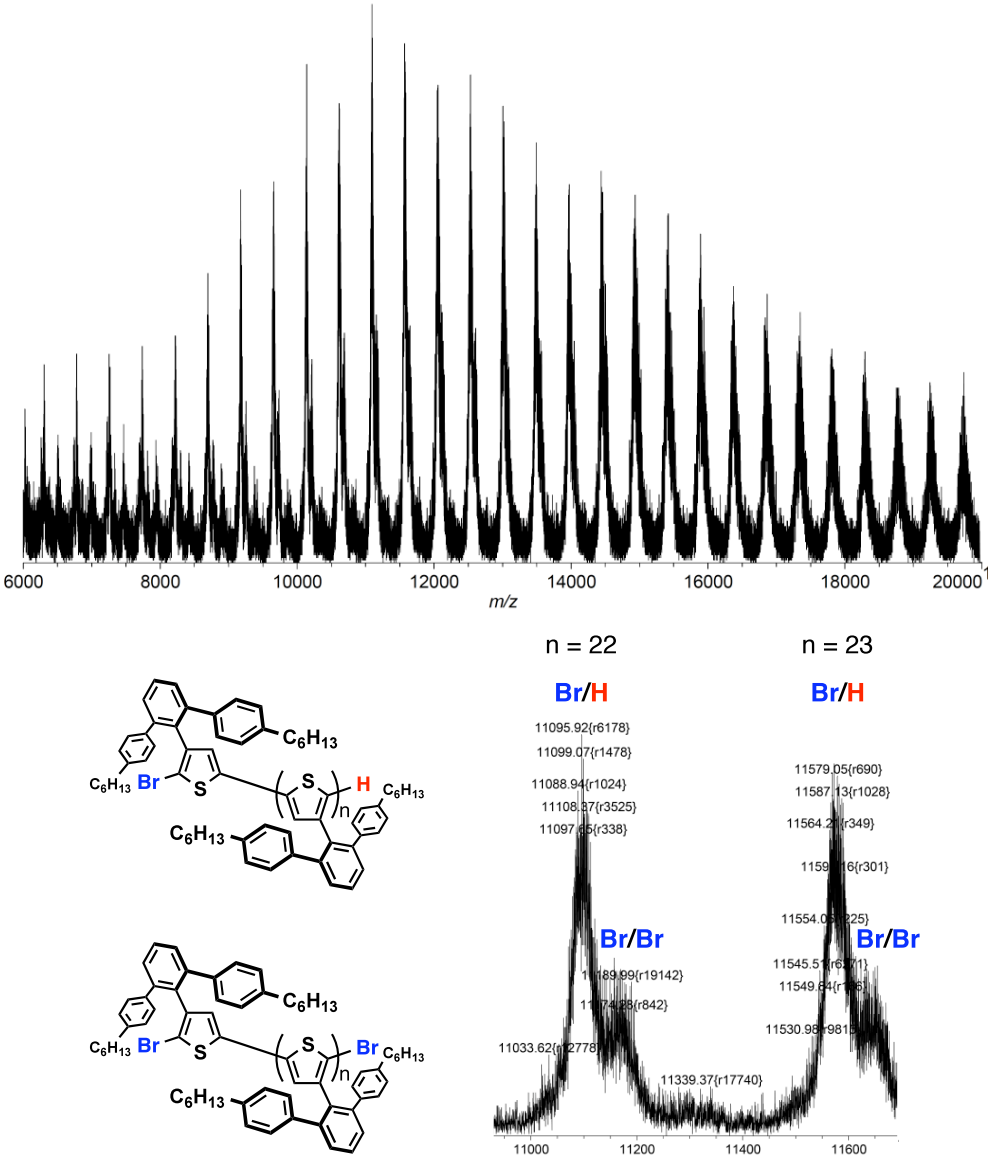

Figure 1-5. MALDI-TOF-Mass spectrum of **P3FT**

Self-threaded bithiophene (**STB**) was brominated by NBS to yield **STBBr$_2$**,[9] which was applied to CTP through the similar procedure for the synthesis of **P3FT** (Scheme 1-4), however, it could not be synthesized through the same procedure, which may shed light on the monomer scope of CTP in terms of steric hindrance (Figure 1-6). Although mechanistic details of the **P3FT** polymerization process are still unclear, we assume that after the reductive elimination step, the aromatic 'fence' can act as a stepping stone and aid the transfer of the Ni catalyst to the propagating terminal. In fact, phenyl monomers are also known to have π-binding affinity for Ni(0), and are applicable to CTP.[13] In addition, such an acrobatic catalyst-transfer process has recently been suggested, in which the Ni catalyst jumps across the neighboring thiophene monomers that are linked through a non-conjugated spacer.[14]

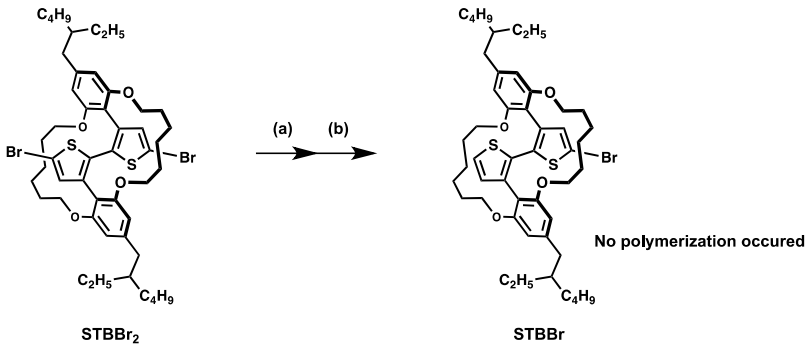

Scheme 1-4. Attempt of CTP of self-threaded bithiophene monomer (**STBBr$_2$**): (a) *i*-PrMgCl, LiCl, THF, (b) Ni(dppp)Cl$_2$, 65 °C.

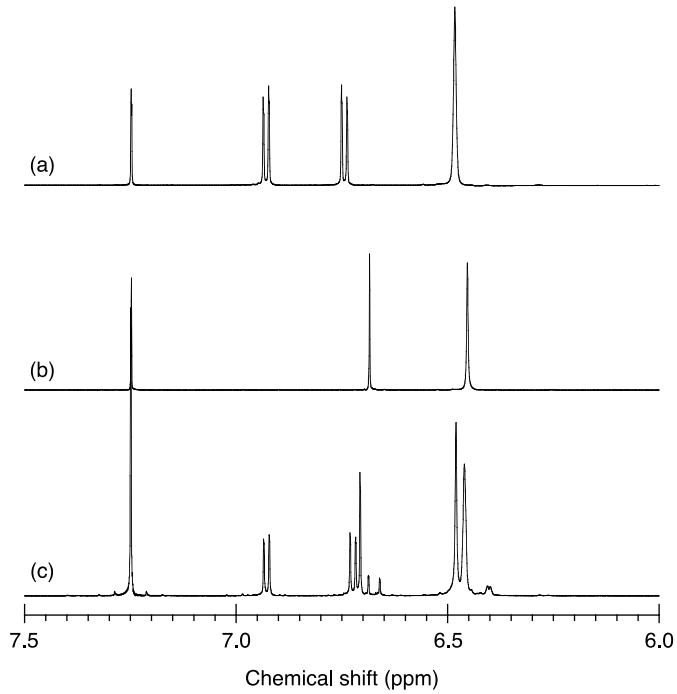

Figure 1-6. ^{1}H-NMR spectra of (a) **STB**, (b) **STBBr$_2$**, and (c) the product obtained after the attempt of CTP, without any purification. Polymerization did not yield **poly(STB)**, instead, monobrominated compound (**STBBr**) was obtained.

Photophysical Properties. Figure 1-7 compares the absorption and fluorescence spectra of **P3HT** and **P3FT** in solution and film forms. As is well known, absorption and fluorescence spectra of **P3HT** show a significant red shift upon film formation due to the strong interchain π–π stacking ($\lambda_{abs.}$: 450 → 600 nm: 5560 cm^{-1}).[15] In stark contrast, the absorption and fluorescence spectra of **P3FT** in solution and film forms are virtually similar. A small blue shift observed in the absorption maximum from solution to the film ($\lambda_{abs.}$: 523 → 488 nm: -1370 cm^{-1}), which has often been observed for other isolated CPs, is probably due to conformational changes.[9] Fluorescence quantum yield of the **P3FT** film (7%) was higher than that of **P3HT** (2%) (Table 1-1), suggesting that exciton migration is suppressed in the **P3FT** film.

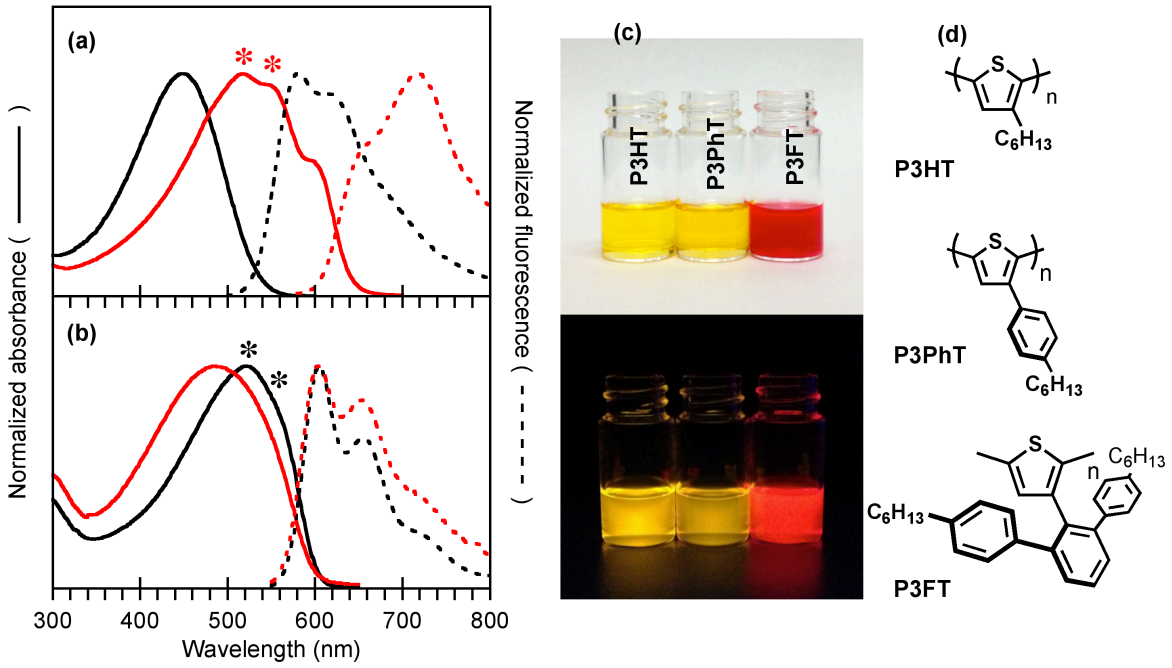

Figure 1-7. Absorption (solid lines) and fluorescence (dotted lines) spectra of (a) **P3HT** and (b) **P3FT** in chloroform solution (black lines) and film form (red lines); electronic transitions marked as * can be attributed to planar polythiophene. (c) Photographs of the solutions of **P3HT**, **P3PhT**, and **P3FT** under ambient (upper panel) and UV (lower panel) light; (d) Chemical structures of **P3HT**, **P3PhT**, and **P3FT**.

The photophysical properties of **P3HT** and **P3FT** are summarized in Table 1-1. The molar extinction coefficient of **P3FT** was 3.95, which is close to that of **P3HT** (3.74). **P3FT** has a better fluorescence quantum yield (Φ_F) (0.33 in chloroform) compared to those of **P3HT** (0.23 in chloroform), which were measured under the same conditions. **P3FT** has small Stokes shift and longer lifetime both in $CHCl_3$ and film form compared to those of **P3HT**. These results indicate that the terphenyl group can effectively prevent the polythiophene backbone from π-π stacking which inhibit the interpolymer interactions and reduce the self-quenching processes of polythiophene backbone.

Table 1-1. Photophysical data of **P3HT** and **P3FT** homopolymers

Compd.[a]	$\lambda_{abs}(\log\varepsilon)$[b] [nm]	λ_{em}[b] [nm]	Stokes Shift [cm^{-1}]	Φ[c]	Lifetime τ_{AVE} [ns][d]
P3HT sol.	450 (3.94)	581	5,011	0.23	0.63
film	517	719	5,434	0.02	0.31
P3FT sol.	523 (3.95)	605	2,592	0.33	0.97
film	488	603	3,908	0.07	0.41

[a] Solutions were prepared from $CHCl_3$; films were prepared by drop-cast from chlorobenzene solutions; [b] only the longest absorption and fluorescence maxima are shown. **P3HT**, and **P3FT** in $CHCl_3$ were excited at 476 nm. **P3HT** film was excited at 518 nm, and **P3FT** film was excited at 520 nm; [c] absolute quantum yields determined with a calibrated integrating sphere system; [d] λ_{ex} = 375 nm; $\lambda_{moni.}$ = 600 nm for **P3FT** and **P3HT** solution, and **P3FT** film; $\lambda_{moni.}$= 700 nm for **P3HT** film. All the lifetime data were fitted by two-exponential decay and the average values were shown here: $\tau_{AVE} = (\tau_1^2 X_1 + \tau_2^2 X_2) / (\tau_1 X_1 + \tau_2 X_2)$.

DSC and UPS measurements. Furthermore, differential scanning calorimetry (DSC) measurement showed that **P3FT** was rather amorphous in nature (Figure 1-8), and ultraviolet photoelectron spectroscopy (UPS) revealed that a **P3FT** film had larger ionization potential (~5.3 eV) than a **P3HT** film (~5.0 eV) (Figure 1-9). These results indicate that terphenyl picket fences prevent the polythiophene backbone from forming π–π stacking.

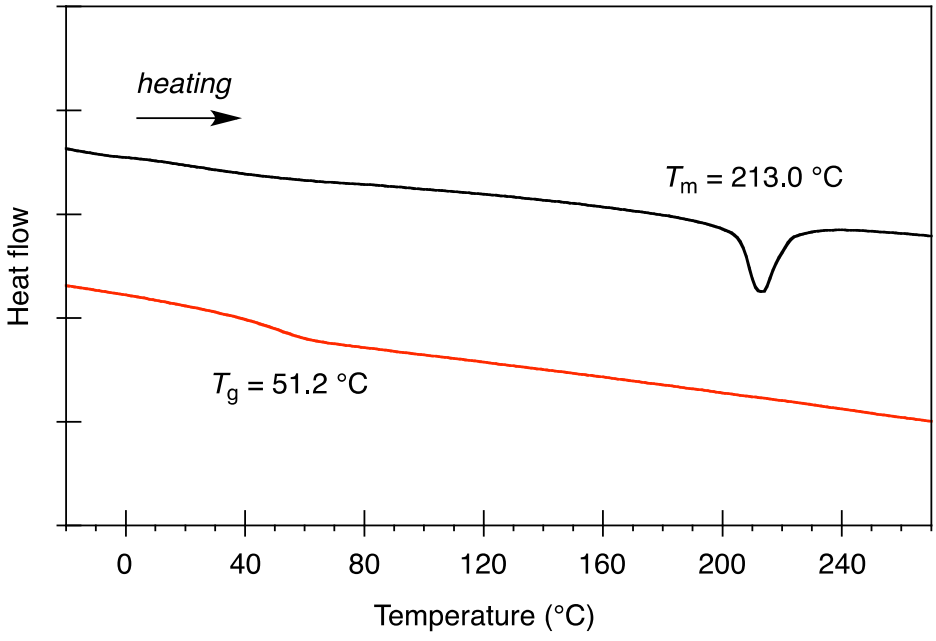

Figure 1-8. Differential scanning calorimetry (DSC) thermograms of **P3HT** (black) and **P3FT** (red) in the third heating cycles.

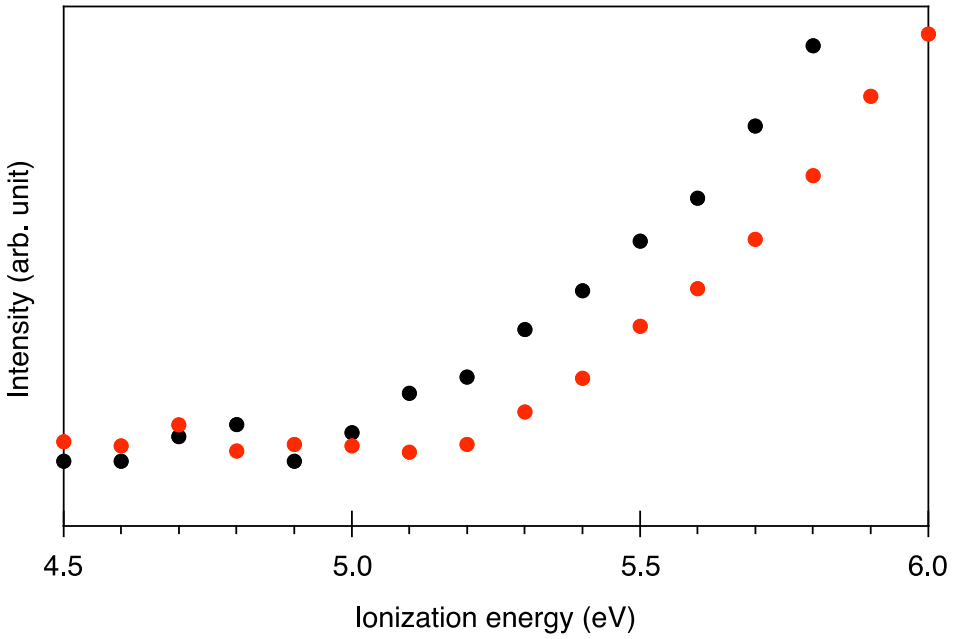

Figure 1-9. Ultraviolet photoelectron spectroscopy (UPS) results of **P3HT** (black dot) and **P3FT** (red dot).

Absorption and CV measurements. Another intriguing feature of **P3FT** was discovered when comparing the absorption spectra of **P3HT**, **P3PhT**, and **P3FT** in solution (Figures 1-7 and 1-10). **P3FT** had an absorption maximum at 523 nm together with a shoulder at 561 nm, which were greatly red-shifted in comparison to those of **P3HT** (λ_{max} = 450 nm) and **P3PhT** (λ_{max} = 453 nm). These red-shifted electronic transitions were also observed for **P3HT** *films* (see the * marks in Figures 1-2a,b), which are attributable to the 0-0 and 0-1 transitions of the planar polythiophene.[15] In addition, **P3FT** showed a lower oxidation potential (0.1 V vs Fc/Fc^{+}) than **P3HT** (0.2 V) in solution (Figure 1-11). These results suggest that **P3FT** exhibits better conjugation than **P3HT** and **P3PhT** in solution.

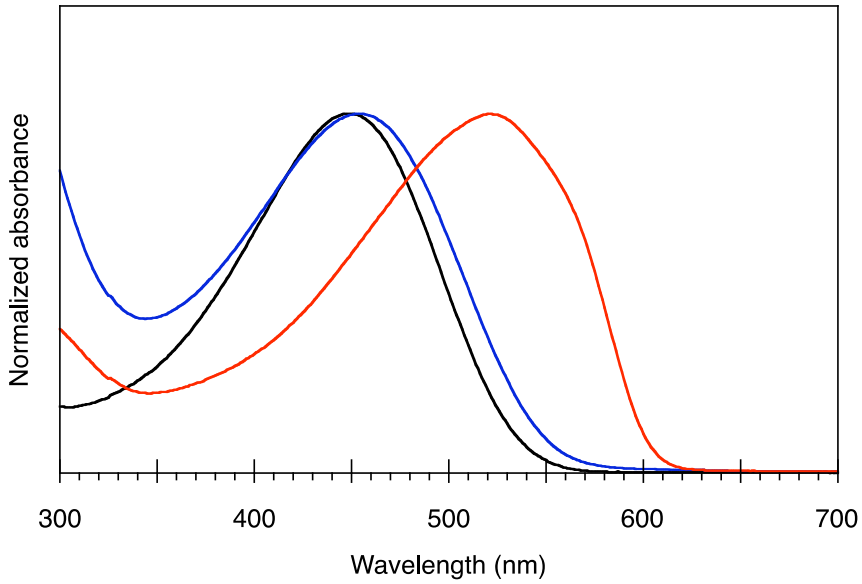

Figure 1-10. Absorption spectra of **P3HT** (black), **P3PhT** (blue) and **P3FT** (red) in chloroform.

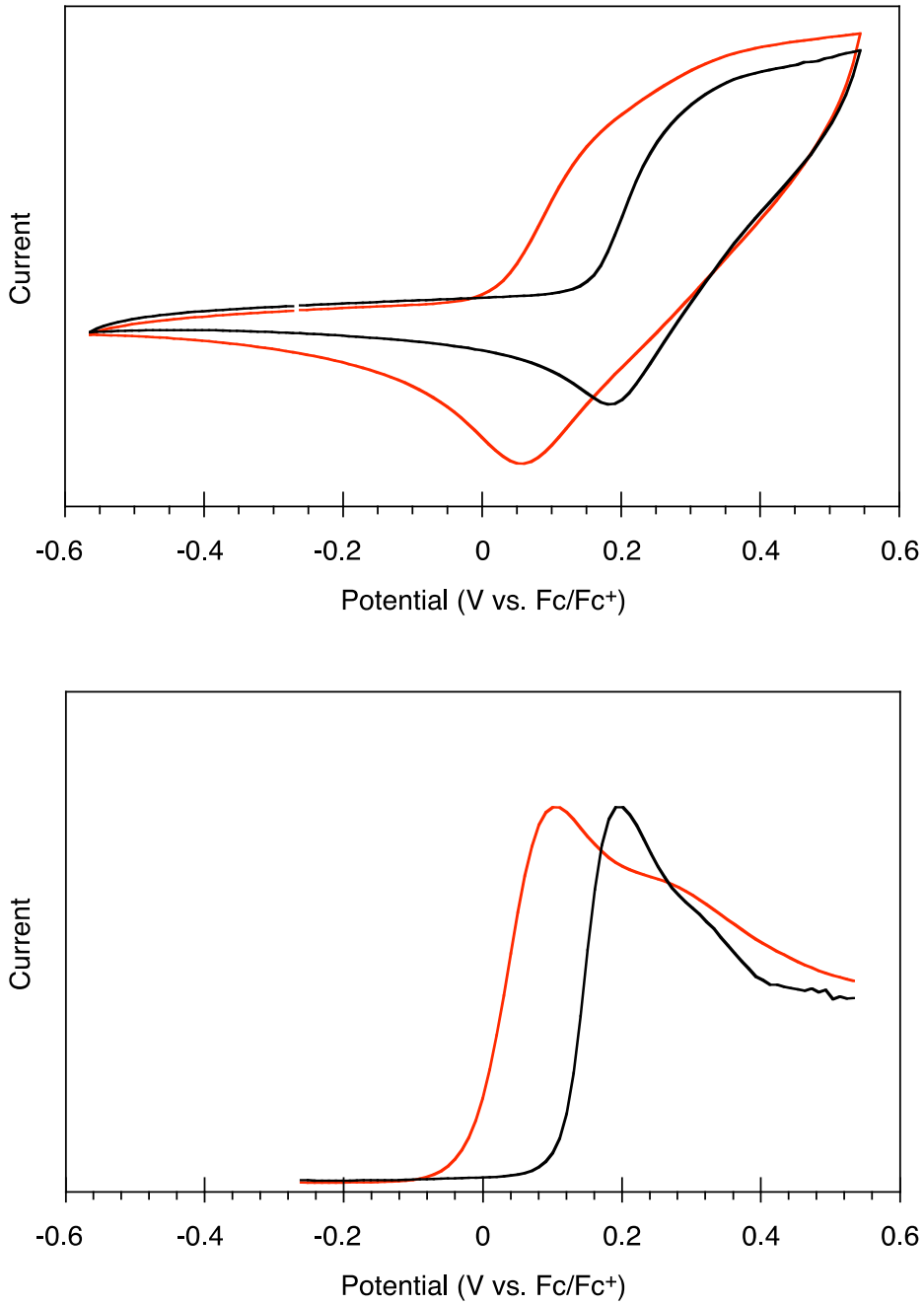

Figure 1-11. Cyclic voltammogram (upper panel) and differential pulse voltammogram (lower panel) of **P3HT** (black) and **P3FT** (red) in CH_2Cl_2 containing 0.1M $TBAPF_6$.

Molecular Model and ^{1}H NMR. A computer-generated model of **P3FT** revealed that regioregular picket fences interlock in a herringbone pattern and planarize the interior polythiophene backbone (Figures 4-12a,b,c).[16] Furthermore, DFT calculations for the oligomers revealed the well-developed molecular orbitals of **P3FT**, which contrasts to those of twisted **P3HT** (Figures 4-13d,e).[17] In fact, the proposed structure was supported by the ^{1}H-NMR spectra: the β-proton of **P3FT** (5.83 ppm) appeared in a higher magnetic field in comparison with those of **P3HT** (6.98 ppm) and **P3PhT** (6.79 ppm), which can be attributed to the magnetic shielding by the aromatic picket fence (Figure 4-13). As such, **P3FT** is a unique polythiophene featuring an isolated, planar backbone with a narrow polydispersity.

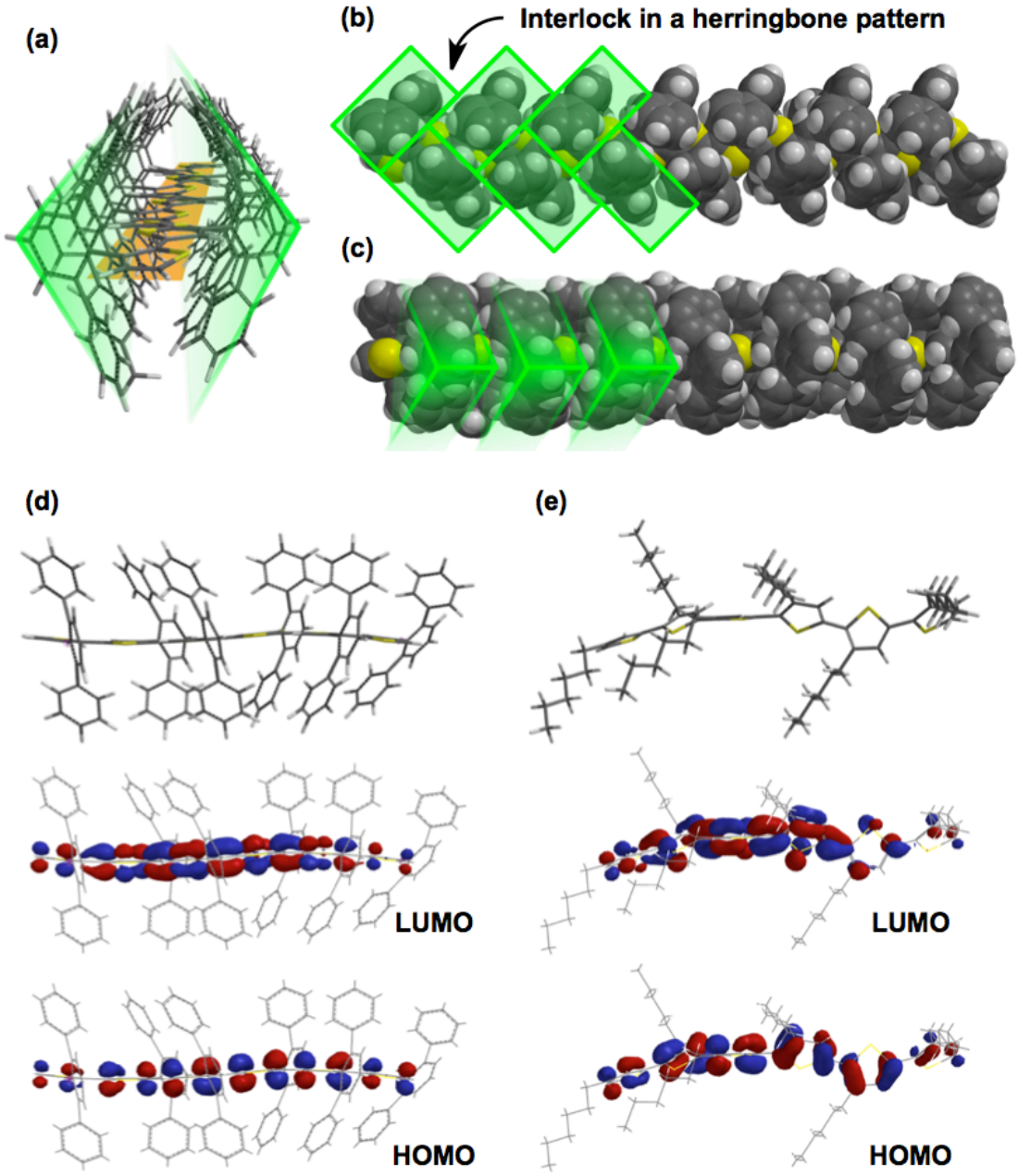

Figure 1-12. Computer-generated model of **P3FT**: (a) axial, (b) top, and (c) lateral views. Note the interdigitation in a herringbone pattern of terphenyl picket fences at both faces of the polythiophene backbone as shown in (b), which extends effective conjugation as shown in (d). Structure and molecular orbitals of (d) **3FT** and (e) **3HT** hexamers (B3LYP/6-31G* levels).

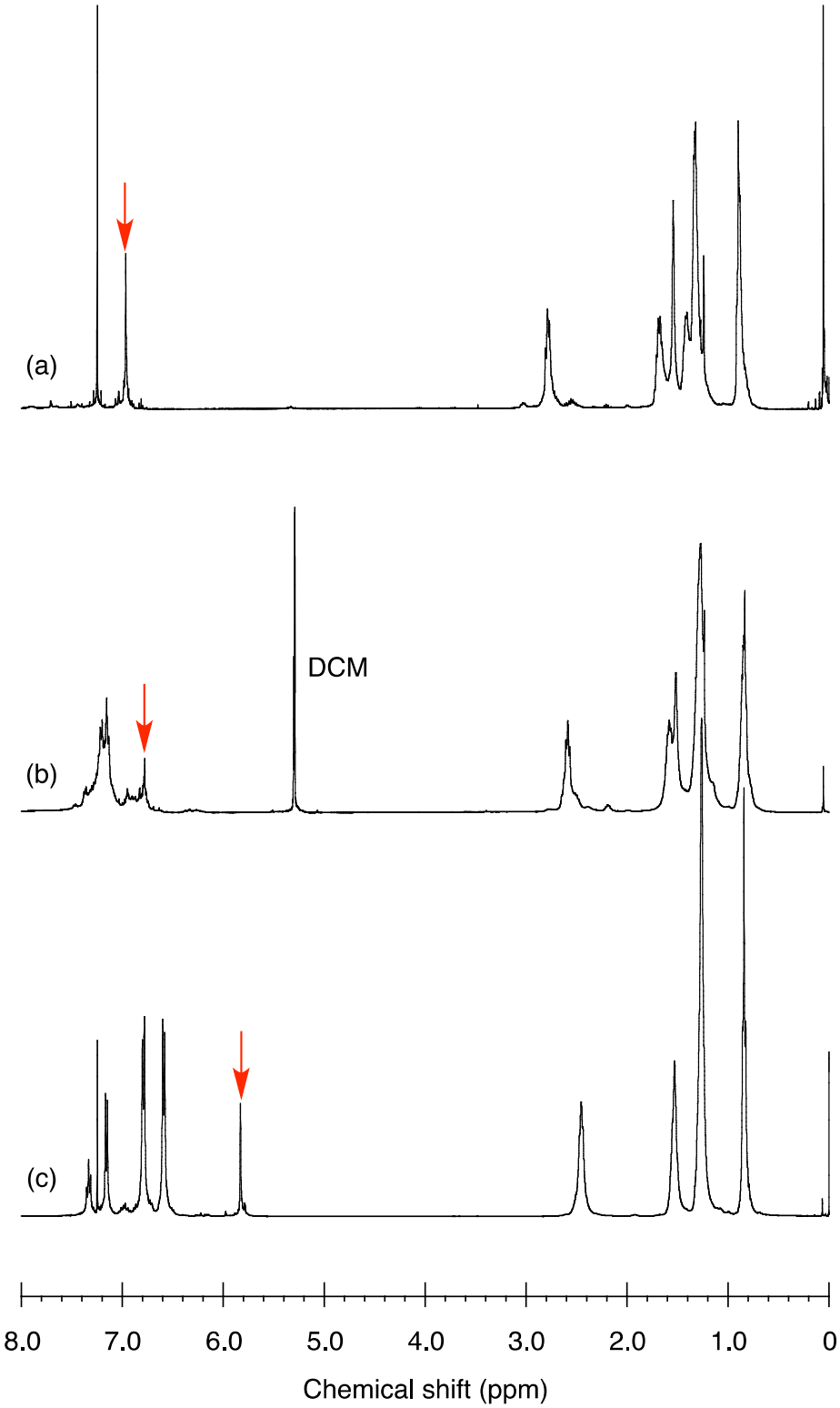

Figure 1-13. ^{1}H NMR spectra of (a) **P3HT**, (b) **P3PhT**, and (c) **P3FT**. **P3FT** and **P3HT** are measured in $CDCl_3$, and **P3PhT** was measured in CD_2Cl_2 to avoid spectral overlap. Red arrows indicate the β-protons of polythiophene backbones: 6.98 ppm for **P3HT**, 6.79 ppm for **P3PhT** (6.78 ppm in $CDCl_3$), and 5.83 ppm for **P3FT**.

CONCLUSION

In conclusion, the present study in this chapter has revealed an unexplored potential of the CTP method in terms of steric hindrance, along with a demonstration of chain-growth polymerization of isolated CPs. **P3FT** has a fenced and well-developed conjugated backbone with a narrow polydispersity (PDI ≤ 1.2), and therefore, can be regarded as a new type of isolated CP.

EXPERIMENTAL SECTION

Air and water sensitive synthetic manipulations were performed under an argon atmosphere using standard Schlenk techniques. All chemicals were purchased from Aldrich, TCI, Kanto Chemical, or Wako and used as received without further purification. NMR spectra were recorded on a JEOL ECS-400 (400 MHz) spectrometer by using tetramethylsilane (0 ppm for ^{1}H NMR) or residual $CHCl_3$ (77 ppm for ^{13}C NMR) as an internal standard. Mass spectral data were obtained using a SHIMADZU AXIMA-CFR Plus MALDI TOF mass spectrometer and using *trans*-2-[3-(4-tert-butylphenyl)-2-methyl-2-propenylidene]malononitrile (DCTB) (for monomers and all the intermediates) and dithranol (for all the polymers) as matrix. Melting points were determined with a Yanako NP-500P micro melting point apparatus. Gel permeation chromatography was performed in THF solution using a TOSHO GPC system (HLC-8320GPC EcoSEC) equipped with two TSK gel Super-Multipore HZ-M columns and a UV detector (254 nm). The molecular weight (M_n) and polydispersity index (PDI) of the polymer samples were calculated on the basis of a polystyrene calibration. Absorption and fluorescence spectra were recorded on a Hitachi U-2900 spectrophotometer and a Hitachi F-7000 spectrophotometer, respectively, in chloroform solution at room temperature (298 K) in a quartz cuvette of 1 cm path length. Fluorescence lifetime measurements were performed by means of time correlated single photon counting (TCSPC) technique by using a FluoroCube spectrometer (HORIBA Jobin Yvon) equipped with a picosecond pulse laser (PB-375L, 375 nm) and a picosecond photon detection module (TBX). Decay analysis and the fitting routine to determine the lifetimes were performed using the DAS6 software provided by IBM. Fluorescence quantum yield was recorded on a Hamamatsu absolute PL quantum yield spectrometer C11347. Spin coating was done on an OSHIGANE SC-300 instrument. DSC measurements were performed on a TA instrument DSC Q2000 by heating 10 °C / min. Cyclic voltammetry (CV) experiments were performed in a solution of tetrabutylammonium hexaflurophosphate ($TBAF_6$) (0.1 M) in DCM at a scan rate of 100 mV /s. UPS measurements were performed using an AC-3E photoemission yield spectrometer (Riken Keiki).

Synthesis of compound 1.4:[18] A 1L three-necked round bottom flask was charged with 1,3-dibromo-2-iodobenzene (10.1 g, 26.8 mmol), 3-thienylboronic acid (10.3 g, 80.4 mmol), sodium carbonate (26 g, 245.3 mmol), and evacuated and back-filled with argon three times. Toluene (260 ml), ethanol (120 ml) and water (100 ml) were added via syringe. The reaction mixture was vigorously stirred at 80 °C for 90 minutes, $Pd(PPh_3)_4$ (800 mg, 0.69 mmol) was then added to the reaction mixture, the stirring was continued for 72 hours, then the solvent was evaporated under reduced pressure. Water was poured into the reaction mixture, extracted with DCM for 3 times, the combined organic layer was washed with brine, dried over $MgSO_4$. The solvent was removed by evaporation under reduced pressure, and the resulting black solid was purified through column chromatography (silica gel, hexane) to afford compound **3** as white powder (5.1 g, 60%).

M.p.: 86.6–87.6 °C. ^{1}H NMR ($CDCl_3$, 400 MHz, TMS, 298 K): δ 7.02–7.06 (m, 2H), 7.22–7.23 (m, 1H), 7.39 (t, J = 4.0 Hz 1H), 7.60 (d, J = 8.0 Hz, 2H). ^{13}C NMR ($CDCl_3$, 100 MHz, TMS, 298 K): δ 124.72, 124.95, 125.05, 128.44, 129.90, 131.78, 138.54, 140.29. Anal. Calcd for $C_{10}H_6Br_2S$: C, 37.77; H, 1.90. Found: C, 37.44; H, 1.87.

Synthesis of compound 1.3: The same procedure for the synthesis of **1.4** was applied using compound **1.4** and 4-hexylphenylboronic acid as starting materials. Yield: 95%, colorless oil.

^{1}H NMR ($CDCl_3$, 400 MHz, TMS, 298 K): δ 0.88 (t, J = 6.6 Hz, 6H), 1.29–1.33 (broad, 12H), 1.56–1.60 (m, 4H), 2.55 (t, J = 7.8 Hz, 4H), 6.45 (dd, J = 4.8 Hz & 1.6 Hz, 1H), 6.53 (dd, J = 2.8 Hz & 1.6 Hz, 1H), 6.91 (dd, J = 4.8 Hz & 2.8 Hz, 1H), 7.01 (broad, 8H), 7.38–7.43 (m, 3H). ^{13}C NMR ($CDCl_3$, 100 MHz, TMS, 298 K): δ 14.09, 22.61, 28.94, 31.26, 31.70, 35.53, 123.35, 124.86, 127.28, 127.62, 129.29, 129.35, 130.53, 134.00, 139.26, 139.66, 140.92, 142.23. MALDI-TOF-MS (Matrix: DCTB): Found m/z = 480.12, Calcd for $[M]^+$ ($C_{34}H_{40}S$) = 480.29. Anal. Calcd for $C_{34}H_{40}S$: C, 84.94; H, 8.39. Found: C, 85.01; H, 7.92.

Synthesis of monomer 1.1: To a solution of **1.3** (6.97 g, 14.52 mmol) in $CHCl_3$ (100 ml) was added Br_2 (4.65 g, 29.04 mmol) in $CHCl_3$ (100 ml) at 0 °C and the solution was stirred for 6 hours with warming up to room temperature. Na_2SO_3 aqueous solution was added to quench the reaction. The organic layer was isolated and the water layer was extracted with $CHCl_3$ for 3 times. The combined organic layer was washed with brine, dried over $MgSO_4$ and evaporated under reduced pressure. The obtained oil was purified through column chromatography (silica gel: hexane) to yield monomer **1.1** as colorless oil (8.3 g, 90 %).

^{1}H NMR ($CDCl_3$, 400 MHz, TMS, 298 K): δ 0.89 (t, J = 7.0Hz, 6H), 1.28–1.33 (broad, 12H), 1.58–1.62 (m, 4H), 2.58 (t, J = 7.8 Hz, 4H), 6.41 (s, 1H), 7.03–7.09 (broad, 8H), 7.39–7.41 (m, 2H), 7.48–7.51 (m, 1H). ^{13}C NMR ($CDCl_3$, 100 MHz, TMS, 298 K): δ 14.12, 22.62, 28.84, 31.23, 31.71, 35.53, 109.48, 111.12, 127.77, 128.53, 128.99, 129.33, 131.18, 133.22, 138.25, 141.39, 141.44, 142.83.

MALDI-TOF-MS (Matrix: DCTB): Found m/z = 640.16, Calcd for $[M]^+$ ($C_{34}H_{38}Br_2S$) = 638.10. Anal. Calcd for $C_{34}H_{38}Br_2S$: C, 63.95; H, 6.00. Found: C, 64.14; H, 6.33.

Synthesis of compound 1.5: The same procedure for the synthesis of **1.3** was applied using compound **1.4** and 4-isopropylphenylboronic acid as starting materials. Yield: 95 %, white powder.
M.p.: 113.5–114.5 °C. ^{1}H NMR ($CDCl_3$, 400 MHz, TMS, 298 K): δ 1.23 (d, J = 6.8 Hz, 12H), 2.83–2.90 (m, 2H), 6.46–6.47 (dd, J = 0.8 Hz and 5.2 Hz, 1H), 6.55 (dd, J = 0.8 Hz and 2.8 Hz, 1H), 6.91–6.93 (dd, J = 2.8 Hz and 5.2 Hz, 1H), 7.02–7.08 (m, 8H), 7.39–7.43 (m, 3H). ^{13}C NMR ($CDCl_3$, 100 MHz, TMS, 298 K): δ 23.94, 33.62, 123.31, 124.90, 125.63, 127.28, 129.33, 129.40, 130.58, 134.00, 139.39, 139.63, 142.21, 146.81. MALDI-TOF-MS (Matrix: DCTB): Found m/z = 396.04, Calcd for $[M]^+$ ($C_{28}H_{28}S$) = 396.19. Anal. Calcd for $C_{28}H_{28}S \bullet 0.2H_2O$: C, 84.04; H, 7.15. Found: C, 84.18; H, 7.44.

Synthesis of monomer 1.2: The same procedure for the synthesis of **1.1** was applied using compound **1.5** as a starting material. Yield: 60 %, pale yellow powder.
M.p.: 116.1–117.2 °C. ^{1}H NMR ($CDCl_3$, 400 MHz, TMS, 298 K): δ 1.24 (d, J = 6.8 Hz, 12H), 2.85–2.92 (m, 2H), 6.39 (s, 1H), 7.05–7.12 (m, 8H), 7.40–7.42 (m, 2H), 7.42–7.49 (m, 1H). ^{13}C NMR ($CDCl_3$, 100 MHz, TMS, 298 K): δ 23.93, 29.70, 33.70, 109.44, 111.16, 125.75, 128.54, 129.03, 129.08, 131.20, 133.24, 138.40, 141.44, 142.79, 147.33. Anal. Calcd for $C_{28}H_{26}Br_2S$: C, 60.66; H, 4.73. Found: C, 60.96; H, 4.97.

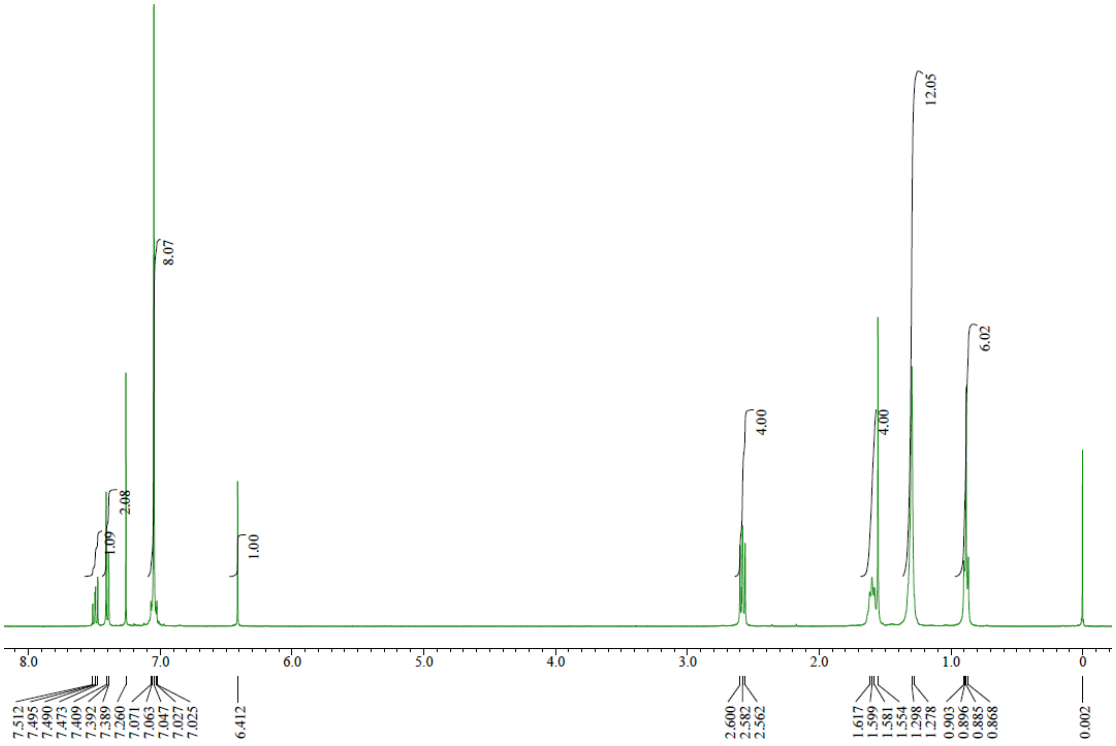

^{1}H NMR Spectrum of monomer **1.1**

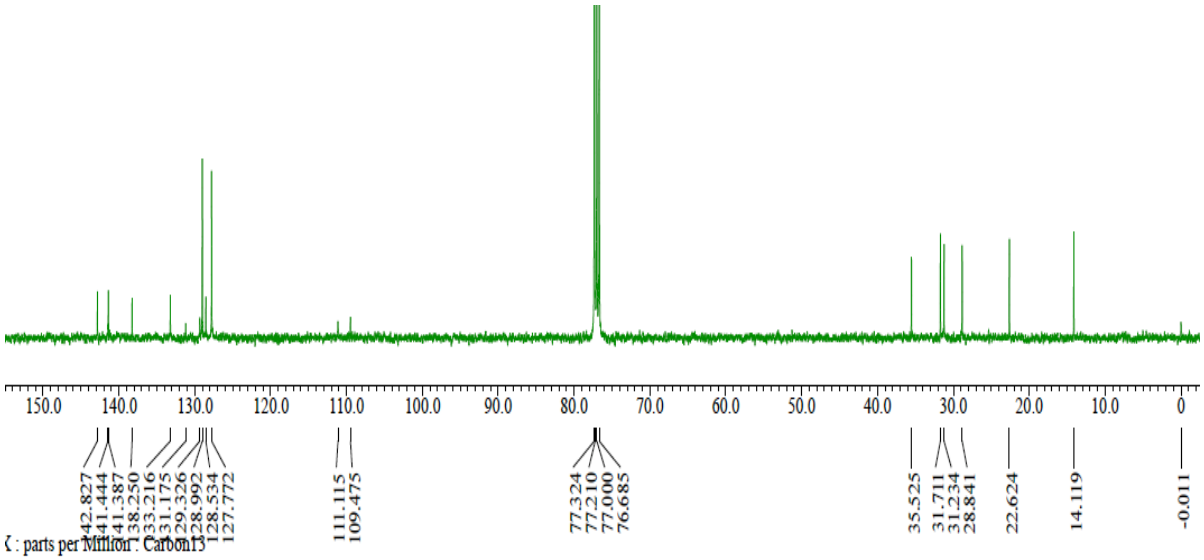

^{13}C NMR Spectrum of monomer **1.1**

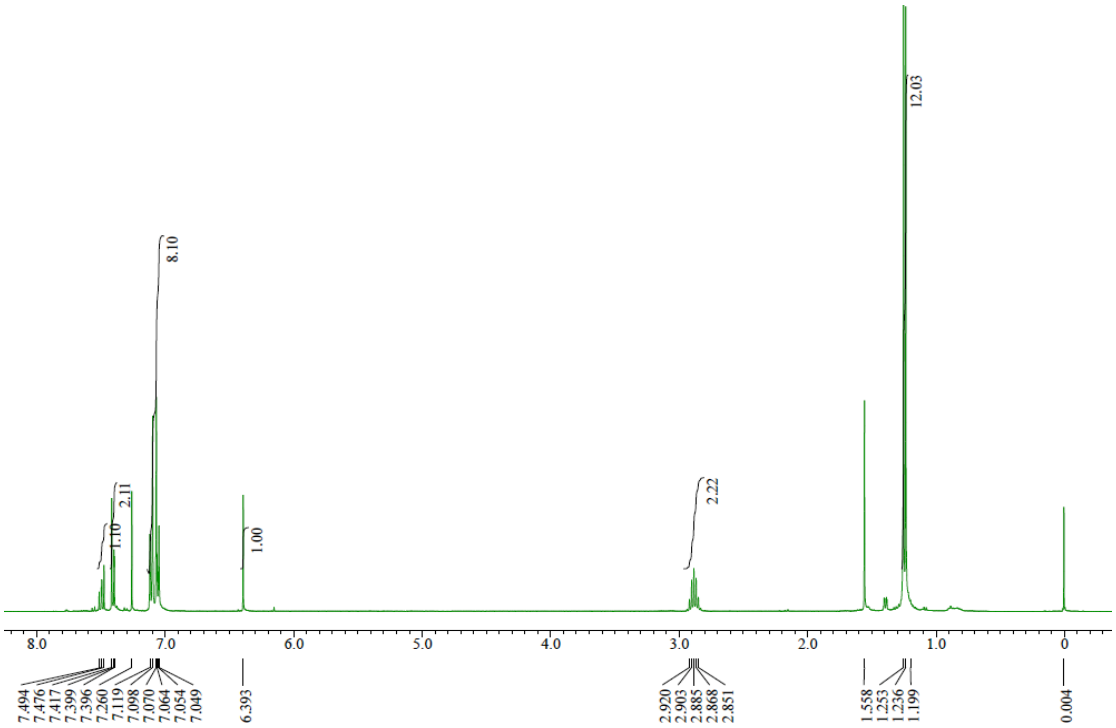

^{1}H NMR Spectrum of monomer **1.2**

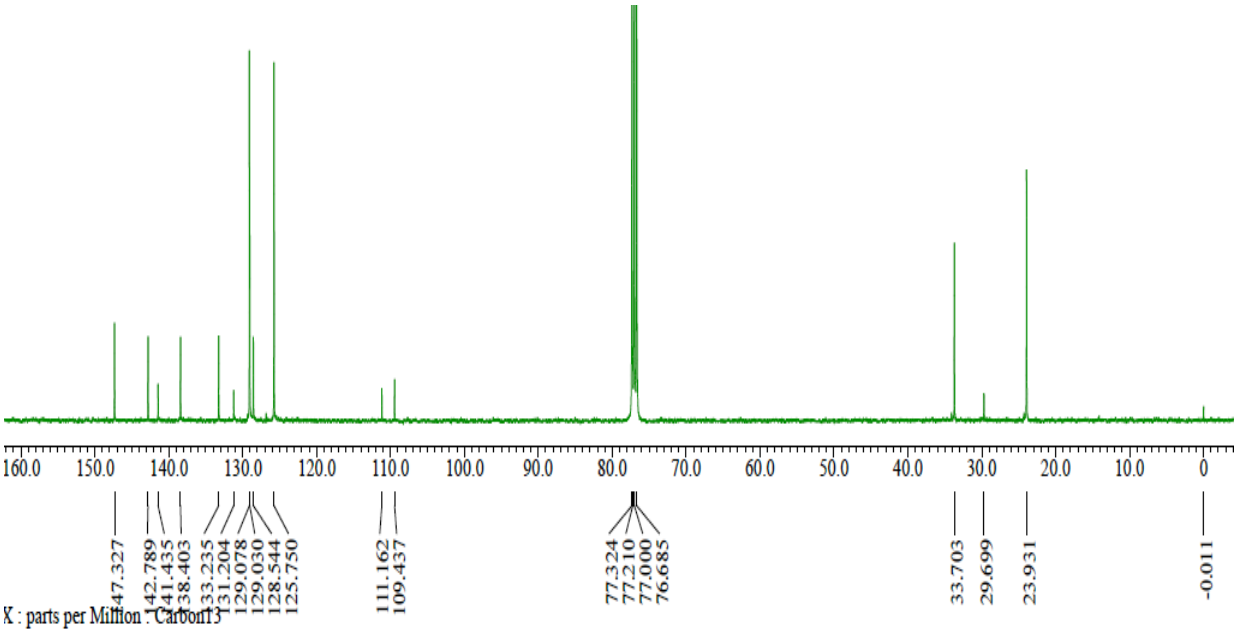

^{13}C NMR Spectrum of monomer **1.2**

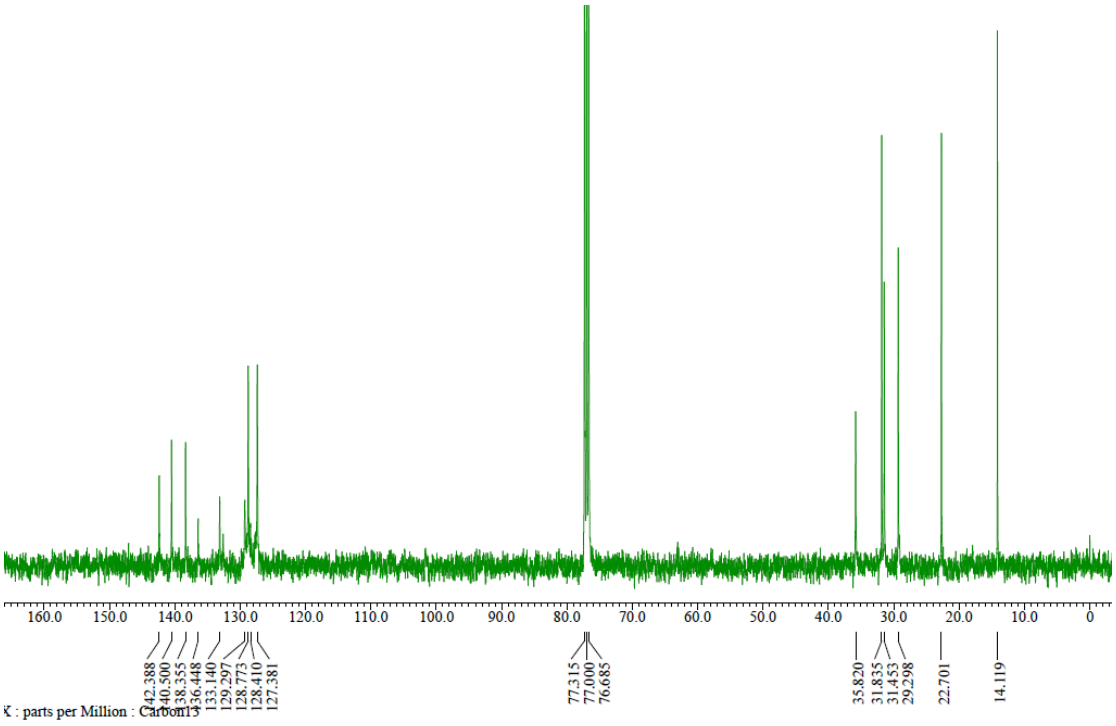

^{13}C NMR Spectrum of **P3FT** (^{1}H-NMR is shown in Figure 1-3)

REFERENCES

[1] R. D. McCullough, *Adv. Mater.* **1998**, *10*, 93.

[2] H. Sirringhaus, N. Tessler, R. H. Friend, *Science* **1998**, *280*, 1741.

[3] M. R. Andersson, O. Thomas, W. Mammo, M. Svensson, M. Theander, O. Inganäs, *J. Mater. Chem.* **1999**, *9*, 1933.

[4] G. Li, V. Shrotriya, J. Huang, Y. Yao, T. Moriarty, K. Emery, Y. Yang, *Nat. Mater.* **2005**, *4*, 864.

[5] H. Sirringhaus, P. J. Brown, R. H. Friend, M. M. Nielsen, K. Bechgaard, B. M. W. Langeveld-Voss, A. J. H. Spiering, R. A. J. Janssen, E. W. Meijer, P. Herwig, D. M. de Leeuw, *Nature* **1999**, *401*, 685.

[6] a)T. Yamamoto, *Bull. Chem. Chem. Soc. Jpn.* **2010**, *83*, 431; b) P. J. Flory, *Chem. Rev.* **1946**, *39*, 137.

[7] a) A. Yokoyama, R. Miyakoshi, T. Yokozawa, *Macromolecules* **2004**, *37*, 1169; b) E. E. Sheina, J. Liu, M. C. Iovu, D. W. Laird, R. D. McCullough, *Macromolecules* **2004**, *37*, 3526.

[8] T. Yokozawa, Y. Ohta, *Chem.Commun*. **2013**, *49*, 8281.

[9] a) K. Sugiyasu, Y. Honsho, R. M. Harrison, A. Sato, T. Yasuda, S. Seki, M. Takeuchi, *J. Am. Chem. Soc.* **2010**, *132*, 14754; b) R. Shomura, K. Sugiyasu, T. Yasuda, A. Sato, M. Takeuchi, *Macromolecules* **2012**, *45*, 3759.

[10] Z. J. Bryan, A. J. McNeil, *Macromolecules* **2013**, *46*, 8395, and references are cited therein.

[11] 'Picket fence polythiophene' was named after 'picket fence porphyrin' in terms of the structural similarity: J. P. Collman, R. R. Gagne, T. R. Halbert, J.-C. Marchon, C. A. Reed, *J. Am. Chem. Soc.* **1973**, *95*, 7868.

[12] R. Miyakoshi, A. Yokoyama, T. Yokozawa, *Macromol. Rapid Commun*. **2004**, *25*, 1663.

[13] a) R. Miyakoshi, K. Shimono, A. Yokoyama, T. Yokozawa, *J. Am. Chem. Soc.* **2006**, *128*, 16012; b) R. Tkachov, V. Senkovskyy, H. Komber, J.-U. Sommer, A. Kiriy, *J. Am. Chem. Soc.* **2010**, *132*, 7803.

[14] S. Wu, Y. Sun, L. Huang, J. Wang, Y. Zhou, Y. Geng, F. Wang, *Macromolecules* **2010**, *43*, 4438.

[15] P. J. Brown, D. S. Thomas, A. Köhler, J. S. Wilson, J. -S. Kim, C. M. Ramsdale, H. Sirringhaus, R. H. Friend, *Phys. Rev. B* **2003**, *67*, 064203.

[16] Similar planarization effects have also been observed for other bulky substituents, see: A. Fukazawa, Y. Li, S. Yamaguchi, H. Tsuji, K. Tamao, *J. Am. Chem. Soc.* **2007**, *129*, 14164, and 4c.

[17] Spartan'08, Wavefunction, Inc. Irvine, CA.

[18] X. Feng, W. Pisula, K. Müllen, *J. Am. Chem. Soc.* **2007**, *129*, 14116.

[19] S. Wu, L. Huang, H. Tian, Y. Geng, F. Wang, *Macromolecules* **2011**, *44*, 7558.

Chapter 2

Synthesis of Head-to-tail Poly (3-hexylthiophene)-block-poly (3-‘fenced’thiophene)s and their Microphase Separations comprising Stacked and Isolated Polythiophenes Ensemble

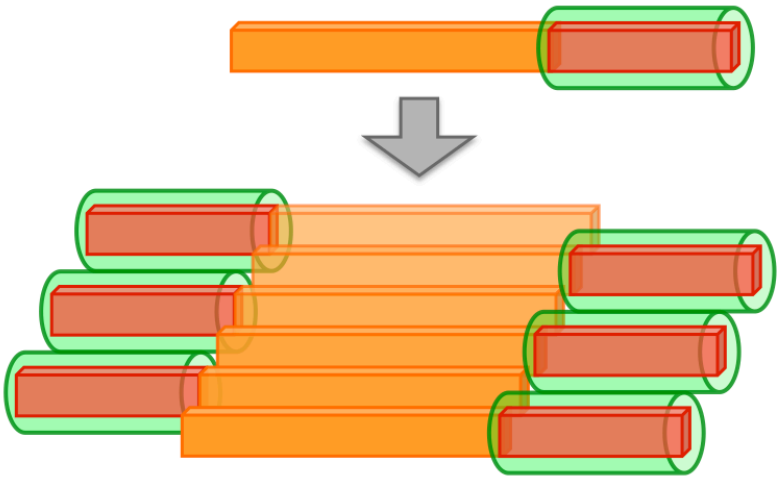

ABSTRACT: *All-polythiophene diblock copolymers, comprising one naked block and one fenced block, were synthesized through catalyst-transfer polycondensation. The naked block self-assembles through π–π stacking, thereby inducing microphase separation. Consequently, as a first, we have succeeded in creating a microphase separation comprising an ensemble of stacked and isolated polythiophenes. This achievement could be extended to various unexplored applications owing to the integration of the contrasting functions of the two blocks.*

INTRODUCTION

The ability to control supramolecular assemblies of CPs in thin films is essential for the development of organic optoelectronic devices because collective functions and properties of the CPs strongly depend on the interpolymer overlap of the molecular orbitals (i.e., π–π stacking).[1] On one hand, arranging π–π stacking facilitates interwire charge carrier transport,[2] whereas, on the other hand, preventing π–π stacking leads to unique photophysical and mechanical properties.[3,4] The aim of our present study was to integrate both the aforementioned contrasting properties in a single polymeric film. Such sophisticated design of CP-based materials should advance organic optoelectronics because complex materials have always led to unprecedented functional systems.[5]

To this end, the approach based on microphase separations (MPSs) of block copolymers is straightforward and promising because it allows the assembly of more than two distinct properties in one system.[6] For example, MPSs comprising resist/sacrificial polymer domains and electron/ion transporting domains are useful for patterning technologies[6a] and electrochemical devices[6b], respectively. CP-based MPSs have also increasingly attracted much attention owing to the recent developments in catalyst-transfer polycondensation (CTP).[7,8] The CTP method has evolved in that it can even afford all-conjugated block copolymers,[9,10] thereby leading to previously inaccessible MPSs such as the ones comprising crystalline/amorphous CP domains[9a] and p-type/n-type CP domains.[10] Likewise, our target—MPSs comprising stacked/isolated CP domains—can be realized through CTP; however, to the best of our knowledge, there have been no such reports to date.

In Chapter 1, we have successfully synthesized a new type of IMWs-**P3FT** through catalyst transfer polycondesation (CTP). Motivated by the results in Chapter 1, we performed block copolymerization of **P3FT** with **P3HT** to synthesize poly(3-hexylthiophene)-*block*-poly(3-'fenced'thiophene)s comprising an ensemble of stacked **P3HT** and isolated **P3FT**.

RESULTS AND DISCUSSION

Synthesis and Characterizations of the Monomers and Polymers. As shown in Scheme 2-1, **P3HT-Ni** (PDI < 1.1) was first prepared according to the reported procedure,[9] and then used as a macroinitiator for the successive CTP of the **P3FT** block. After block copolymerization, the gel permeation chromatography (GPC) retention curve showed a peak shift in comparison to the macroinitiator **P3HT**, while maintaining the low PDI value (≤ 1.2) (Figure 2-1). This result evidences the controlled propagation of the **P3FT** block from the **P3HT** block. We prepared several **P3HT(x)-*b*-P3FT(y)** species with different x/y ratios, which were determined based on the ^{1}H-NMR spectral data (see Figure 2-3, here, x and y represent the percentage composition of m and n, respectively).

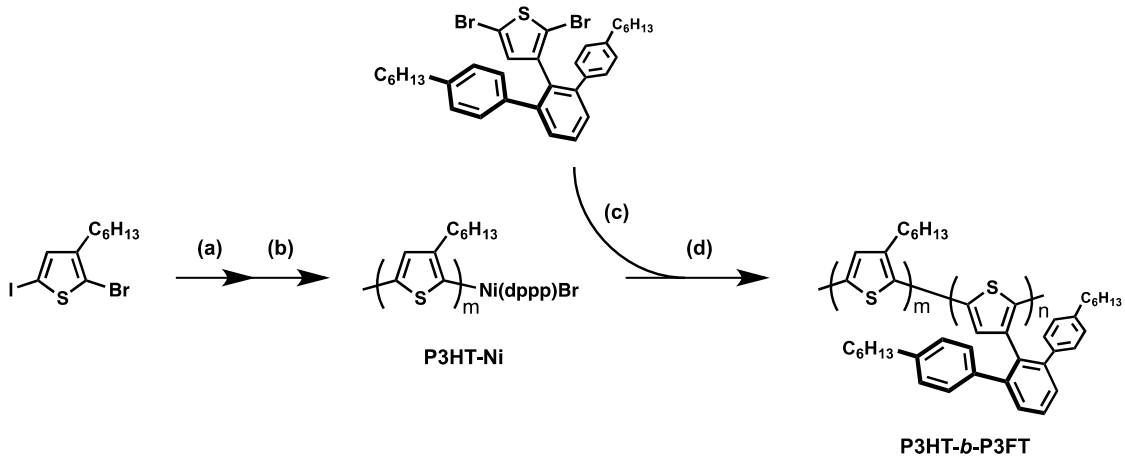

Scheme 2-1. Block copolymerization to P3HT-*b*-P3FT: (a) *i*-PrMgCl, (b) Ni(dppp)Cl_2, 35 °C, (c) LiCl, *i*-PrMgCl, THF, (d) 65 °C.

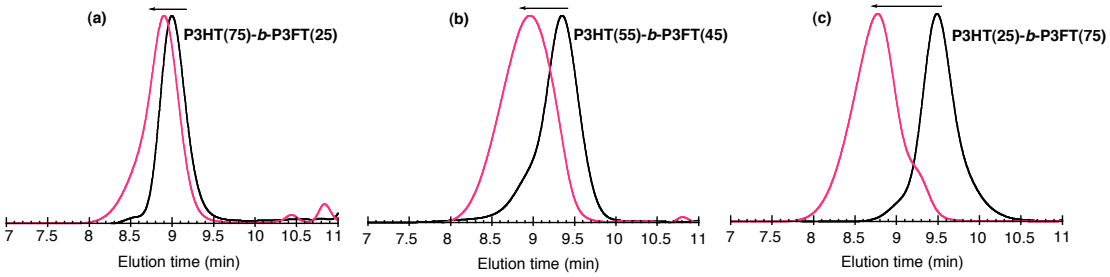

Figure 2-2. GPC profiles of **P3HT-*b*-P3FT** with block ratio of 75:25 (a), 55:45 (b) and 25:75 (c). The black and red lines show the GPC traces of the **P3HT** macroinitiator and **P3HT-*b*-P3FT**, respectively.

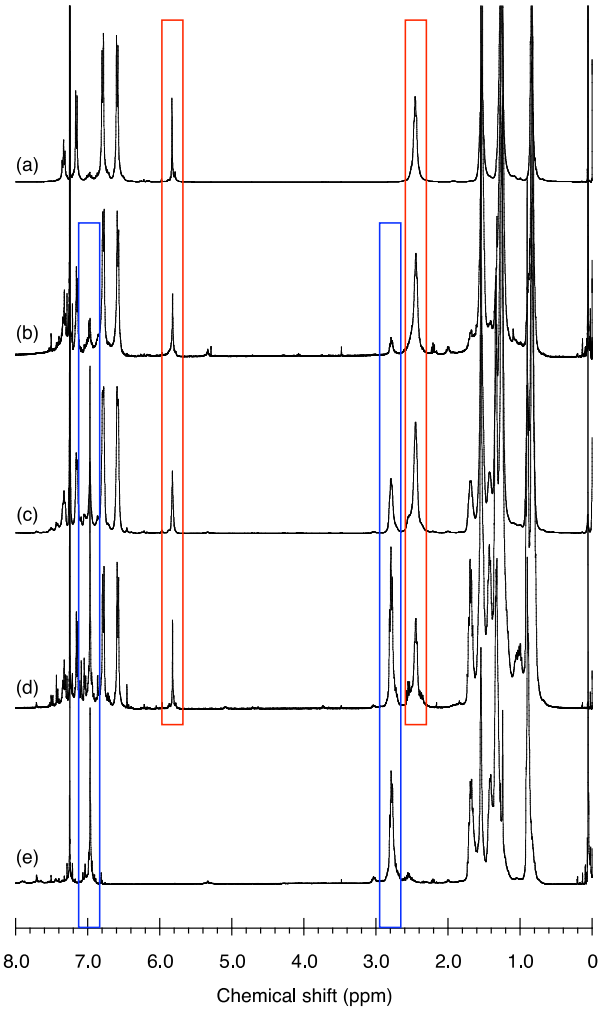

Figure 2-2. ^{1}H NMR spectra of (a) **P3FT**, (b) **P3HT(25)-*b*-P3FT(75)**, (c) **P3HT(55)-*b*-P3FT(45)**, (d) **P3HT(75)-*b*-P3FT(55)**, and (e) **P3HT** (400 MHz in chloroform-*d* at room temperature): Red and blue squares highlight peaks for **P3HT** and **P3FT** blocks, respectively.

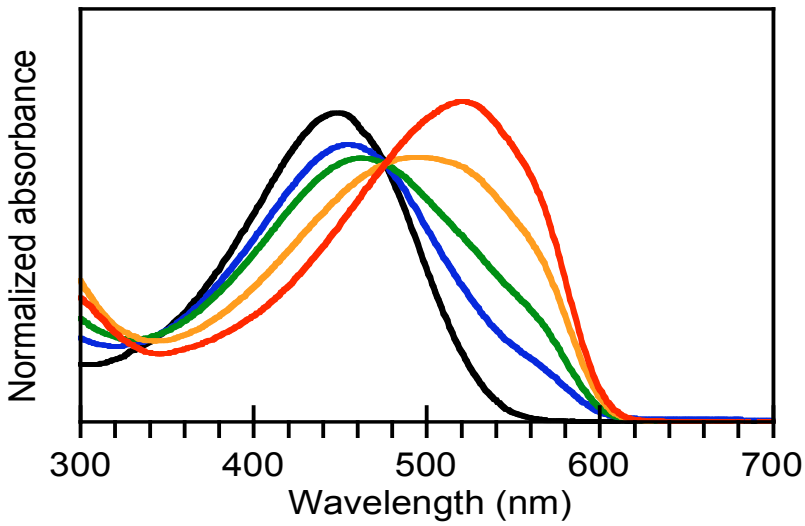

Figure 2-3. Absorption spectra of **P3HT(x)-*b*-P3FT(y)** for x:y ratios of 100:0 (black), 75:25 (blue), 55:45(green), 25:75 (orange), and 0:100 (red), in chloroform, normalized at 476 nm.

Because **P3HT** and **P3FT** have the same molar absorption coefficient at 476 nm ($\log\varepsilon_{476} = 3.88$), all the spectra of these diblock polymers were normalized at this wavelength and are displayed in Figure 2-3. The spectra could be deconvoluted into those of **P3HT** and **P3FT** (Figure 2-4), and the determined ratios between the blocks showed good agreement with those resolved by ^{1}H-NMR. This result indicates that **P3HT(x)-*b*-P3FT(y)**s comprise two distinct π-conjugated systems.

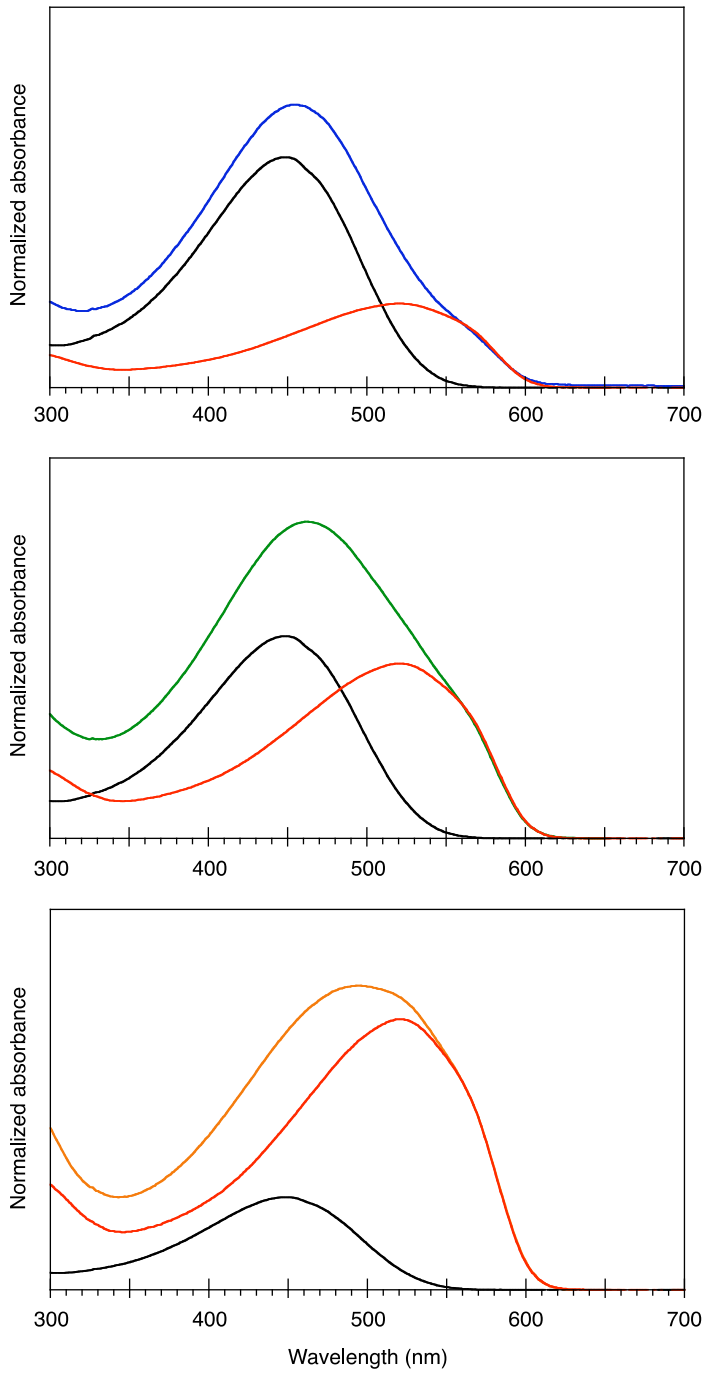

Figure 2-4. Absorption spectra of (blue) **P3HT(75)-*b*-P3FT(55)**, (green) **P3HT(55)-*b*-P3FT(45)**, and (orange) **P3HT(25)-*b*-P3FT(75)**, which can be deconvoluted into the absorption spectra of **P3HT** (black) and **P3FT** (red).

Photophysical Properties. We next investigated the photophysical properties of all the obtained block copolymers in detail. Figure 2-5 shows the fluorescence spectra of **P3HT** homopolymer, **P3HT-*b*-P3FT** with different block ratios, and **P3FT** homopolymer in chloroform at room temperature. **P3FT** shows different fluorescence as compared to that of **P3HT**. All the spectra were excited at 476 nm. Based on the absorption spectra, we can normalize the fluorescence intensities by the optical density (absorption) at 476 nm. We found that **P3FT** shower much higher intensity than that of **P3HT**, and the fluorescence intensity of the block polymers gradually enhanced with increasing the **P3FT** block ration.

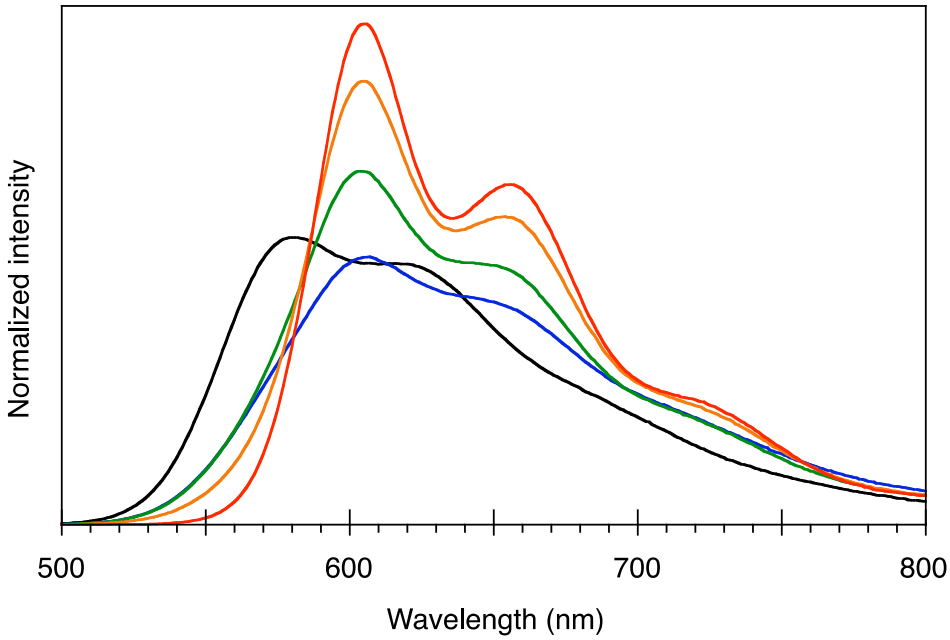

Figure 2-5. Fluorescence spectra of **P3HT** (black), **P3HT(75)-*b*-P3FT(25)** (blue), **P3HT(55)-*b*-P3FT(45)** (green), **P3HT(25)-*b*-P3FT(75)** (orange), and **P3FT** (red) in $CHCl_3$. The spectra were obtained with an excitation wavelength of 476 nm, and then, the intensities were normalized by the optical density at 476 nm.

The photophysical data of **P3HT(x)-*b*-P3FT(y)** was summarized in Table 2-1. It can be clearly observed that the absorption spectral maxima were shifted from 452 nm of **P3HT(75)-*b*-P3FT(25)** and 460 nm of **P3HT(55)-*b*-P3FT(45)** to 505 nm of **P3HT(25)-*b*-P3FT(75)** in chloroform. However, the absorption spectral maxima of those block copolymers in film state were shifted from 505 nm to 499 nm to 480 nm due to that the distinct absorption spectra of **P3HT** in solution and film state. In the contrast, the fluorescence spectra for the mentioned three block copolymers are more or less the same.

Table 2-1. Photophysical data of of **P3HT(x)-*b*-P3FT(y)**

Compd.	Molar ratio[b]	λ_{abs} [nm]	λ_{em} [nm]	Φ	M_n[a] (kg/mol)	PDI[a]
P3HT-*b*-P3FT	75:25				11	1.17
sol.		452	607	0.26		
film		505	659	0.01		
P3HT-*b*-P3FT	55:45				0.9	1.2
sol.		460	604	0.32		
film		499	664	0.03		
P3HT-*b*-P3FT	25:75				12	1.2
sol.		505	605	0.30		
film		482	655	0.03		

[a] The M_n and PDI were determined by GPC by using polystyrene as a standard, judging from the ^{1}H-NMR and absorption spectroscopic data, the M_ns of **P3FT** determined by polystyrene calibration seem to be underestimated; [b] the molar ratios were determined by ^{1}H-NMR.

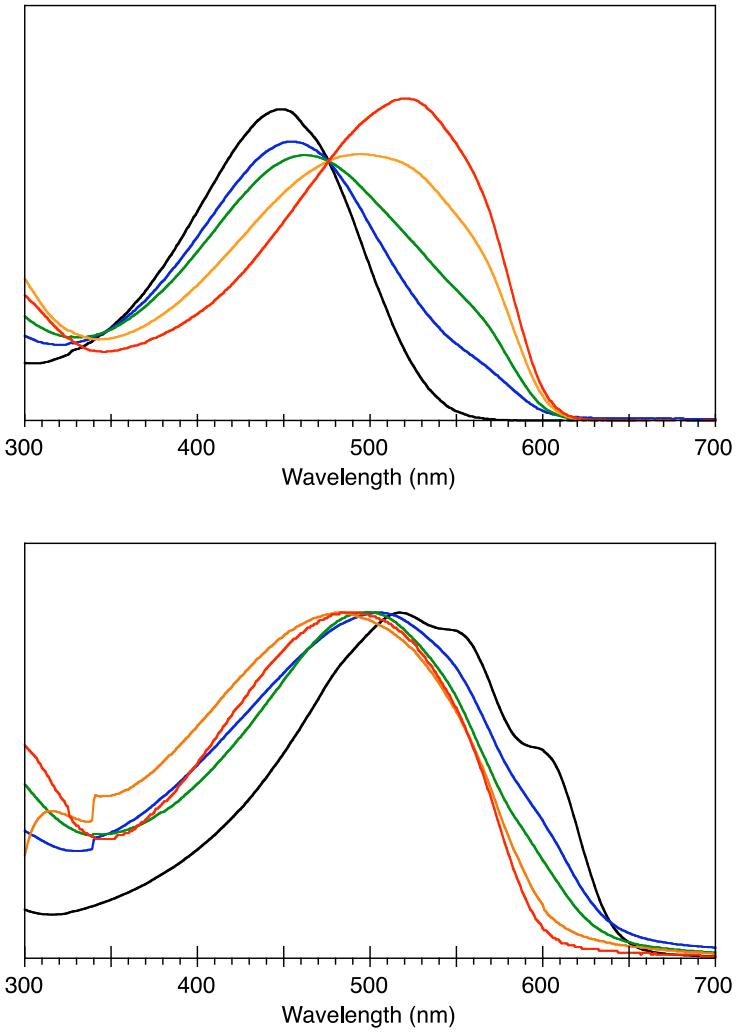

Figure 2-6. Absorption spectra of **P3HT** (black), **P3HT(75)-*b*-P3FT(25)** (blue), **P3HT(55)-*b*-P3FT(45)** (green), **P3HT(25)-*b*-P3FT(75)** (orange), **P3FT** (red) in solution (upper panel) and in their film forms (lower panel).

Thin Film Properties. Upon spin-coating, the absorption spectra of **P3HT-*b*-P3FT** changed significantly (Figures 2-6). Given that the absorption spectrum of **P3FT** is insensitive to film formation (Figure 1-7, Chapter 1), the observed spectral change indicates the π–π stacking formation of the **P3HT** block. The onset (650 nm) and shoulder (600 nm) of the absorption spectra of **P3HT-*b*-P3FT** indeed correspond with those of **P3HT** in its film form. It is noteworthy that these **P3HT-*b*-P3FT** films were still fluorescent as compared to **P3PhT**, and **P3HT-*b*-P3PhT** films (Figure 2-7).

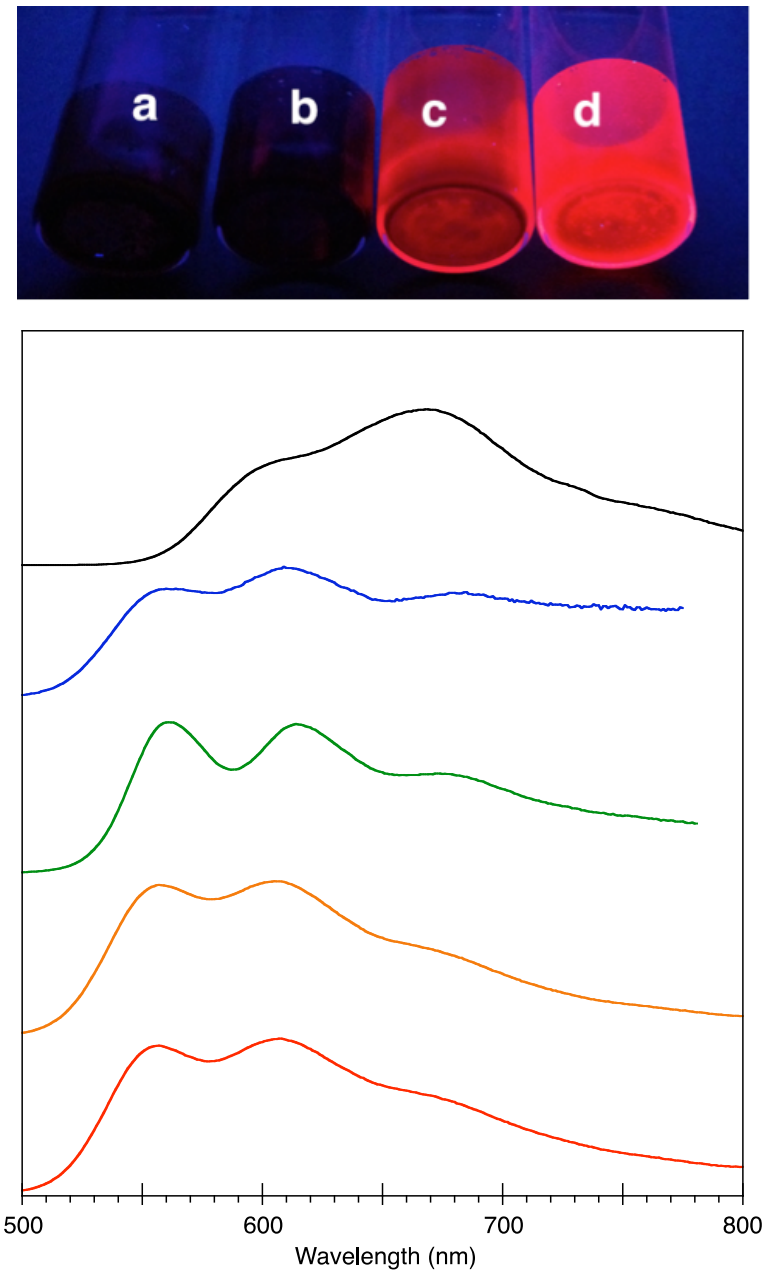

Figure 2-7. (upper panel) Photographs of film states of (a) **P3PhT**, (b) **P3HT(50)-*b*-P3PhT(50)**, (c) **P3HT(55)-*b*-P3FT(45)** and **P3FT**, which were taken under UV irradiation at 365 nm; the polymer solutions were dried in glass vials and the films were formed at the bottom of the vials. (lower panel) fluorescence spectra of **P3HT** (black), **P3HT(75)-*b*-P3FT(25)** (blue), **P3HT(55)-*b*-P3FT(45)** (green), **P3HT(25)-*b*-P3FT(75)** (orange), **P3FT** (red) in their film forms (λ_{ex} = 490 nm).

The spin-coated film of **P3HT-*b*-P3FT** on a silicon substrate was investigated by atomic force microscopy (AFM) after solvent annealing. Although **P3HT(55)-*b*-P3FT(45)** and **P3HT(25)-*b*-P3FT(75)** (with lower **P3HT** contents) did not show any particular morphology (data not shown), **P3HT(75)-*b*-P3FT(25)** exhibited microphase separation resulting in a worm-like structure of width of approximately 15 nm (Figure 2-8b). Physical blending of **P3HT** and **P3FT** did not result in well-defined morphology (Figure 2-10). We could thus conclude that the driving force for the microphase separation is the π–π stacking of the **P3HT** block. Considering the larger girth and shorter length of the **P3FT** block relative to the **P3HT** block, the periodicity must have emerged from an interdigitated structure as shown in Figure 2-8c. To the best of our knowledge, this is the first example of microphase separation of all-conjugated diblock copolymers in which one block is stacked and the other is isolated.

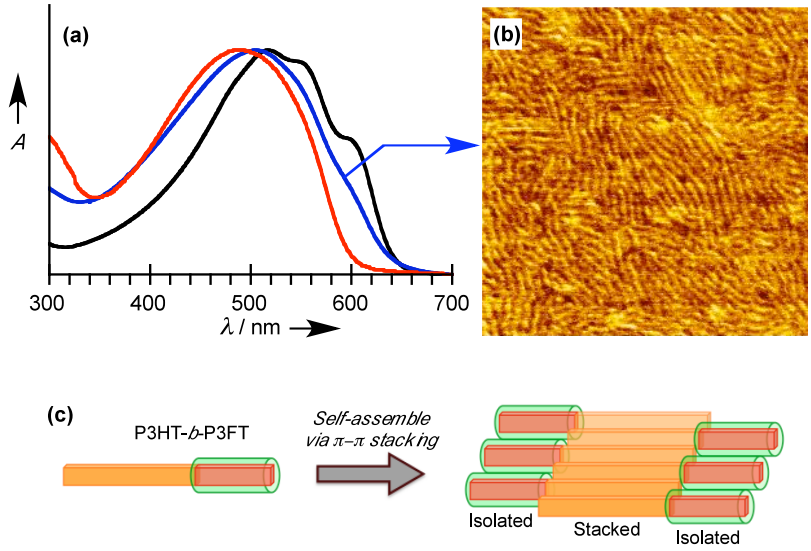

Figure 2-8. (a) Normalized absorption spectra of **P3HT** (black), **P3FT** (red), and **P3HT(75)-*b*-P3FT(25)** (blue) in their film forms. (b) AFM image of microphase separation of **P3HT(75)-*b*-P3FT(25)** (700 nm × 700 nm.(c) illustration of the plausible self-assembled structure.

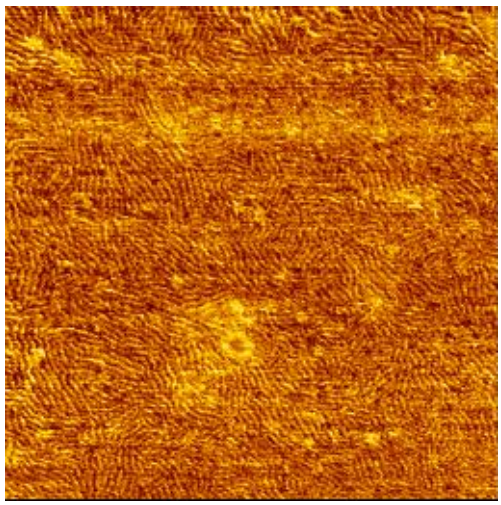

Figure 2-9. AFM phase image of **P3HT(75)-*b*-P3FT(25)** in large area; 1.5 μm x 1.5 μm.

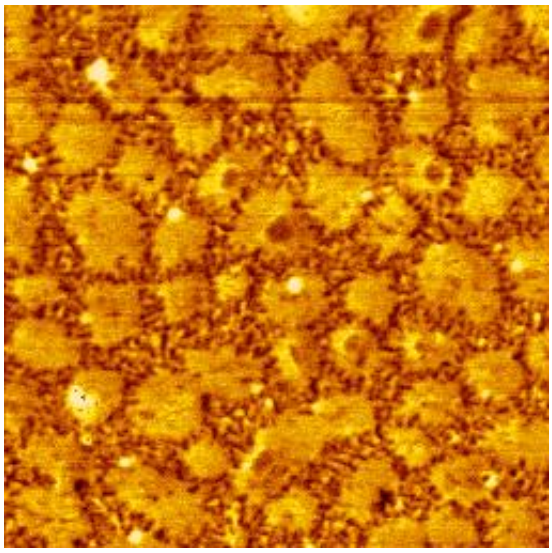

Figure 2-10. AFM phase image of a blended film of **P3HT** and **P3FT**; 75:25 mol/mol blend ratio, 1.5 μm x 1.5 μm.

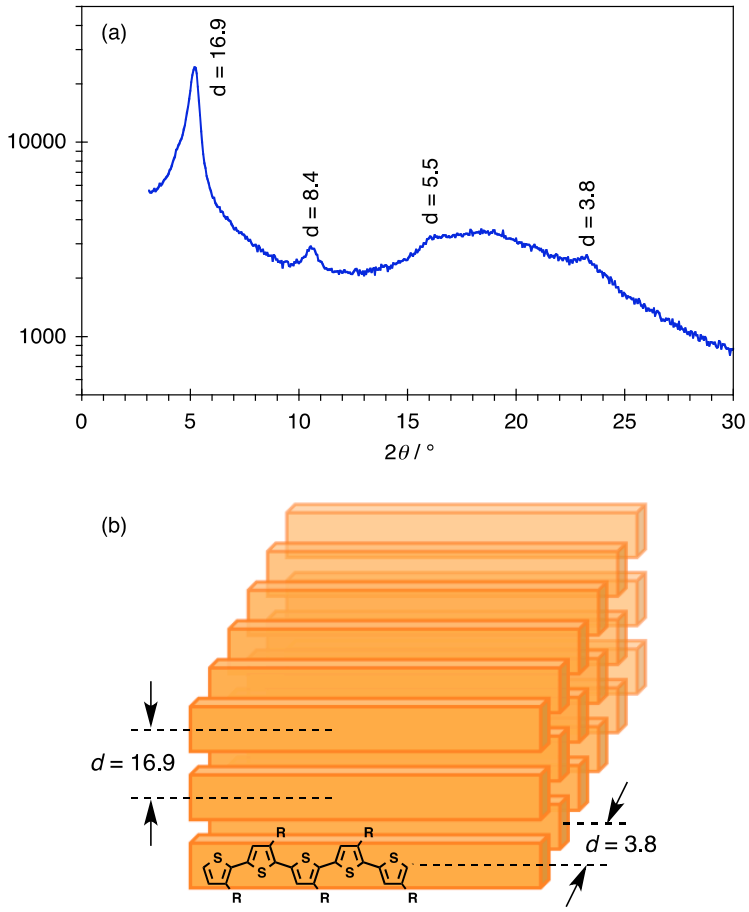

Figure 2-11. (a) Wide-angle X-ray diffraction of **P3HT(75)-*b*-P3FT(25)**. (b) Schematic representation of crystalline lamellar structure of **P3HT** domain.

We carried out wide-angle X-ray diffraction measurement of **P3HT(75)-*b*-P3FT(25)** in the film state. Polymer was firstly dissolved in chloroform and drop-casted to the silicon substrate to form thick polymer films. The film was solvent annealed in chlorobenzene vapor for 12 hours and dried under vacuum. The result obtained from the XRD measurement is displayed in Figure 2-11. Peaks at the 2θ angle of 5.2 (d = 16.9 Å), 10.6 (d = 8.4 Å), 16.1 (d = 5.5 Å) correspond to first-, second-, and third-order reflections from (100), (200), and (300) planes of crystalline **P3HT**, respectively. Peak at the 2θ angle of 23.3 (d = 3.8 Å) corresponds to π–π stacking distance. In the schematic representation of crystalline lamellar structure of **P3HT** domain: for clarity, **P3FT** domain is not shown. These periodicities are consistent with those reported in the literatures of **P3HT**-based all conjugated block copolymers.[9]

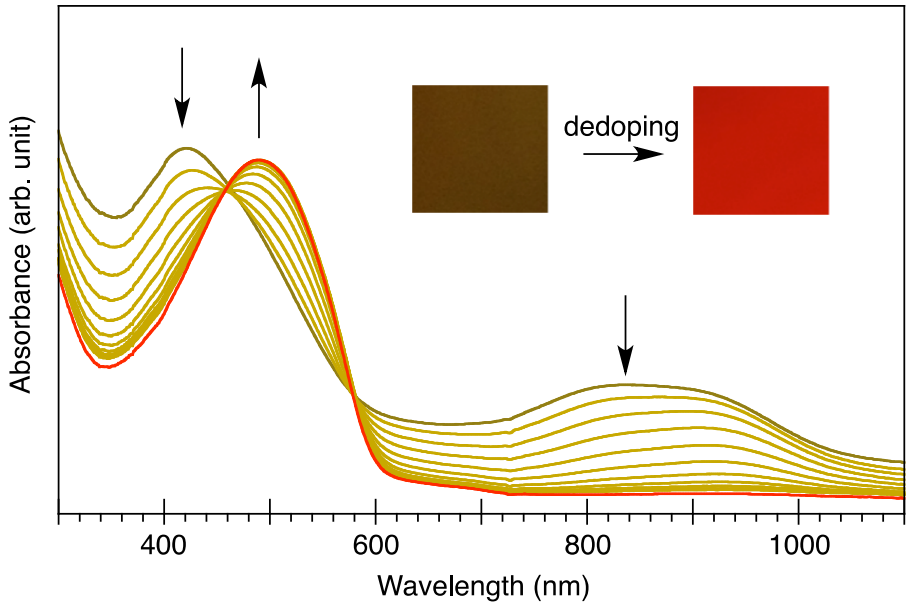

Figure 2-12. UV/vis/NIR absorption spectral changes of the I_2 doped **P3FT** film observed during the exhalation of I_2 from the film.

Polythiophene films can be doped with iodine vapor. Interestingly, doped **P3FT** films are readily de-doped to their neutral undoped states within a few seconds once they are taken out from the iodine vapor atmosphere (Figure 2-12). The doping/de-doping process of **P3FT** occurs quickly and reversibly, presumably due to the absence of the π–π stacking that stabilizes the charge carriers.[11] The changes in absorption spectra of **P3FT** induced by doping/de-doping are accompanied by isosbestic points, whose presence can be attributed to the neutral/polaron equilibrium (Figure 2-12). The spectral change was taken in a sealed sample compartment, otherwise the process occurs too quickly to be monitored. The inset picture shows the color change upon de-doping.

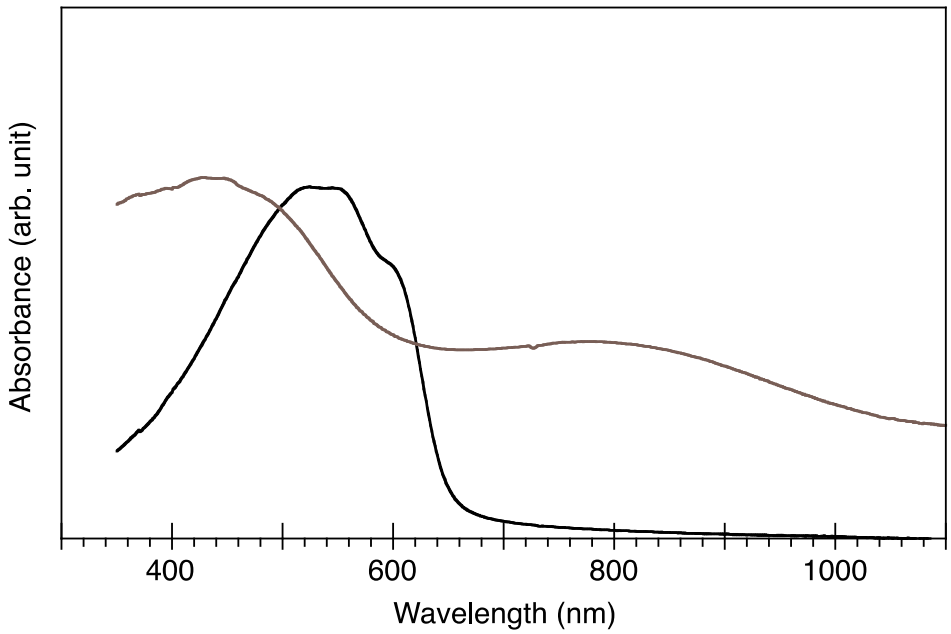

Figure 2-13. UV/vis/NIR absorption spectra of **P3HT** in neutral state (black line) and doped state (dark brown line).

As is well known, in contrast to **P3FT**, the doped state of **P3HT** is stable and electronically conductive (Figure 2-13). By taking advantage of the difference in the kinetic stabilities of the respective doped states of **P3HT** and **P3FT**, one can selectively dope the **P3HT** domain in a microphase separation. Consequently, the absorption spectrum of the iodine-doped **P3HT-*b*-P3FT** film consists of the summation of spectra of doped **P3HT** and neutral **P3FT** (Figure 2-14).

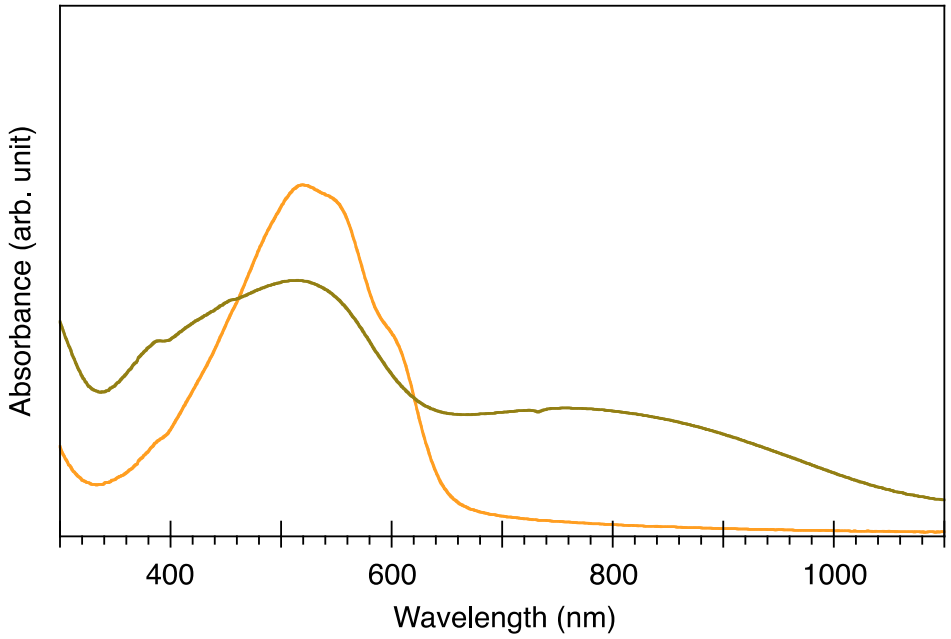

Figure 2-14. UV/vis/NIR absorption spectra of the **P3HT(75)-*b*-P3FT(25)** before (orange) and after doping with I_2 vapor (gold).

It is worth to mention that the conductivity of the film of **P3HT(75)-*b*-P3FT(25)** was 0.5 S/cm, which was comparable to that of **P3HT** (0.7 S/cm) measured under the same conditions. Given that the **P3FT** domain in the doped **P3HT-*b*-P3FT** film is not electronically conductive, the ~28% decrease in the conductivity of **P3HT-*b*-P3FT** relative to the **P3HT** film is reasonable. Hence, we assert that the stacked **P3HT** domain provides a continuous carrier transport pathway in the MPSs of **P3HT-*b*-P3FT** films.[12]

CONCLUSION

We have synthesized all-polythiophene diblock copolymer, in which one block is naked and the other is fenced. The naked **P3HT** block self-assembles through π–π stacking, thereby inducing microphase separation. As a consequence, we have succeeded, for the first time, in creating a microphase separation comprising an ensemble of stacked and isolated polythiophenes. We believe that such a sophisticated control over π–π stacking in a polymeric thin film will extend the use of these materials into various unprecedented applications owing to the synergy of the contrasting properties of the two blocks.

EXPERIMENTAL SECTION

General procedure of synthesizing block copolymers:[13,14] Since all the experiments of synthesizing block copolymers were conducted in the same manner, only the polymerization of **P3HT(55)-*b*-P3FT(45)** is described as follows: 2-bromo-3-hexyl-5-iodothiophene (347.3 mg, 0.93 mmol) was placed in flask A under argon, and then evacuated and back-filled with argon three times. After adding dry THF (10 ml) into the flask via a syringe, the solution was mixed at 0 °C. 2 mol/L solution of *i*-PrMgCl in THF (0.49 ml, 0.98 mmol) was added via a syringe, and the mixture was stirred at 0 °C for 30 min (solution A). In the second vial B, monomer **1.1** (275 mg, 0.43 mmol) was reacted with *i*-PrMgCl (0.24 ml, 0.47 mmol) in the same manner (solution B, THF with 0.5 M LiCl) at room temperature for 2 hours. Solution A was heated up to 35 °C and then injected to a prepared flask with Ni(dppp)Cl_2 catalyst (8.20 mg, 0.015 mmol). After stirring for 1 h, an aliquot of solution (2 ml) was withdrawn and injected to solution B via a syringe, and the resulting solution was stirred for 12 h at 65 °C. The reaction was quenched 5 M HCl. The crude polymer was extracted using $CHCl_3$ and dried over $MgSO_4$. The solvent was removed by evaporation to give a red solid as crude product, the solid was purified by precipitation using THF/acetone mixture and collected by centrifugation (6000 rpm, 90 min), **P3HT-*b*-P3FT** was obtained as a dark red solid. Yield (calculated based on the monomer **1.1**) is ranging from 10 % to 30 %.

P3HT (75)-*b*-P3FT (25): M_n = 11 K, PDI = 1.17. ^{1}H NMR ($CDCl_3$, 400 MHz, TMS, 298 K): δ 0.85–0.93 (m, 15H), 1.26–1.35 (m, 28H), 1.42–1.44 (m, 6H), 1.67–1.72 (m, 6H), 2.46 (m, 4H), 2.79–2.82 (m, 6 H), 5.83 (s, 1H), 6.59 (d, J = 7.6 Hz, 4H), 6.79 (d, J = 7.6 Hz, 4H), 6.98 (s, 3H), 7.16 (d, J = 7.2 Hz, 2H), 7.34 (t, J = 7.2 Hz, 1H).

P3HT (55)-*b*-P3FT (45): M_n = 0.9 K, PDI = 1.2. ^{1}H NMR (400 MHz, $CDCl_3$, TMS, 298 K): δ 0.85–0.91 (m, 9.66H), 1.27–1.34 (m, 20.88H), 1.44 (m, 2.44H), 1.69–1.71 (m, 2.44H), 2.46 (m, 4H), 2.80 (m, 2.44 H), 5.84 (s, 1H), 6.59-6.60 (m, 4H), 5.79-6.80 (m, 4H), 6.98 (s, 1.22 H), 7.16 (d, J = 7.2 Hz, 2H), 7.34 (t, J = 7.2 Hz, 1H). ^{13}C NMR (400 MHz, $CDCl_3$): δ 14.11, 22.69, 29.30, 29.45, 29.69, 30.50, 31.44, 31.68, 31.84, 35.82, 127.38, 127.72, 128.59, 128.76, 129.28, 132.61, 133.14, 138.36, 139.88, 140.49, 142.39.

P3HT (25)-*b*-P3FT (75): M_n = 12 K, PDI = 1.2. ^{1}H NMR ($CDCl_3$, 400 MHz, TMS, 298 K): δ 0.85–0.91 (m, 7H), 1.26–1.33 (m, 17.32H), 1.42 (m, 0.66H), 1.69–1.70 (m, 0.66H), 2.46 (m, 4H), 2.79–2.80 (m, 0.66H), 5.83 (s, 1H), 6.59 (d, J = 7.6 Hz, 4H), 6.79 (d, J = 7.2 Hz, 4H), 6.98 (s, 1H), 7.16 (d, J = 7.2 Hz, 2H), 7.34 (t, J = 7.2 Hz, 1H).

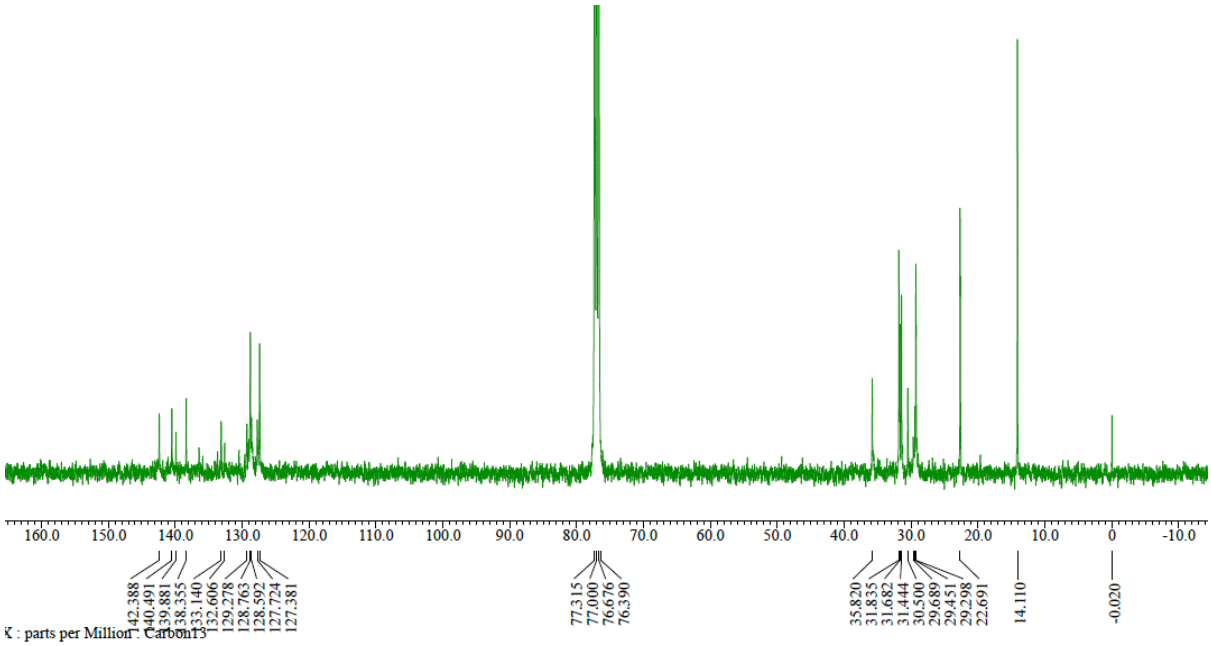

^{13}C NMR Spectrum of **P3HT-*b*-P3FT** (55:45) (^{1}H-NMR is shown in Figure 2-2)

The monomer, **P3PhT** and **P3HT-*b*-P3PhT** were prepared according to the previously reported procedures.[14]

P3PhT: M_n = 3.8 K, PDI = 1.5. ^{1}H NMR (CD_2Cl_2, 400 MHz, TMS, 298 K): δ 0.84–0.87 (m, 3H), 1.24–1.28 (m, 6H), 1.58–1.59 (m, 2H), 2.58–2.61 (m, 2H), 6.79 (s, 1H), 7.09–7.29 (m, 4H).

P3HT-*b*-P3PhT: M_n = 16 K, PDI = 1.4. ^{1}H NMR ($CDCl_3$, 400 MHz, TMS, 298 K): δ 0.85–0.93 (m, 6H), 1.30–1.44 (m, 10H), 1.42–1.44 (m, 2H), 1.58–1.63 (m, 2H), 1.67–1.72 (m, 2H), 2.61 (t, J = 7.8 Hz, 2H), 2.80 (t, J = 7.8 Hz, 2H), 6.78 (s, 1H), 7.00 (s, 1H), 7.14–7.16 (m, 2H), 7.21–7.24 (m, 2H).

REFERENCES

[1] *Handbook of Conducting Polymers, Conjugated Polymers* (Eds.: T. A. Skotheim, J. R. Reynolds), CRC, Boca Raton, **2007**

[2] H. Sirringhaus, P. J. Brown, R. H. Friend, M. M. Nielsen, K. Bechgaard, B. M. W. Langeveld-Voss, A. J. H. Spiering, R. A. J. Janssen, E. W. Meijer, P. Herwig, D. M. de Leeuw, *Nature* **1999**, *401*, 685.

[3] Reviews see: a) M. J. Frampton, H. L. Anderson, *Angew. Chem.* **2007**, *119*, 1046; *Angew. Chem. Int. Ed.* **2007**, *46*, 1028; b) D. J. Cardin, *Adv. Mater.* **2002**, *14*, 553; c) J. Terao, *Polym. Chem.* **2011**, *2*, 2444; d) T. M. Swager, *Acc. Chem. Res.* **2008**, *41*, 1181.

[4] a) Recent selected examples of isolated CPs, see: a) F. Cacialli, J. S. Wilson, J. J. Michels, C. Daniel, C. Silva, R. H. Friend, N. Severin, P. Samorì, J. P. Rabe, M. J. O'Connell, P. N. Taylor, H. L. Anderson, *Nat. Mater.* **2002**, *1*, 160; b) J. Terao, S. Tsuda, Y. Tanaka, K. Okoshi, T. Fujihara, Y. Tsuji, N. Kambe, *J. Am. Chem. Soc.* **2009**, *131*, 16004; c) Y. Ie, A. Han, T. Otsubo, Y. Aso, *Chem. Commun.* **2009**, 3020; d) K. Sugiyasu, Y. Honsho, R. M. Harrison, A. Sato, T. Yasuda, S. Seki, M. Takeuchi, *J. Am. Chem. Soc.* **2010**, *132*, 14754; e) R. Shomura, K. Sugiyasu, T. Yasuda, A. Sato, M. Takeuchi, *Macromolecules* **2012**, *45*, 3759; f) C. Pan, K. Sugiyasu, Y. Wakayama, A. Sato, M. Takeuchi, *Angew. Chem.* **2013**, *125*, 10975; *Angew. Chem. Int. Ed.* **2013**, *52*, 10775.

[5] P. Samorì, F. Cacialli, H. L. Anderson, A. E. Rowan, *Adv. Mater.* **2006**, *18*, 1235.

[6] a) R. Ruiz, H. Kang, F. A. Detcheverry, E. Dobisz, D. S. Kercher, T. R. Albrecht, J. J. de Pablo, P. F. Nealey, *Science* **2008**, *321*, 936; b) S. N. Patel, A. E. Javier, K. M. Beers, J. A. Pople, V. Ho, R. A. Segalman, N. P. Balsara, *Nano Lett.* **2012**, *12*, 4901; c) H.-A. Klok, S. Lecommandoux, *Adv. Mater*. **2001**, *13*, 1217.

[7] a) A. Yokoyama, R. Miyakoshi, T. Yokozawa, *Macromolecules* **2004**, *37*, 1169; b) E. E. Sheina, J. Liu, M. C. Iovu, D. W. Laird, R. D. McCullough, *Macromolecules* **2004**, *37*, 3526; c) Z. J. Bryan, A. J. McNeil, *Macromolecules* **2013**, *46*, 8395, and references are cited therein.

[8] M. C. Stefan, M. P. Bhatt, P. Sista, H. D. Magurudeniya, *Polym. Chem*. **2012**, *3*, 1693.

[9] a) Y. Zhang, K. Tajima, K. Hirota, K. Hashimoto, *J. Am. Chem. Soc*. **2008**, *130*, 7812; b) Y. Zhang, K. Tajima, K. Hashimoto, *Macromolecules* **2009**, *42*, 7008; c) A. Yokoyama, A. Kato, R. Miyakoshi, T. Yokozawa, *Macromolecules* **2008**, *41*, 7271; d) J. Hollinger, A. A. Jahnke, N. Coombs, D. S. Seferos, *J. Am. Chem. Soc*. **2010**, *132*, 8546; e) D. Gao, J. Hollinger, D. S. Seferos, *ACS Nano* **2012**, *6*, 7114; f) X. Yu, H. Yang, S. Wu, Y. Geng, Y. Han, *Macromolecules* **2012**, *45*, 266; g) M. Sommer, H. Komber, S. Huettner, R. Mulherin, P. Kohn, N. C. Greenham, W. T. S. Huck, *Macromolecules* **2012**, *45*, 4142; h) T. Higashihara, K. Ohshimizu, Y. Ryo, T. Sakurai, A. Takahashi, S. Nojima, M. Ree, M. Ueda, *Polymer* **2011**, *52*, 3687; i) J. Ge, M. He, F. Qiu, Y. Yang, *Macromolecules* **2010**, *43*, 6422; j) C.-C. Ho, Y.-C. Liu, S.-H. Lin, W.-S. Su, *Macromolecules* **2012**, *45*, 813; k) E. F. Palermo, A. J. McNeil, *Macromolecules* **2012**, *45*, 5948.

[10] Although p-type/n-type diblock copolymer has not yet been synthesized soley through CTP method, the CTP combined with step-growth polymerization can provide such a new type of functional polymers; see: a) D. Izuhara, T. M. Swager, *Macromolecules* **2011**, *44*, 2678; b) S.-Y. Ku, M. A. Brady, N. D. Treat, J. E. Cochran, M. J. Robb, E. J. Kramer, M. L. Chabinyc, C. J. Hawker, *J. Am. Chem. Soc.* **2012**, *134*, 16040; c) M. J. Robb, S.-Y. Ku, C. J. Hawker, *Adv. Mater.* **2013**, *25*, 5686.

[11] R. Österbacka, C. P. An, X. M. Jiang, Z. V. Vardeny, *Science* **2000**, *287*, 839, and 4c.

[12] In fact, several groups reported that polythiophene-based MPSs showed even better charge carrier mobility than polythiophene films, which was attributed to the homogeneous film morphologies, see: a) X. Yu, K. Xiao, J. Chen, N. K. Lavrik, K. Hong, B. G. Sumpter, D. B. Geohegan, *ACS Nano* **2011**, *5*, 3559; b) W.-C. Chen, Y.-H. Lee, C.-Y. Chen, K.-C. Kau, L.-Y. Lin, C.-A. Dai, C.-G. Wu, K.-C. Ho, J.-K. Wang, L. Wang, *ACS Nano* **2014**, *8*, 1254.

[13] R. Miyakoshi, A. Yokoyama, T. Yokozawa, *J. Am. Chem. Soc.* **2005**, *127*, 17542.

[14] T. W. Holcombe, C. H. Woo, D. F. J. Kavulak, B. C. Thompson, J. M. J. Fréchet, *J. Am. Chem. Soc.* **2009**, *131*, 14160.

Chapter 3

Thermoplastic Fluorescent Conjugated Polymers: Benefits of Preventing π−π Stacking

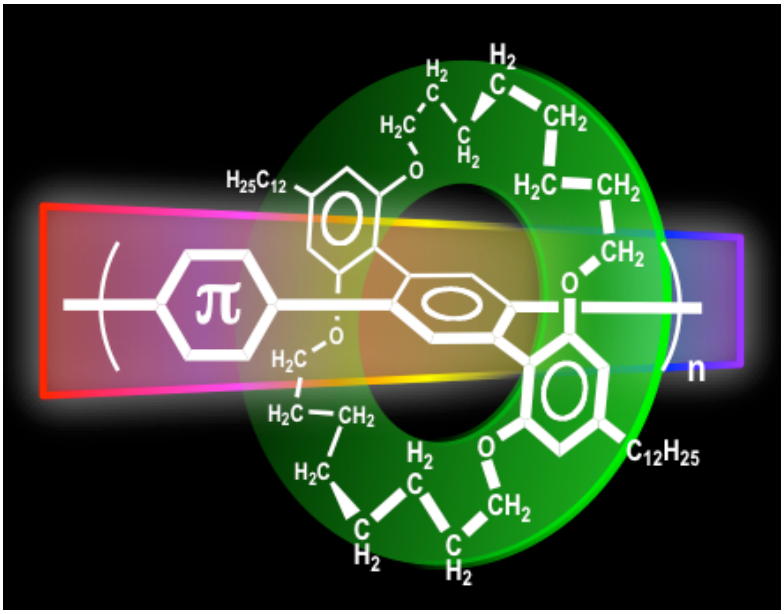

ABSTRACT: *Fluorescent conjugated polymers that are sheathed within their own cyclic side chains have been synthesized. Owing to the unique three-dimensional architecture, the polymers are light-emissive, even in the film state, miscible, allowing the combination of various fluorescence colors, and thermoformable, like conventional plastics.*

INTRODUCTION

Organic materials that emit colorful fluorescence in condensed phases such as solids (crystals, thin films, or glasses),[1–5] liquid crystals,[6] and liquids[7] are useful for various applications ranging from organic light-emitting diodes and wavelength-tunable lasers to ultrasensitive sensors. Under these extremely concentrated conditions, however, photophysical processes are rather complex involving energy migration/transfer, charge separation, self-absorption and excimer formation, which often give rise to low fluorescence quantum yields (Φ_F).[8] Therefore, rational molecular designs are essential, and inevitably, the intermolecular interactions in the condensed phases that govern these nonradiative decay processes need to be taken into consideration.

Among fluorescent organic materials, CPs are attractive for organic optoelectronic applications owing to their distinguishing mechanical properties, processability, and electronic conductivity. In fact, CPs have been key materials in the field of organic optoelectronics.[9] An effective strategy for attaining solid-state emissive CPs is to isolate the π-conjugated backbone and inhibit interpolymer interactions.[3–5] For example, Swager et al.[3] have created a variety of highly emissive CPs that have rigid protecting frameworks such as triptycenes, and Anderson et al.[4] have exploited polyrotaxane-type CPs, i.e., CPs that are sheathed by many CDs. In addition to these pioneering researches, some so-called IMWs were found to be emissive even in the solid state due to the absence of π–π stacking interactions; $\Phi_{F(film)}$ values of the IMWs in the literature are in the range of 4–62% and are generally around 10–20%.[3–5] However, conjugated systems have been limited to mostly poly(phenylene ethynylene) and polyphenylene systems, and accordingly, the hues of the fluorescence are still insufficient for filling the entire visible spectrum. This shortcoming behind small molecular fluorophores[1] arises mainly from the difficulty in designing and synthesizing IMWs in which three-dimensional architectures are equipped along the one-dimensional polymer backbones.

In this chapter, we introduce a new monomer, which is readily available and versatile, for producing a variety of IMWs. Our IMWs are intriguing not only from a photophysical point of view but because of their physical properties as polymeric materials; the polymers are miscible and thermoformable which are less developed properties with respect to CPs. All of the unique properties are a result of the absence of π-π stacking, and we describe the structure–property relationships of these IMWs.

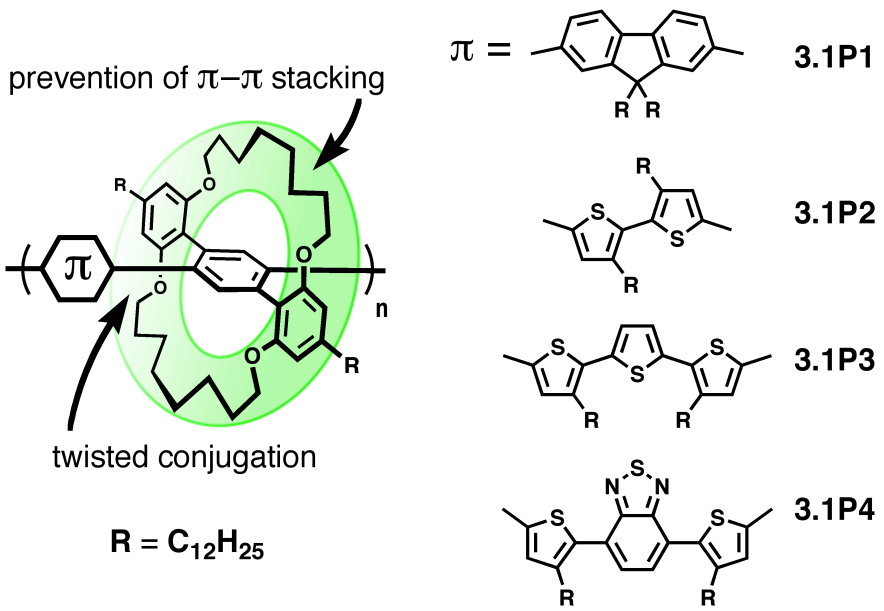

Figure 3-1. Chemical structures of the CPs studied in this chapter.

RESULTS AND DISCUSSION

Synthesis of the Monomers and Polymers. On the basis of our previous reports on thiophene-based IMWs,[10] new monomers **3M1** and **3M1H** were synthesized through five well-established reaction steps with a total yield of over 80% (Scheme 3-1). The double ring closing metathesis (RCM) reaction is a key step in producing the three-dimensional architecture;[11] notably, this double RCM is so efficient, even without highly diluted conditions, that all the steps are scalable to a multiple gram reaction scale. The X-ray crystal structure of **3M1H** gives clear evidence of the cyclic structure in which the 1,4-dibromobenzene monomer is isolated while leaving the terminal bromide groups for further modification and polymerization (**Figure 3-2**). Starting from monomer **3M1** (having solubilizing dodecyl chains), four kinds of IMWs were synthesized through Suzuki–Miyaura, Yamamoto, or Stille coupling reactions (i.e., **3.1P1** to **3.1P4**, Scheme 3-2). In this study, thiophene-based polymers were mainly developed (**3.1P2**, **3.1P3**, and **3.1P4**) because the installation of thiophene effectively influences the HOMO–LUMO gaps, and thus, various fluorescence colors can be realized.[12] All of the polymers are highly soluble in common organic solvents, and the molecular weights were determined by gel permeation chromatography (GPC) using a polystyrene standard (Figure 3-3 and Table 3-1). The repeating units are analogous to a tetra-aryl benzene scaffold that poses a propeller-like conformation,[13] thereby twisting the conjugated backbone. We expect that the exciton is confined not only intermolecularly (by the sheath) but also intramolecularly (by the twisting), which can limit energy migration and lead to high $\Phi_{F(film)}$.[14]

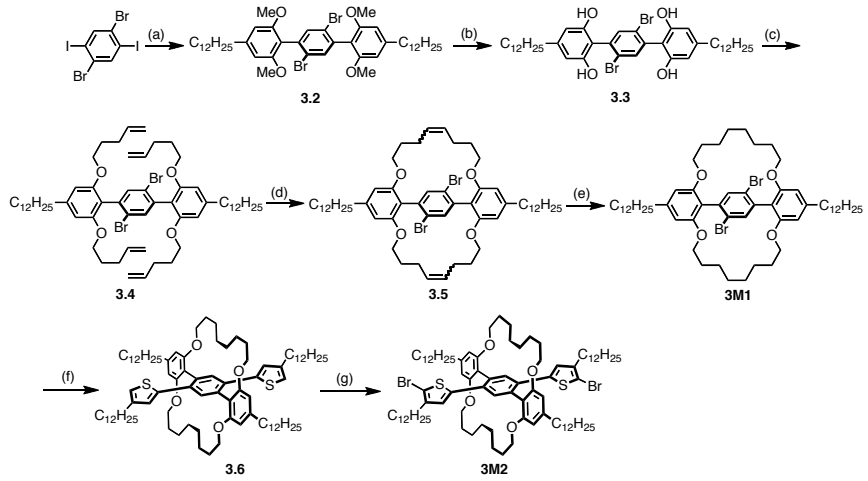

Scheme 3-1. Synthetic route of monomers **3M1** and **3M2**: (a) $ArB(OH)_2$, $Pd(PPh_3)_4$, Na_2CO_3, Toluene, EtOH, H_2O, reflux; (b) BBr_3, DCM, RT; (c) 5-Bromo-1-pentene, Cs_2CO_3, DMSO, 100 ^oC; (d) second generation Grubbs catalyst, DCM, reflux; (e) Wilkinson's catalyst, THF, *t*-BuOH, H_2, 40 ^oC; (f) 3-dodecylthiophene-2-boronic acid pinacol ester, $Pd(PPh_3)_4$, K_2CO_3, dioxane, H_2O, 120 ^oC, overnight; (g) NBS, THF, r.t., 2h.

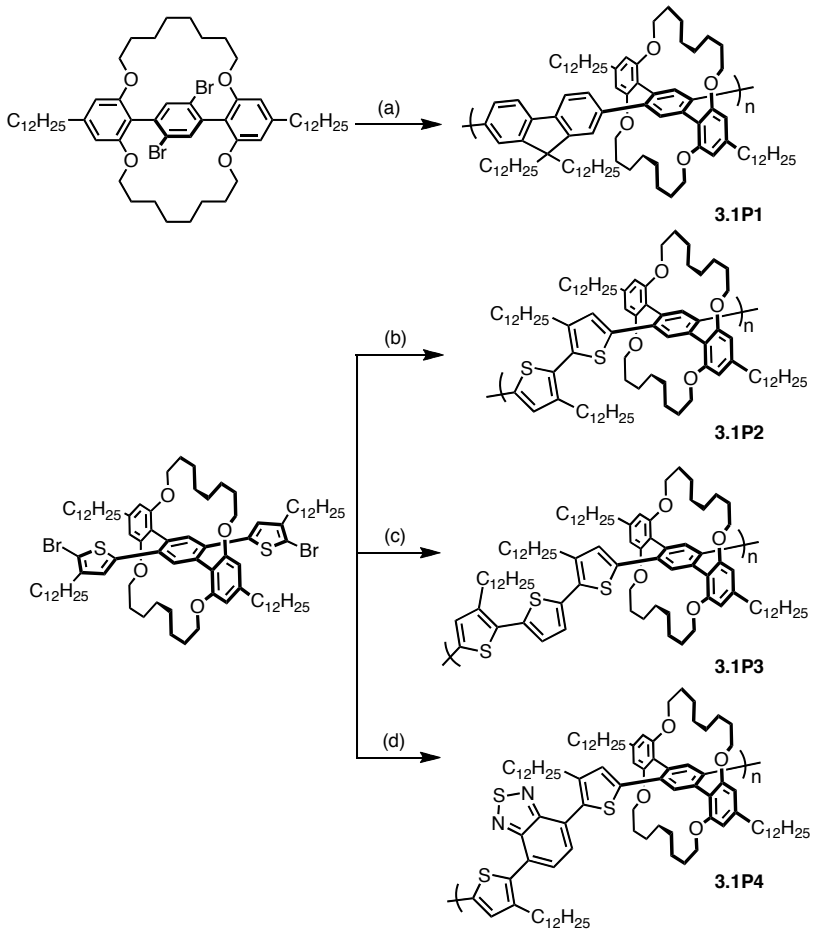

Scheme 3-2. Synthetic route of the polymers: (a) 9, 9-dioctylfluorene-2, 7-diboronic acid bispinacol ester, $Pd(PPh_3)_4$, Aliquat 336, potassium carbonate (2 M), toluene, 105 ^oC; (b) $Ni(COD)_2$, 2, 2'-bipyridyl, COD, toluene, DMF; (c)2,5-Bis(trimethylstannyl)thiophene, $Pd_2(dba)_3$, $P(o\text{-}tol)_3$,toluene; (d) 2,1,3-Benzothiadiazole-4,7-bis(boronicacid pinacol ester), $Pd(PPh_3)_4$, Aliquat 336, potassium carbonate (2 M), toluene, 105 ^oC.

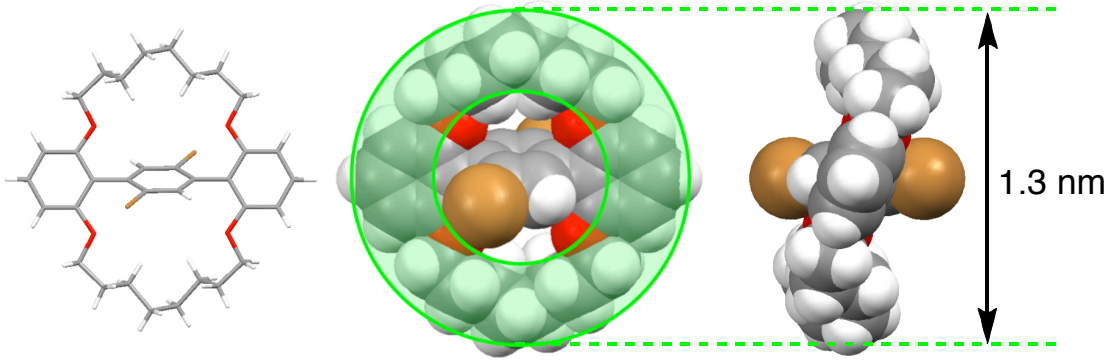

Figure 3-2. Axial (left and middle) and lateral (right) views of **3M1H** in crystallized form.

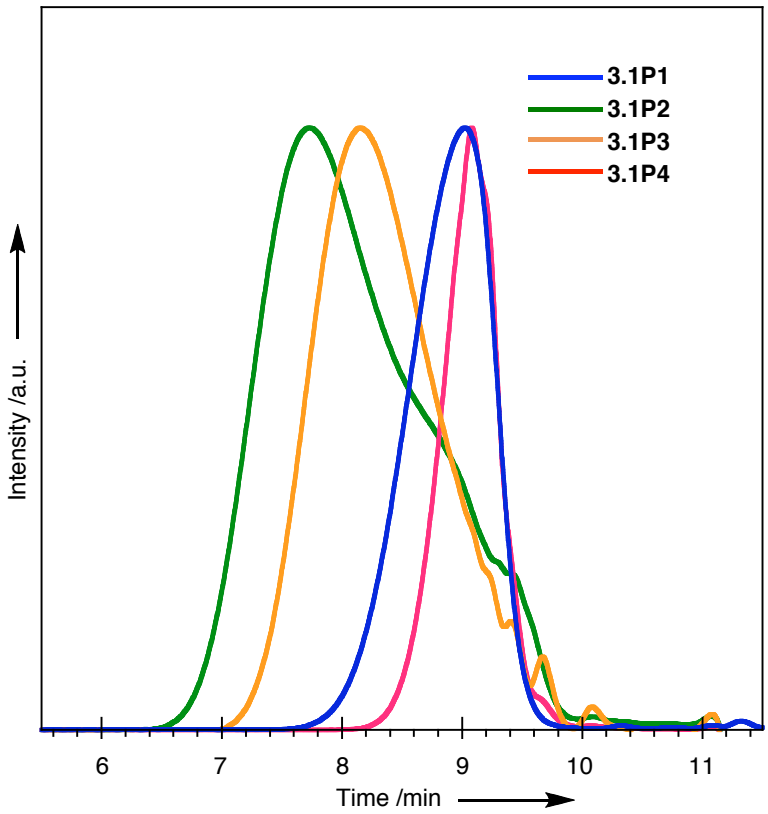

Figure 3-3. GPC chromatogram of polymers **3.1P1**, **3.1P2**, **3.1P3**, and **3.1P4**.

Table 3-1. Summary of the copolymers.

Polymers	M_n	PDI
3.1P1	10.6 K	1.3
3.1P2	22.6 K	2.9
3.1P3	21.2 K	1.8
3.1P4	8.4 K	1.2

Photophysical Properties of the Polymers. In general, CPs show significant absorption and fluorescence spectral changes upon film formation due to the interpolymer interactions.[15] In contrast, the spectra of our polymers in both solution and film form are quite similar (Figure 3-4). Small peak shifts, for which we could not ascribe to any particular feature of the family, are probably due to solvent effects and/or a restriction of the conformational motion in the solid films. These results indicate that the cyclic side chains can effectively prevent the conjugated backbone from π–π stacking. The fluorescence colors of **3.1P1**, **3.2P2**, **3.3P3**, and **3.4P4** were violet, green, yellow, and red, respectively; that is, the primary colors plus yellow (Y). All of the polymers showed relatively large Stokes shifts thought to be due to the twisted backbone, which is advantageous for attaining high $\Phi_{F(film)}$ values by limiting self-absorption and energy migrations. The absolute quantum yields (Φ_F) and fluorescence lifetimes (τ) of these polymers in solution and film form are summarized in Tables 1-2 and 1-3, respectively. **3.1P1** to **3.1P4** have moderate Φ_F values even in the film state, retaining roughly half the value of that determined in solution: see, ρ ($\Phi_{F(film)}/\Phi_{F(solution)}$) in Table 1-2.[16] These values are comparable with those of IMWs highlighted as solid-state emissive materials in the literature,[3–5] and the moderate $\Phi_{F(film)}$ values of the yellow (**3.1P3**) and red fluorescence (**3.1P4**), which are rare for IMWs, should be particularly noteworthy.

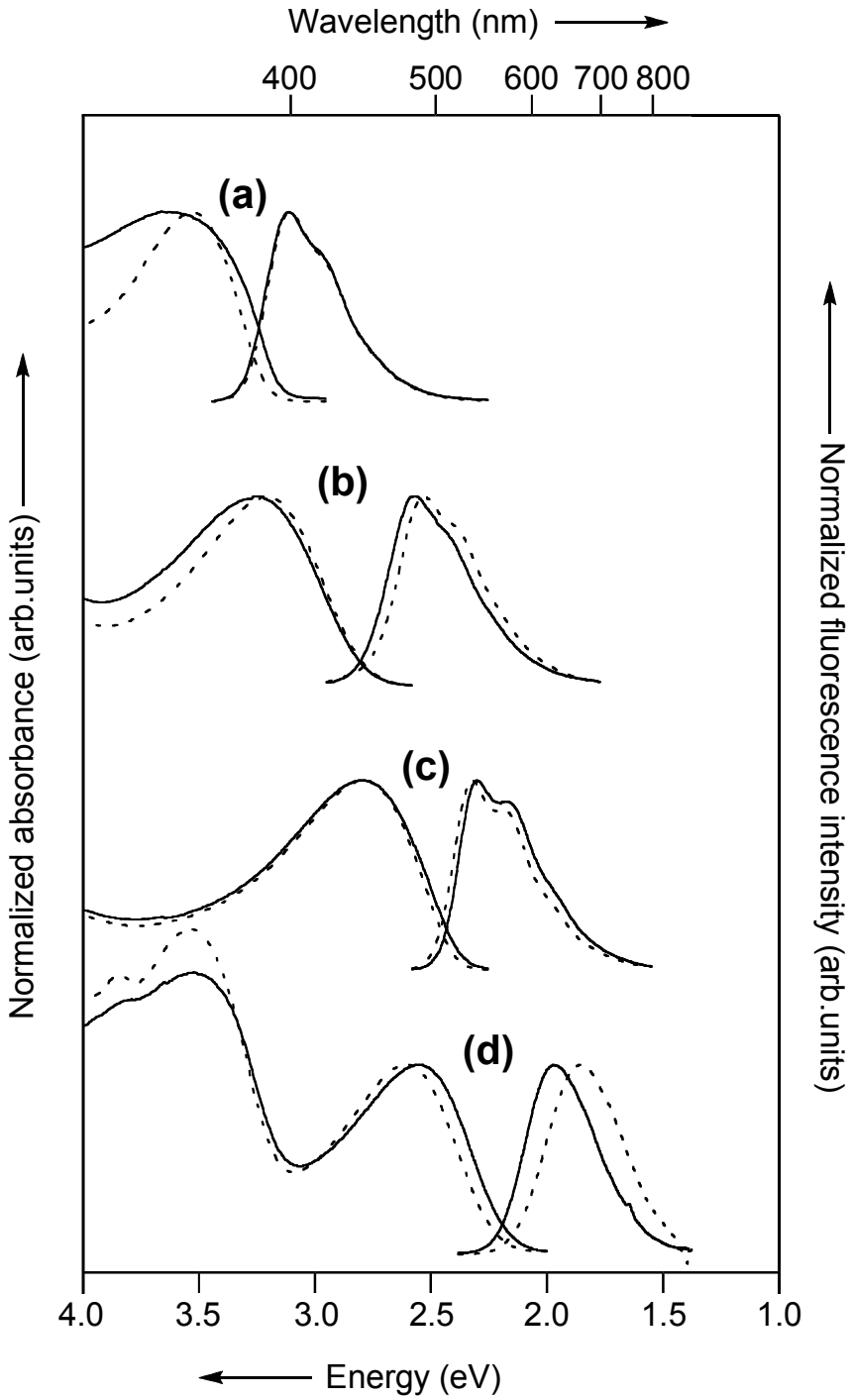

Figure 3-4. UV/Vis absorption (left) and fluorescence spectra (right: excited at the absorption maxima) of a) **3.1P1**, b) **3.1P2**, c) **3.1P3** and d) **3.1P4** in DCM (solid line) and drop-cast film form (dashed line).

Table 3-2. Photophysical data of the copolymers. [a]

Compd.		λ_{abs} [b] (logε) [nm]	λ_{em} [b] [nm]	Stokes shift [cm^{-1}]	Φ [c]	ρ: $\Phi_{F(film)}/\Phi_{F(solution)}$
3.1P1	sol.	351 (4.59)	399	3,430	0.92	0.48
	film	338	398	4,460	0.44	
3.1P2	sol.	386 (4.48)	490	5,500	0.16	0.75
	film	381	482	5,500	0.12	
3.1P3	sol.	443 (4.62)	534	3,850	0.33	0.55
	film	443	539	4,020	0.18	
3.1P4	sol.	476 (4.20)	669	6,060	0.39	0.33
	film	481	631	4,940	0.13	

[a] Solutions were prepared from DCM, which was drop-cast to prepare the films. [b] Only the longest absorption and fluorescence maxima are shown. [c] Absolute quantum yields determined with a calibrated integrating sphere system.

Table 3-3. Time resolved fluorescence decays of **3.1P1**, **3.1P2**, **3.1P3** and **3.1P4** in solution (DCM) and film state, λ_{ex} = 375 nm.

Compd.	Solution (DCM)		Film	
	λ_{moni} (nm)	τ (ns)	λ_{moni} (nm)	τ (ns)
3.1P1	399	0.57	398	0.19 (0.63), 0.44 (0.37)
3.1P2	500	0.17 (0.57), 0.34 (0.43)	482	0.05 (0.76), 0.34 (0.24)
3.1P3	534	0.55	539	0.29 (0.35), 0.01 (0.59), 1.57 (0.06)
3.1P4	669	1.04 (0.20), 3.8 (0.59) 0.003 (0.21)	631	0.72 (0.43), 0.005 (0.23), 2.04 (0.33)

Phase Separation of Polymer Blends. Polymer blend is an important research field in polymer science.[17] However, blending polymers to combine their fluorescence colors has been practically difficult because of phase separation; one needs to carefully consider the complex phase diagrams of the polymer blends and optimize both the blending processes and conditions (e.g., the solvents and temperature). Furthermore, blended films with phase separation may not be optically clear and often deteriorate over time as the photophysical properties change. To address this issue, CPs with pendant or end-capping fluorophores have been synthesized.[18] In addition, a supramolecular copolymer approach that enables fluorescent components to be randomly mixed has recently been reported.[19] We envisage that our IMWs will be an alternative to these protocols in that phase separation does not occur when the IMWs are blended since all the polymers are sheathed with the same cyclic sidechains regardless of the conjugated backbones. To test this idea, a solution of **3.1P1**/**3.1P3** (1:1 wt/wt) was spin-coated onto glass plates, and we found that a homogeneous transparent film without any light scattering was formed (transmittance at 800 nm (T_{800}) >99%, thickness = 100 nm). In contrast, the T_{800} values of **3.1P1**/polystyrene (**PS**: amorphous polymer) and **3.1P1**/**P3HT** (crystalline polymer) blended films decreased slightly to 95% (60 nm thick) and 92% (60 nm thick), respectively, suggesting the formation of heterogeneous structures. In fact, atomic force microscopy (AFM) images of the films clearly showed phase separation in the **3.1P1**/**PS** and **3.1P1**/**P3HT** films, whilst that of the **3.1P1**/**3.1P3** film was uniformly flat (Figure 3-5a-b). Furthermore, even after annealing (100 °C for 3 h: Figure 3-5b or RT for 3 months: Figure 3-6), we did not observe any phase separation in the **3.1P1**/**3.1P3** film. These observations indicate that no discrimination occurs with our IMWs and there is no phase separation in the blended films. We deduced that the Flory–Huggins parameters of our IMWs blends are small owing to not only their structural similarity but also the intrinsically weak interpolymer interaction, although this expectation is still preliminary in the absence of consideration of the molecular weights.

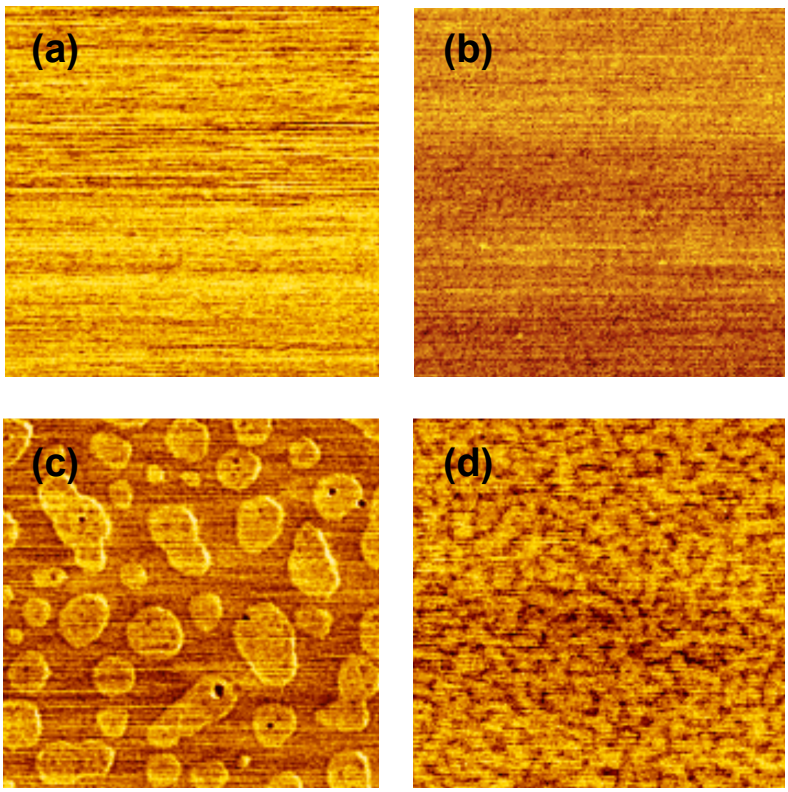

Figure 3-5. AFM phase images of the **3.1P1**/**3.1P3** blend (a) before and (b) after annealing at 100 °C for 3 h and the (c) **3.1P1**/**PS** and (d) **3.1P1**/**P3HT** polymer blends; 2 μm × 2 μm.

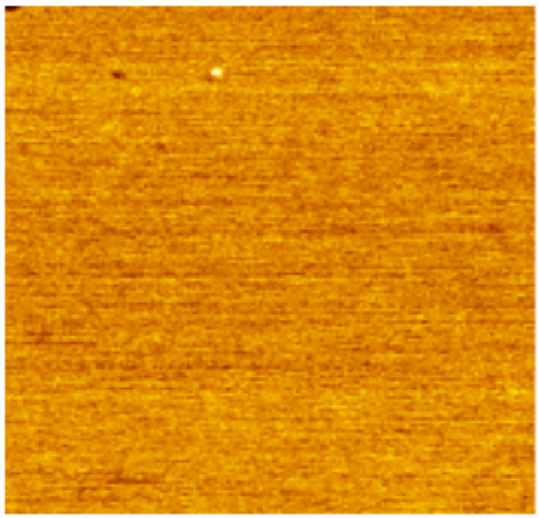

Figure 3-6. AFM phase image of the **3.1P1**/**3.1P3** blend left at RT for 3 months (2 μm × 2 μm).

Photophysical Properties of Polymers Blends. By taking advantage of the mutual compatibility of our IMWs, we mixed the IMWs to mix their fluorescence in the film state. Combinations of these four emission colors can in principle generate any fluorescence color, and in fact, sky-blue (**B1**), orange (**B2**), pink (**B3**), and even white (**B4**) fluorescence were prepared (Figures 3-7 and 3-8). For example, the white emission (CIE coordinate: [0.33, 0.34]) was obtained by mixing **3.1P1**, **3.1P3**, and **3.1P4** at a ratio of 200:3:1 (molar ratio of the repeating units). Considering that **3.1P1** has the highest $\Phi_{F(film)}$ and is mainly excited in the mixture (λ_{ex} = 338 nm), excited energy is transferred from **3.1P1** to **3.1P3** and **3.1P4**. This notion was indeed supported by additional experiments as described in the supporting information; for example, the fluorescence intensity and lifetime of **3.1P1** decreased with blending **3.1P3** (Figure 3-9). All the blended films retained reasonable $\Phi_{F(film)}$ values as indicated in Figure 3-7, from which we infer that the acceptor polymers can act as an energy sink (a dead end of the energy migration) in the polymer blends and thus do not decrease the total $\Phi_{F(film)}$ significantly.[20] In fact, **3.1P4** in the **3.1P1** matrix showed a better $\Phi_{F(film)}$ than the pure **3.1P4** film (Figure 3-10). Importantly, the preparation of these homogeneous fluorescent films was reproducible and independent of the film preparation conditions (solvents and temperature), and the fluorescence color was stable for more than three months at room temperature.

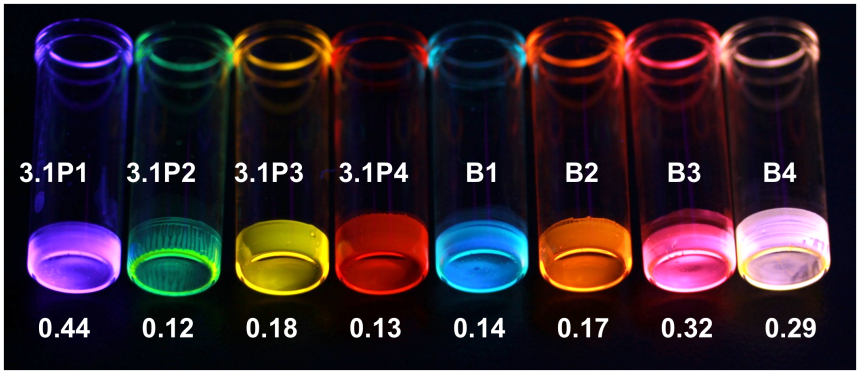

Figure 3-7. Photographs of the films of **3.1P1**–**3.1P4** and blend films **B1**–**B4** taken under UV (365 nm) illumination. The blending ratios **3.1P1/3.1P2/3.1P3/3.1P4** of **B1**, **B2**, **B3**, and **B4** are 100/10/0/0, 0/0/100/5, 100/0/0/5, 200/0/3/1, respectively. The polymer solutions were dried in glass vials and the films were formed at the bottom of the vials.

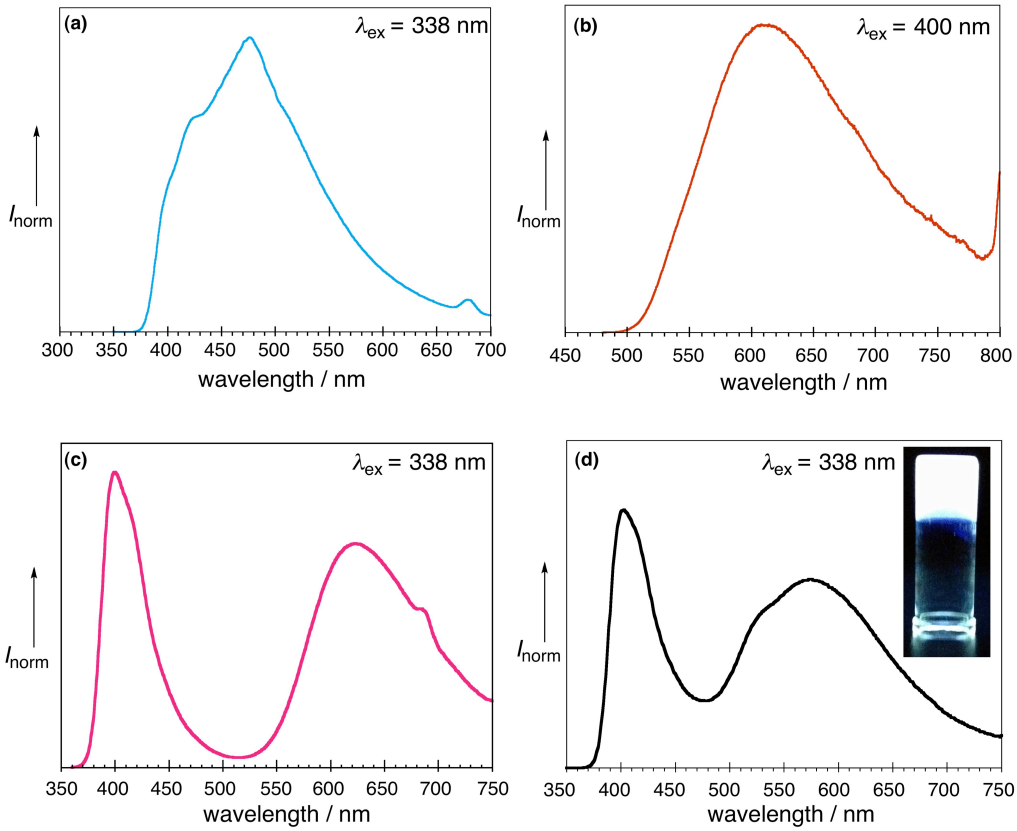

Figure 3-8. Normalized fluorescence spectra of **B1** (a), **B2** (b), **B3** (c) and **B4** (d), inset in figure (d) is the picture of **B4** blend film taken under UV irradiation at 365 nm.

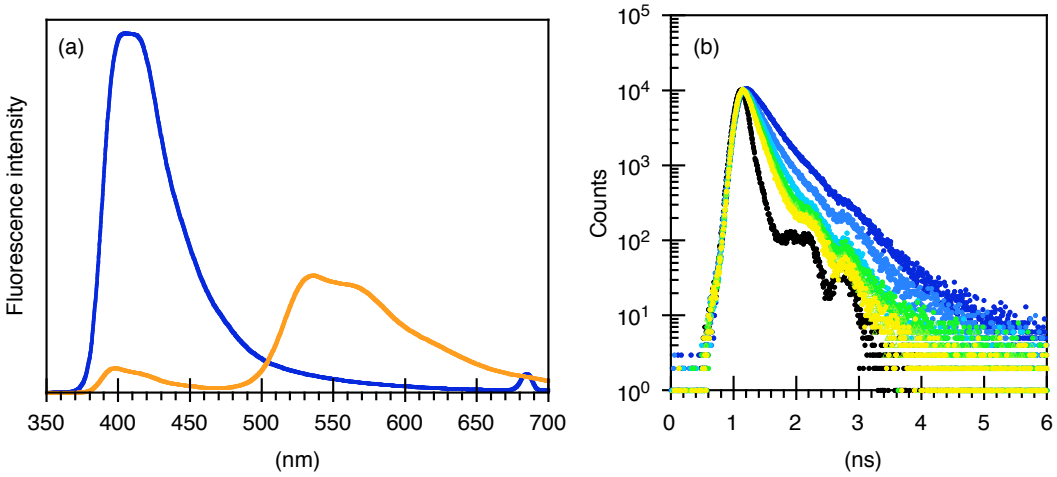

Figure 3-9. (a) Fluorescence spectra of **3.1P1** (blue) and **3.1P1/P3** blend (orange) with 5 % of **3.1P3**, λ_{ex} = 338 nm. (b) Time resolved fluorescence decay of **3.1P1**/**3.1P3** blend: outer (blue) to inner (yellow), 0, 1, 3, 5, 7, 9% of **3.1P3** was blended into **3.1P1**: black: IRF, λ_{ex} = 375 nm, λ_{moni} = 420 nm. These results indicate the excited energy transfer from **3.1P1** to **3.1P3** in the blend films.

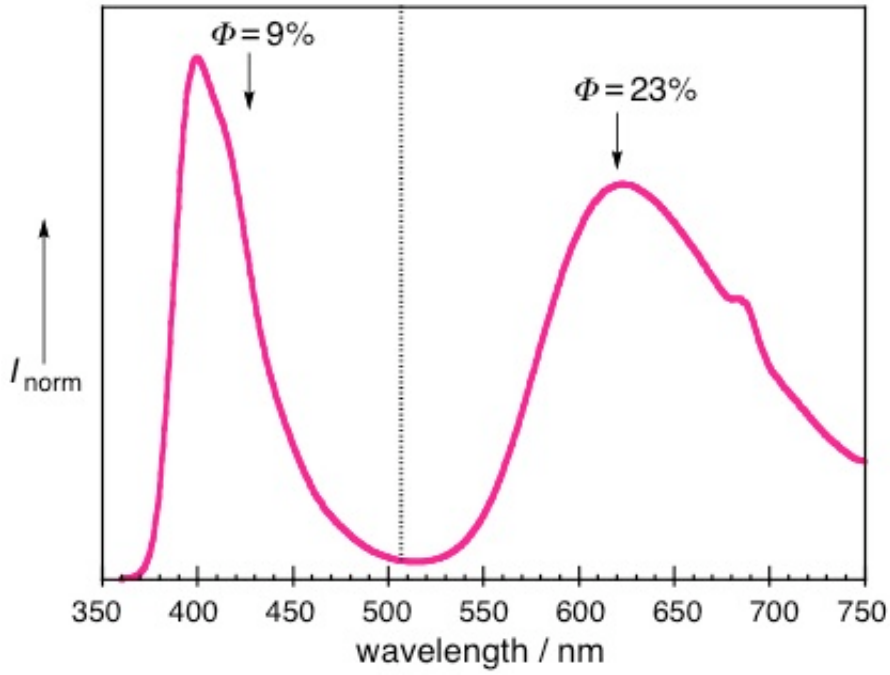

Figure 3-10. Normalized fluorescence spectra of **3.1P1/3.1P4** (100:5), λ_{ex} = 338 nm, the quantum yield of **3.1P1** was decreased from 44 % to 9 %, while the quantum yield of **3.1P4** was increased from 13 % to 23 %.

Thermal and Mechanical Properties. Another intriguing physical property of our IMWs was revealed during differential scanning calorimetry (DSC) measurements (Figure 3-11; −50 to 300 °C, 3 cycles). In the first scan, the as-synthesized polymers showed relatively low melting points. In the following scans, the glass transition at around 20–60 °C was observed, and after the measurements, plastic-like transparent lumps of the IMWs were recovered. The material did not show any X-ray diffraction peaks (data not shown), which is indicative of the amorphous nature of our IMWs. In addition, ^{1}H-NMR spectra of the recovered materials confirmed no decomposition of the polymer structures. Thus, our IMWs are thermoplastic quite unlike common CPs; accordingly, we explored the possibility of thermal processing.

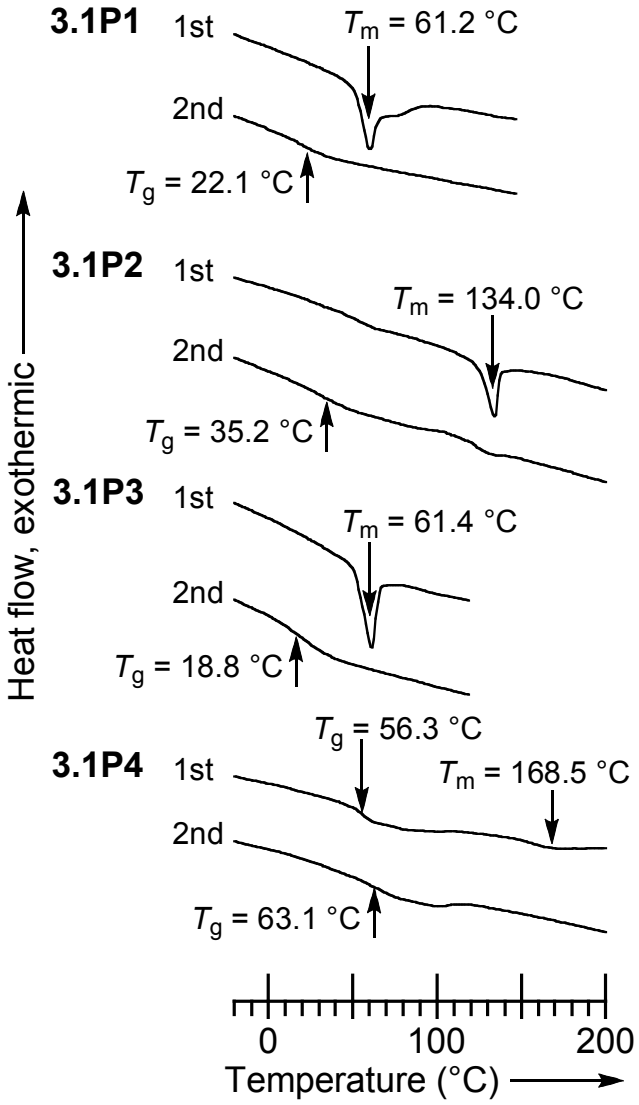

Figure 3-11. The first and second heating traces of the DSC thermograms of **3.1P1, 3.1P2, 3.1P3, and 3.1P4.**

A drop-cast film of **3.1P3** prepared on a Teflon plate was thermally annealed at 80 °C for 30 min, peeled off the substrate, and then dried overnight, thereby we obtained a fluorescent flexible self-standing film (Figures 3-12 and 3-13). A small piece of the film (80 μm thick and 5 mm wide) could sustain a weight of more than 200 g (>5 MPa of tensile stress), was stretchable (>300% of tensile strain), and even foldable without the formation of any cracks (Figure 3-14). Given the relatively low molecular weight and weak interpolymer interactions of our IMWs, the mechanical strength is remarkable. We assume that the internal free volume between the repeating units along the shish-kebab-like structure can physically interlock the polymer backbones, as has been reported by Swager and Thomas[21] for their triptycence containing polyesters (Figure 3-15).

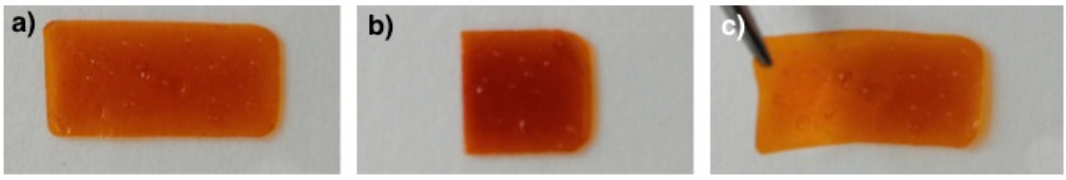

Figure 3-12. Photos of **3.1P3** film: the film (a) was folded into half (b) and unfolded (c), but no crack was observed.

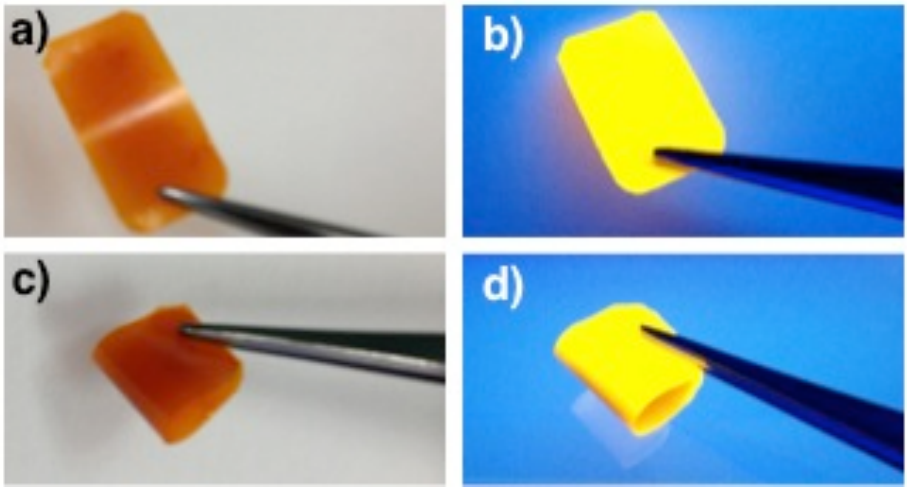

Figure 3-13. Images of **3.1P3** self-standing film (20 mm ×10 mm) under room (a, c) and UV (b, d) light. The preparation procedure for **3.1P3** self-standing film: The thick film was prepared from a 23 mg / 0.5 ml THF solution by drop casting on a Teflon substrate and annealed at 80 ^{o}C for 30 min, and the self-standing film was peeled off the substrate

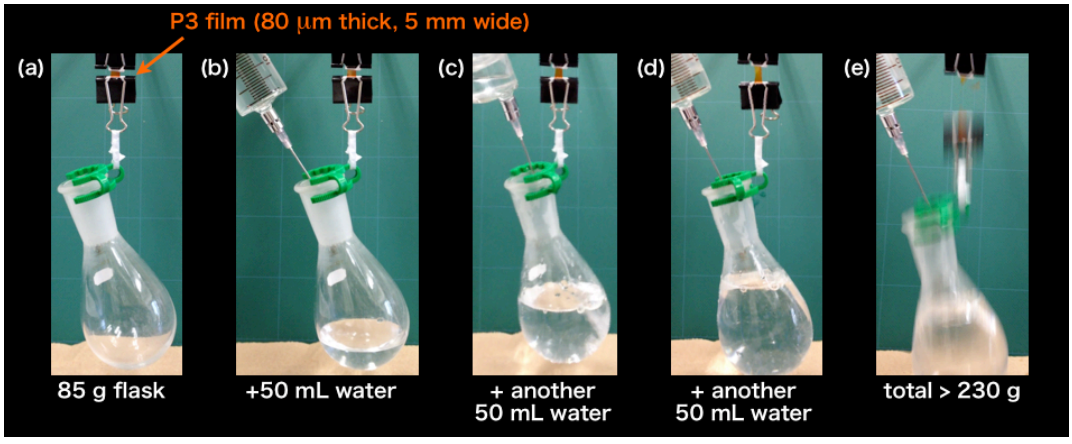

Figure 3-14. Snapshots (a) of the **3.1P3** film sustaining a flask and (b-e) taken while water was added to the flask.

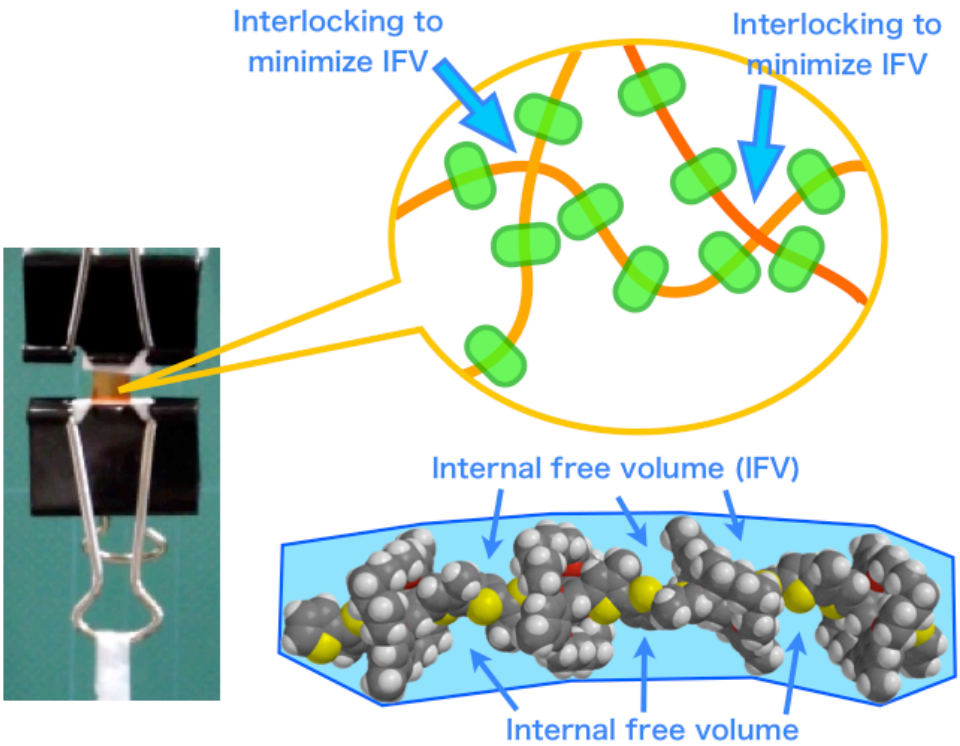

Figure 3-15. Cartoon showing proposed interlocking of **3.1P3** through minimizing internal free volume between the repeating units. Dodecyl chains are replaced with methyl groups to clarify.

Nanoimprint of 3.1P1 Film. In addition, we also attempted thermal patterning of the IMWs using a silicon mold. A spin-coated film of **3.1P1** was pressed with the mold at 100 °C. or 30 min and then cooled to room temperature (Figures 3-16 and 3-17). The patterned structure showed structural coloration due to Bragg reflection, which indicates that the periodic structure covered a large area. In addition, strong fluorescence was observed after the patterning process, and such highly fluorescent periodic structures could find potential use as a gain medium for lasing.[22] Importantly, these mechanical and thermal properties can be modified by the molecular design, for example, by simply changing the length and number of the solubilizing alkyl chains. Thus, **3.1M1** is a versatile building unit that can provide a variety of IMWs with tunable photophysical and mechanical properties.

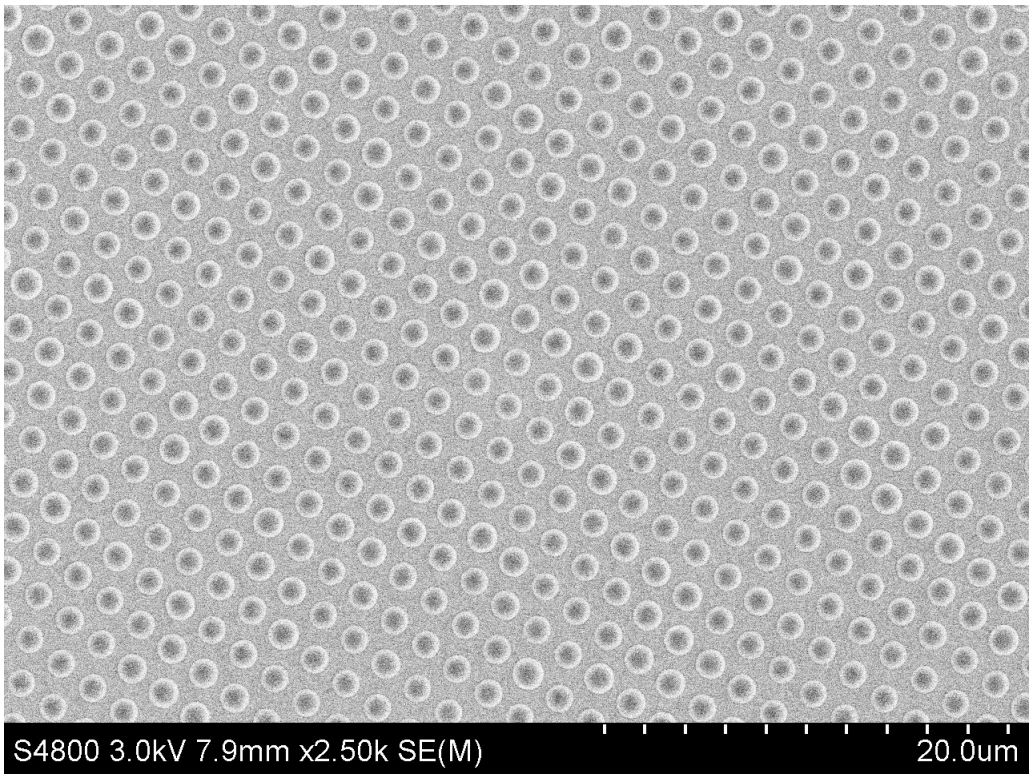

Figure 3-16. SEM image of **3.1P1** pattern.

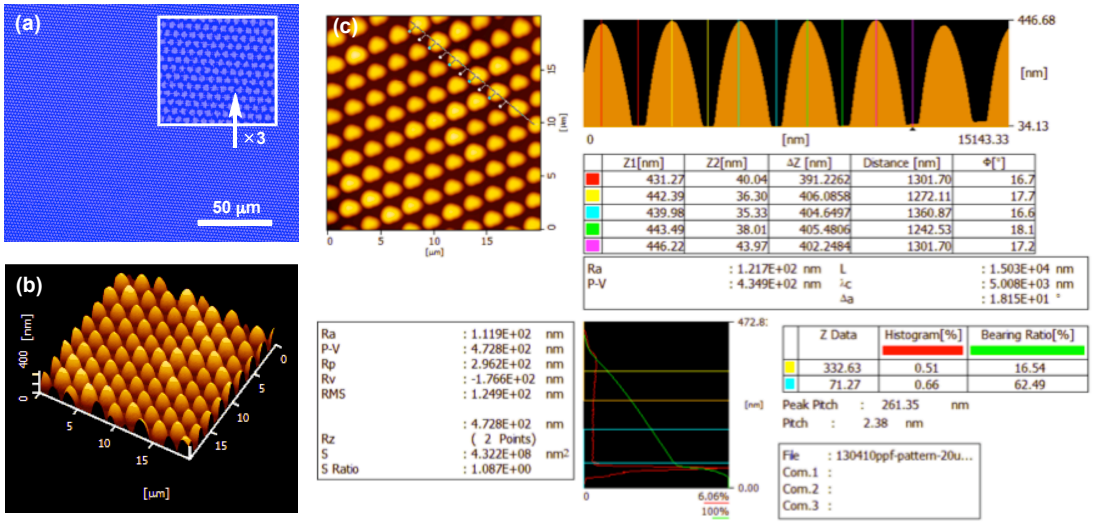

Figure 3-17. (a) Fluorescence microscopic, (b) AFM three-dimentional height images of the patterned **3.1P1** film, and (d) AFM image of **3.1P1** pattern.

CONCLUSION

In this chapter, we have synthesized a new family of IMWs based on a monomer that is readily available, versatile, and able to produce IMWs with a variety of conjugated systems. Our IMWs are (1) emissive in entire visible region, even in the film state, (2) miscible, allowing the combination of various fluorescence colors, and (3) thermoformable, like conventional plastics. These features have been rarely developed for CPs and can be attributed to the unique three-dimensional architectures, which distinguish our polymers from other organic fluorescent materials reported previously.[1-7] Simple structural customization on the basis of **3.1M1** is expected to provide IMWs with a myriad of properties, which we believe will be useful in various plastic optoelectronic applications such as electroluminescence, sensors, and lasers.

EXPERIMENTAL SECTION

Air and water sensitive synthetic manipulations were performed under an argon atmosphere using standard Schlenk techniques. All chemicals were purchased from Aldrich, TCI, Kanto Chemical, or Wako and used as received without further indication. NMR spectra were recorded on a Bruker Biospin DRX-600 (600 MHz) spectrometer or JEOL ECS-400 (400 MHz) spectrometer by using tetramethylsilane (0 ppm for ^{1}H NMR) or $CDCl_3$ (77 ppm for ^{13}C NMR) as an internal standard. Mass spectral data were obtained using a SHIMADZU AXIMA-CFR Plus MALDI TOF mass spectrometer and using *trans*-2-[3-(4-*tert*-butylphenyl)-2-methyl-2-propenylidene]malononitrile (DCTB) as matrix. Melting points were determined with a Yanako NP-500P micro melting point apparatus. Elemental analysis (C, H, N) was performed on a Perkin-Elmer 2400 CHN Elemental Analyzer. Gel permeation chromatography for copolymers was performed in THF solution using a TOSHO GPC system (HLC-8320GPC EcoSEC) equipped with two TSK gel Super-Multipore HZ-M columns and a UV detector (254 nm). The molecular weight (M_n) and polydispersity index (PDI) of the polymer samples were calculated on the basis of a polystyrene calibration. Absorption and fluorescence spectra were recorded on a Hitachi U-2900 spectrophotometer and a Hitachi F-7000 spectrophotometer, respectively, in dichloromethane (DCM) solution at room temperature (298 K) in a quartz cuvette of 1 cm path length. Fluorescence lifetime measurements were performed by means of time correlated single photon counting (TCSPC) technique by using a FluoroCube spectrometer (HORIBA Jobin Yvon) equipped with a picosecond pulse laser (PB-375L, 375 nm) and a picosecond photon detection module (TBX). Decay analysis and the fitting routine to determine the lifetime(s) were performed using the DAS6 software provided by IBM. Fluorescence quantum yield was recorded on a Hamamatsu absolute PL quantum yield spectrometer C11347. Spin coating was done by using OSHIGANE SC-300. Differential scanning calorimetry (DSC) measurements were performed on a TA instrument DSC Q2000 by heating 10 ^{o}C / min. Atomic force microscope (AFM) measurements were carried out on a NanoNavi S-image (SII, Japan) using fresh mica as the substrate. **P1** pattern was characterized by SEM (S-4800, Hitachi, 10 kV), AFM and upright fluorescence microscopy (DMI6000 B, Leica). Film thickness was measured by using the microfigure measuring instrument (Surfcorder ET200, Kosaka Laboratory Ltd., Tokyo, Japan).

Synthesis of compound 3.2:[23] A 300 ml two-necked round bottom flask was charged with 1, 4-dibromo-2, 5-diiodobenzene (7.0 g, 14.4 mmol), 4-dodecyl-2, 6-dimethoxylphenylboronic acid (15.2 g, 43.4 mmol), sodium carbonate (9.2 g, 87 mmol), and evacuated and back-filled with argon three times. Toluene (160 ml), ethanol (40 ml) and water (40 ml) were added via syringe. The reaction mixture was vigorously stirred at 80 ^{o}C for 1 hour, $Pd(PPh_3)_4$ (503 mg, 0.435 mmol) was then added to the reaction mixture, the stirring was continued for 24 hours, then the solvent was evaporated by reduced pressure. Water was poured into the reaction mixture, extracted with DCM for 3 times, the combined organic layer was washed with brine, dried over $MgSO_4$. The solvent was removed by evaporation under reduced pressure, and the resulting black solid was purified through column chromatography (silica gel, hexane/DCM = 2/1) to afford compound **2** crude product, then small amount of DCM was added to the crude product, further precipitation from methanol to give pure compound **3.2** as white powder (11.03 g, 91%).

M.p.: 127.9-128.4 ^{o}C. ^{1}H NMR ($CDCl_3$, 600 MHz, TMS, 298 K): δ 0.88 (t, J = 7.2 Hz, 6H), 1.27–1.39 (m, 36H), 1.66–1.71 (m, 4H), 2.65 (t, J = 8.1 Hz, 4H), 3.76 (s, 12H), 6.46 (s, 4H), 7.48 (s, 2H). ^{13}C NMR (150 MHz, $CDCl_3$, TMS, 298 K): δ 14.11, 22.69, 29.36, 29.55, 29.64, 29.66, 29.69, 31.38, 31.92, 36.87, 55.89, 104.15, 115.24, 123.67, 135.54, 136.18, 139.10, 145.13, 157.47. MALDI-TOF-MS (Matrix: DCTB): Found m/z = 844.98, Calcd for [M]+ ($C_{46}H_{68}Br_2O_4$) = 844.35. Anal. Calcd for $C_{46}H_{68}Br_2O_4$: C, 65.40; H, 8.11. Found: C, 65.57; H, 8.01.

Synthesis of compound 3.3:[10a] A 300 ml two-necked round bottom flask was charged with compound 3.**2** (7.0 g, 8.3 mmol), and evacuated and back-filled with argon three times. Anhydrous DCM (100 ml) was added to the flask via syringe, BBr_3 (49.7 ml, 49.7 mmol) was added to the reaction mixture slowly at 0 ^{o}C and the solution was stirred for 36 hours at room temperature. Methanol was then added slowly to quench the reaction and the solvent was removed by evaporation under reduced pressure. The resulting dark brown powder was washed with water, extracted with EtOAc for three times, the combined organic layer was washed with brine and dried over $MgSO_4$. The solvent was evaporated and the obtained oil residue was purified through column chromatography (silica gel, Hexane / EtOAc = 2/1) to afford compound **3.3** as white powder quantitatively.

M.p.: 138.6-139.6 ^{o}C. ^{1}H NMR ($CDCl_3$ / MeOD, 600 MHz, TMS, 298 K): δ 0.89 (t, J = 7.2 Hz, 6H), 1.27–1.36 (m, 36H), 1.62–1.64 (m, 4H), 2.53 (t, J = 7.8 Hz, 4H), 6.36 (s, 4H), 7.66 (s, 2H). ^{13}C NMR (150 MHz, $CDCl_3$ / MeOD, TMS, 298 K): δ 13.78, 22.44, 29.12, 29.22, 29.34, 29.42, 29.46, 30.85, 31.69, 35.81, 107.03, 112.13, 124.94, 136.40, 136.57, 145.29, 154.08. MALDI-TOF-MS (Matrix: DCTB): Found m/z = 789.28, Calcd for [M]+ ($C_{42}H_{60}Br_2O_4$) = 788.28. Anal. Calcd for $C_{42}H_{60}Br_2O_4 \cdot 1.05H_2O$: C, 62.46; H, 7.75. Found: C, 62.36; H, 7.65.

Synthesis of compound 3.4:[24] A 300 ml two-necked round bottom flask was charged with compound **3.3** (5.7 g, 7.23 mmol), cesium carbonate (23.2 g, 71.21 mmol) and 5-bromo-1-pentene (10.6 g, 71.13 mmol), and evacuated and back-filled with argon three times. Anhydrous DMSO (100 ml) was added to the flask via syringe and the solution was heated up to 100 ^{o}C overnight. Water was added to quench the reaction and the solvent was distilled under reduced pressure. The resulting solid was washed with water, extracted with DCM for three times, the combined organic layer was washed with brine and dried over $MgSO_4$. The solvent was evaporated and the obtained yellow oil was purified through column chromatography (silica gel, Hexane / DCM = 2/1) to give compound **3.4** as colorless oil (7.29 g, 95 %), the colorless oil gradually solidified after keeping it at room temperature overnight.

M.p.: 29.4-30.1 ^{o}C. ^{1}H NMR ($CDCl_3$, 400 MHz, TMS, 298 K): δ 0.88 (t, J = 7.0 Hz, 6H), 1.27–1.35 (m, 36H), 1.62–1.73 (m, 12H), 2.03–2.09 (m, 8H), 2.61 (t, J = 7.6 Hz, 4H), 3.91 (t, J = 6.0 Hz, 8H), 4.91-5.01 (m, 8H), 5.71–5.78 (m, 4H), 6.43 (s, 4H), 7.49 (s, 2H). ^{13}C NMR ($CDCl_3$, 100 MHz, TMS, 298 K): δ 14.11, 22.68, 28.38, 29.36, 29.50, 29.55, 29.65, 29.69, 29.96, 31.37, 31.92, 36.76, 67.56, 105.32, 115.00, 116.22, 123.28, 135.39, 136.23, 137.98, 144.86, 156.85. MALDI-TOF-MS (Matrix: DCTB): Found m/z =1061.83, Calcd for [M]+ ($C_{62}H_{92}Br_2O_4$) = 1060.53. Anal. Calcd for $C_{62}H_{92}Br_2O_4$: C, 70.17; H, 8.74. Found: C, 69.75; H, 8.74.

Synthesis of compound 3.5:[10a] A 2 L three-necked round bottom flask was charged with compound **3.4** (4.2 g, 3.96 mmol) and evacuated and back-filled with argon three times. Anhydrous DCM (1L) was added to the flask and second generation Grubbs catalyst (200 mg, 0.24 mmol) in DCM (100 ml) was slowly added to the reaction mixture. The solution was heated up to 40 ^{o}C overnight. After cooling to room temperature, the reaction mixture was passed through short silica gel pad to remove catalyst. The solution was concentrated by evaporation under reduced pressure and MeOH was added to the flask to produce compound **3.5** as white powder quantitatively.

M.p.: 136.4-137.4 ^{o}C. ^{1}H NMR ($CDCl_3$, 600 MHz, TMS, 298 K): δ 0.88 (t, J = 7.2 Hz, 6H), 1.27–1.39 (m, 36H), 1.62–1.67 (m, 12H), 2.03–2.12 (m, 8H), 2.63 (t, J = 7.8 Hz, 4H), 3.95–4.01 (m, 8H), 5.22–5.39 (m, 4H), 6.43 (s, 4H), 7.53(s, 2H). ^{13}C NMR ($CDCl_3$, 150 MHz, TMS, 298 K): δ 14.12, 22.69, 24.83, 24.99, 29.37, 29.55, 29.62, 29.66, 29.69, 30.19, 30.31, 31.41, 31.93, 36.88, 68.19, 104.01, 104.26, 115.00, 123.45, 129.56, 130.84, 135.41, 136.18, 144.89, 156.90. MALDI-TOF-MS (Matrix: DCTB): Found m/z = 1004.84, Calcd for [M]+ ($C_{58}H_{84}Br_2O_4$) = 1004.47. Anal. Calcd for $C_{58}H_{84}Br_2O_4$: C, 69.31; H, 8.42. Found: C, 69.06; H, 8.41.

Synthesis of compound 3M1: [25] A 300 ml two-necked round bottom flask was charged with compound **3.5** (4.0 g, 3.98 mmol) and evacuated and back-filled with argon three times. Anhydrous THF/*tert*-Butyl alcohol (1/1, 50 ml) was added to the flask and Wilkinson's catalyst (370 mg, 0.40 mmol) was added to the reaction mixture, the stirring was continued for 3 days at 40 ^{o}C. After cooling

to room temperature, the reaction mixture was passed through short silica gel pad to remove catalyst. The solution was concentrated by evaporation under reduced pressure and MeOH was added to the flask to produce compound **3M1** as white powder quantitatively.

M.p.: 158.6-159.3 ^{o}C. ^{1}H NMR ($CDCl_3$, 600 MHz, TMS, 298 K): δ 0.89 (t, J = 7.2 Hz, 6H), 1.28–1.38 (m, 52H), 1.65–1.70 (m, 8H), 1.65–1.70 (m, 4H), 2.62 (t, J = 7.8 Hz, 4H), 3.91–3.97 (m, 8H), 6.41 (s, 4H), 7.50 (s, 2H). ^{13}C NMR ($CDCl_3$, 150 MHz, TMS, 298 K): δ 14.12, 22.70, 24.04, 27.23, 29.15, 29.38, 29.54, 29.56, 29.63, 29.68, 29.70, 31.40, 31.94, 36.89, 68.43, 103.78, 114.70, 123.44, 135.48, 136.09, 144.79, 157.09. MALDI-TOF-MS (Matrix: DCTB): Found m/z = 1008.84, Calcd for [M]+ ($C_{58}H_{88}Br_2O_4$) = 1008.50. Anal. Calcd for $C_{58}H_{88}Br_2O_4$: C, 69.03; H, 8.79. Found: C, 68.85; H, 8.63.

Synthesis of compound 3.1Th: A 30 ml two-necked round bottom flask was charged with **3M1** (100 mg, 0.099 mmol), 3-dodecylthiophene-2-boronic acid pinacol ester (112.5 mg, 0.3 mmol), potassium carbonate (136.8 mg, 0.99 mmol), and evacuated and back-filled with argon three times. 1, 4-dioxane (6 ml) and H_2O (0.5 ml) were added to the flask via syringe, $Pd(PPh_3)_4$ (5.7 mg, 0.005 mmol) was then added to the reaction mixture, the reaction mixture was heated up to 120 ^{o}C overnight, then the solvent was evaporated by reduced pressure. Water was poured into the black powder, extracted with DCM for 3 times, the combined organic layer was washed with brine, dried over $MgSO_4$. The solvent was removed by evaporation under reduced pressure, and the resulting black solid was purified through column chromatography (silica gel, hexane/DCM = 5/1) to afford compound **3.1Th** crude product, then small amount of DCM was added to the crude product, further precipitation from methanol to give pure compound **3.1Th** as white powder (120 mg, 90 %).

M.p.: 85.4-86.6 ^{o}C. ^{1}H NMR ($CDCl_3$, 400MHz, TMS, 298 K): δ 0.87–0.90 (m, 12H), 1.26–1.46 (m, 92H), 1.42–1.46 (m, 8H), 1.64–1.70 (m, 4H), 2.39 (t, J = 7.4 Hz 4H), 2.63 (t, J = 7.8 Hz, 4H), 3.69–3.74 (m, 4H), 3.87–3.92 (m, 4H), 6.38 (s, 4H), 6.58 (s, 2H), 6.62 (s, 2H), 7.53 (s, 2H). ^{13}C NMR (CD_2Cl_2, 100 MHz, 298 K): δ 14.12, 22.70, 23.88, 27.14, 29.07, 29.21, 29.38, 29.52, 29.61, 29.68, 29.74, 30.51, 31.63, 31.93, 36.84, 68.30, 104.01, 115.78, 118.86, 125.70, 130.71, 132.05, 132.54, 142.13, 143.85, 144.17, 157.87. MALDI-TOF-MS (Matrix: DCTB): Found m/z = 1351.84, Calcd for [M]+ ($C_{90}H_{142}O_4S_2$) = 1351.03. Anal. Calcd for $C_{90}H_{142}O_4S_2 \cdot 1.05CH_2Cl_2$: C, 75.87; H, 10.08. Found: C, 75.94; H, 10.16.

Synthesis of compound 3M2: A 30 ml two-necked round bottom flask was charged with **3.1Th** (110 mg, 0.08 mmol) in THF (3 ml), and NBS (29 mg, 0.16 mmol) was added to the flask slowly. The reaction mixture was stirred under dark for 2 hours, then saturated NaOH solution was poured into the reaction mixture to quench the reaction, the mixture was extracted with $CHCl_3$ for 3 times, the combined organic layer was washed with brine, dried over $MgSO_4$. The solvent was removed by evaporation under reduced pressure, and the resulting yellow solid was purified through column chromatography (silica gel, hexane/DCM = 5/1) to afford compound **3M2** crude product, then small

amount of $CHCl_3$ was added to the crude product, further precipitation from methanol to give pure compound **3M2** as white powder (80 mg, 66 %).

M.p.: 103.6-104.2°C. ^{1}H NMR ($CDCl_3$, 600 MHz, TMS, 298 K): δ 0.87–0.90 (m, 12H), 1.26–1.42 (m, 92H), 1.48–1.50 (m, 8H), 1.67–1.70 (m, 4H), 2.36 (t, J = 7.8 Hz, 4H), 2.64 (t, J = 7.8 Hz, 4H), 3.75–3.77 (m, 4H), 3.88–3.91 (m, 4H), 6.39 (s, 4H), 6.55 (s, 2H), 7.44 (s, 2H). ^{13}C NMR ($CDCl_3$, 150 MHz, 298 K): δ 14.13, 22.71, 23.90, 27.12, 29.05, 29.14, 29.39, 29.43, 29.50, 29.63, 29.70, 29.74, 29.77, 31.58, 31.95, 36.85, 68.36, 104.18, 107.84, 114.91, 125.19, 130.88, 131.52, 132.28, 140.95, 143.42, 144.76, 157.84. MALDI-TOF-MS (Matrix: DCTB): Found m/z = 1509.61, Calcd for [M]+ ($C_{90}H_{140}Br_2O_4S_2$) = 1508.85. Anal. Calcd for $C_{90}H_{140}Br_2O_4S_2 \cdot 0.05CHCl_3$: C, 71.35; H, 9.31. Found: C, 71.04; H, 9.34.

Synthesis of compound 3.2H:[23] A 300 ml two-necked round bottom flask was charged with 1, 4-dibromo-2, 5-diiodinebenzene (1.13 g, 2.32 mmol), 2, 6-dimethoxylphenylboronic acid (1.06 g, 5.82 mmol), potassium carbonate (3.18 g, 23.01mmol), and evacuated and back-filled with argon three times. 1, 4-dioxane (80 ml) and H_2O (5 ml) were added via syringe, $Pd(PPh_3)_4$ (80 mg, 0.069 mmol) was then added to the reaction mixture, the reaction mixture was heated up to 120 °C for 30.5 hours, then the solvent was evaporated by reduced pressure. Saturated NaOH solution was poured into the reaction mixture, filtered and collected the solid, $CHCl_3$ was added to the residual solid and compound **3.2H** was precipitated as white powder (720 mg, 61%).

M.p.: >300 °C. ^{1}H NMR ($CDCl_3$, 600 MHz, TMS) δ 3.78 (s, 12H), 6.65 (d, J = 8.40 Hz, 4H), 7.35 (t, J = 8.40 Hz, 2H), 7.50 (s, 2H). ^{13}C NMR ($CDCl_3$, 150 MHz, 298 K): δ 55.97, 103.96, 117.79, 123.50, 129.71, 135.37, 136.12, 157.78. MALDI-TOF-MS (Matrix: DCTB): Found m/z = 508.55, Calcd for [M]+ ($C_{22}H_{20}Br_2O_4$) = 507.97. Anal. Calcd for $C_{22}H_{20}Br_2O_4$: C, 51.99; H, 3.97. Found: C, 51.66; H, 4.21.

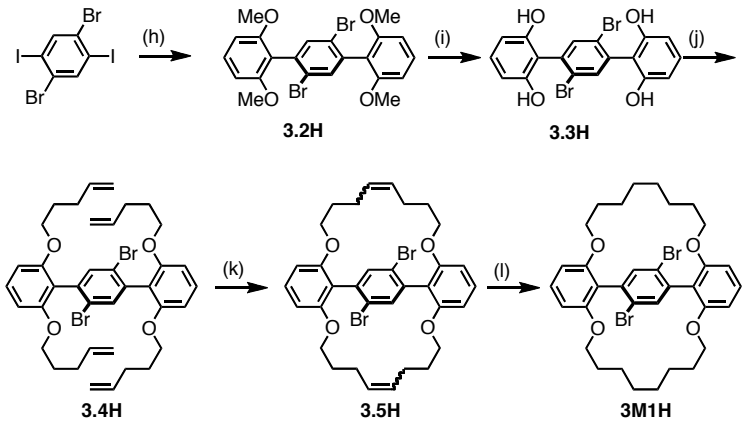

Scheme 3-3. Synthetic routes of monomers **3M1H**: (h) $ArB(OH)_2$, $Pd(PPh_3)_4$, K_2CO_3, dioxane, H_2O, reflux; (i) BBr_3, DCM, RT; (j) PPh_3, DIAD, 3-butene-1-ol, THF, high concentration/sonication method; (k) Second generation Grubbs catalyst, DCM, reflux; (l) Wilkinson's catalyst, THF, *t*-BuOH, H_2, 40 °C.

Synthesis of 3.3H: The same procedure for the synthesis of **3.3** was applied using compound **3.2H** as a starting material. Yield: > 98 %, white powder.

M.p.: >300 ^{o}C.^{1}H NMR ($CDCl_3$ / MeOD, 600 MHz, TMS) δ 6.49 (d, J = 7.80 Hz, 4H), 7.11 (t, J = 7.80 Hz, 2H), 7.64 (s, 2H). ^{13}C NMR ($CDCl_3$ / MeOD, 150 MHz, 298 K): δ 106.52, 114.65, 124.23, 129.25, 135.81, 136.43, 154.49. MALDI-TOF-MS (Matrix: DCTB): Found m/z = 453.55, Calcd for [M]+ ($C_{18}H_{12}Br_2O_4$) = 451.91. Anal. Calcd for $C_{18}H_{12}Br_2O_4$: C, 47.82; H, 2.68. Found: C, 47.45; H, 2.95.

Synthesis of compound 3.4H:[10a]A 30 ml two-necked round bottom flask was charged with compound **3.3H** (400 mg, 0.88 mmol) and PPh_3 (1.38 g, 5.28 mmol), and evacuated and back-filled with argon three times, 4-pentene-1-ol (455 mg, 5.28 mmol) and anhydrous THF (1.5 ml) was added to the flask, DIAD (1.42 g, 7.0 mmol) was then added slowly, heat was generated during the process of adding DIAD. The mixture was then sonicated overnight. The solvent was removed by evaporation under pressure and the solid residue was purified through column chromatography (silica gel, Hexane / DCM = 2 /1) to afford compound **3.4H** as white powder (420 mg, 66 %).

M.p.: 66.6-67.6^{o}C.^{1}H NMR ($CDCl_3$, 600 MHz, TMS, 298 K): δ 1.71–1.74 (m, 8H), 2.07 (m, 8H), 3.92–3.94 (m, 8H), 4.92–5.00 (m, 8H), 5.72–5.78 (m, 4H), 6.61 (d, J = 8.4 Hz, 4H), 7.26–7.50 (m, 2H, overlapped with $CHCl_3$), 7.50 (s, 2H). ^{13}C NMR ($CDCl_3$, 150 MHz, 298 K): δ 28.32, 29.94, 67.60, 105.00, 115.08, 118.73, 123.13, 129.49, 135.22, 136.21, 137.90, 157.17. MALDI-TOF-MS (Matrix: DCTB): Found m/z = 725.24, Calcd for [M]+ ($C_{38}H_{44}Br_2O_4$) = 724.16. Anal. Calcd for $C_{38}H_{44}Br_2O_4$: C, 62.99; H, 6.12. Found: C, 62.61; H, 5.89.

Synthesis of 3.5H: The same procedure for the synthesis of **3.5** was applied using compound **3.4H** as a starting material. Yield: > 98 %, White powder.

M.p.: 268.5-269.3^{o}C.^{1}H NMR ($CDCl_3$, 600 MHz, TMS, 298 K): δ 1.60–1.70 (m, 8H), 2.03–2.15 (m, 8H), 3.94–4.03(m, 8H), 5.22–5.24 (m, 0.4H), 5.34–5.39 (m, 3.6H), 6.61 (m, 4H), 7.30–7.32 (m, 2H), 7.55–7.56 (m, 2H). ^{13}C NMR ($CDCl_3$, 150 MHz, 298 K): δ 24.81, 24.96, 28.81, 30.16, 30.27, 68.24, 68.32, 103.87, 104.02, 104.73, 117.61, 123.30, 129.55, 130.86, 135.24, 136.18, 139.10, 156.96, 157.21. MALDI-TOF-MS (Matrix:): Found m/z = 668.63, Calcd for [M]+ ($C_{34}H_{36}Br_2O_4$) = 668.10. Anal. Calcd for $C_{34}H_{36}Br_2O_4 \cdot 0.1CHCl_3$: C, 60.2; H, 5.35. Found: C, 60.31; H, 5.42.

Due to the existence of the *cis* and *trans* isomers, NMR spectra are slightly complicated.

Synthesis of 3M1H: The same procedure for the synthesis of **3.1** was applied using compound **3.5H** as a starting material. Yield: > 98 %, White powder.

M.p.: 281.9-282.9 ^{o}C.^{1}H NMR ($CDCl_3$, 600 MHz, TMS, 298 K): δ 1.38 (broad, 16H), 1.56–1.62 (m, 8H), 3.91–3.98 (m, 8H), 6.59 (d, J = 8.40 Hz, 4H), 7.29 (t, J = 8.40 Hz, 2H), 7.51 (s, 2H). ^{13}C NMR ($CDCl_3$, 150 MHz, 298 K): δ 23.97, 27.14, 29.07, 68.58, 103.59, 117.21, 123.28, 129.48, 135.30,

136.05, 157.37. MALDI-TOF-MS (Matrix: DCTB): Found m/z = 673.18, Calcd for [M]+ ($C_{34}H_{40}Br_2O_4$) = 672.13. Anal. Calcd for $C_{34}H_{40}Br_2O_4 \cdot 0.25CH_2Cl_2$: C, 59.30; H, 5.88. Found: C, 59.23; H, 5.75.

Synthesis of 3.1P1:[26] A Schlenk flask was charged with compound **3M1** (100 mg, 0.099 mmol), 9, 9-dioctylfluorene-2, 7-diboronic acid bispinacol ester (74.80 mg, 0.099 mmol), $Pd(PPh_3)_4$ (5.70 mg, 0.005 mmol), Aliquat 336 (1 drop), and evacuated and backfilled with argon three times. An aqueous solution of potassium carbonate (2 M, 1 ml) and toluene (2 ml) was added via syringe. The reaction mixture was stirred for 72 h at 105 ^oC under Ar, and then it was cooled to room temperature and extracted with $CHCl_3$ for three times. The resulting organic layer was washed with brine, dried over $MgSO_4$ and concentrated by evaporation under pressure. The residue was dissolved in a small amount of chloroform and the solution was precipitated in Methanol, white powder was obtained by centrifugation (6000 rpm, 60 min). The crude product was dissolved in a small amount of THF and the solution was precipitated in acetone and pure white **3.1P1** powder was obtained by centrifugation (6000 rpm, 60 min) (50 mg, 37%).

T_g: 22.1 ^oC, T_m: 61.2 ^oC. ^1H NMR (CD_2Cl_2, 400 MHz, TMS, 298 K): δ 0.33 (m, 4H), 0.81–0.91 (m, 12H), 1.13–1.34 (m, 88H), 1.54–1.57 (m, 16H), 2.52 (broad, 4H), 3.68 (broad, 4H), 3.88 (broad, 4H), 6.28 (s, 4H), 7.15 (s, 2H), 7.25 (broad, 4H), 7.39 (d, J = 7.6 Hz, 2H). ^{13}C NMR (CD_2Cl_2, 100 MHz, 298 K): δ 14.70, 23.51, 24.96, 28.09, 30.20, 30.40, 30.50, 30.54, 30.72, 31.12, 32.26, 32.76, 37.63, 68.87, 104.26, 117.46, 118.88, 123.53, 128.33, 132.54, 133.92, 139.71, 141.06, 141.66, 144.24, 150.57, 158.07.

Synthesis of 3.1P2:[10a] A small vial was charged with compound **3M2** (50 mg, 0.033 mmol), $Ni(COD)_2$ (36.23 mg, 0.132 mmol), 2, 2'-bipyridyl (20.66 mg, 0.132 mmol) under Ar, A solution of COD (0.133 mmol) in toluene (1.70 ml) and DMF (0.5 ml) were added to the vial and sealed, the reaction mixture was stirred at 80 ^oC for 72 h. After cooling to room temperature, the solution was diluted with $CHCl_3$, washed with 1 M HCl aq., sat. EDTA aq., and then with water. The organic layer was dried over $MgSO_4$. The solvent was removed by evaporation under reduced pressure, the solid was purified by precipitation using $CHCl_3$/MeOH mixture and collected by centrifugation (6000 rpm, 60 min), **3.1P2** was obtained as green powder (30 mg, 67%).

T_g: 35.2 ^oC, T_m: 134.0 ^oC. ^1H NMR (CD_2Cl_2, 400 MHz, TMS, 298 K): δ 0.78–0.83 (m, 12H), 1.03–1.28 (m, 100H), 1.58 (broad, 4H), 2.16 (broad, 4H), 2.52 (broad, 4H), 3.65 (broad, 4H), 3.82 (broad, 4H), 6.32 (s, 4H), 6.51(s, 2H), 7.38 (s, 2H). ^{13}C NMR (CD_2Cl_2, 100 MHz, 298 K): δ 14.71, 23.53, 24.79, 28.01, 29.66, 29.95, 30.22, 30.25, 30.41, 30.54, 30.57, 30.62, 31.56, 32.51, 32.78, 37.67, 69.23, 104.91, 116.12, 126.88, 128.81, 131.49, 132.67, 132.93, 142.05, 143.68, 145.38, 158.50.

Synthesis of 3.1P3:[27] A Schlenk flask was charged with compound **3M2** (100 mg, 0.066 mmol), 2,5-Bis(trimethylstannyl)thiophene (28.27 mg, 0.069 mmol), $Pd_2(dba)_3$ (3.00 mg, 0.0033 mmol), $P(o\text{-}tol)_3$ (8.0 mg, 0.026 mmol) under Ar. Anhydrous toluene (2 ml) was added to the flask and sealed, the reaction mixture was stirred at 110 ^oC for 72 h. The solution was diluted with $CHCl_3$, washed with water. The organic layer was dried over $MgSO_4$. The solvent was removed by evaporation under reduced pressure, the solid was purified by precipitation using $CHCl_3$/MeOH mixture and collected by centrifugation (6000 rpm, 60 min), **3.1P3** was obtained as red powder (90 mg, 95%).
T_g: 18.8 ^oC, T_m: 61.4 ^oC. ^1H NMR (CD_2Cl_2, 400 MHz, TMS, 298 K): δ 0.77–0.81 (m, 12H), 1.18–1.35 (m, 100 H), 1.60–1.62 (broad, 4H), 2.50-2.59 (m, 8H), 3.71 (broad, 4H), 3.86 (broad, 4H), 6.38 (s, 4H), 6.54 (s, 2H), 6.78 (s, 2H), 7.44 (s, 2H). ^{13}C NMR (CD_2Cl_2, 100 MHz, 298 K): δ 14.71, 23.52, 24.85, 28.01, 29.89, 30.22, 30.28, 30.38, 30.40, 30.51, 30.57, 31.39, 32.59, 32.77, 37.60, 69.31, 105.06, 115.90, 125.68, 128.63, 130.14, 131.76, 132.71, 132.84, 136.77, 139.81, 142.19, 145.68, 158.56.

Synthesis of 3.1P4: The dark red powder was prepared according to the procedure described for the synthesis of **3.1P1** using compound **3M2 (**81.69 mg, 0.054 mmol), 2,1,3-Benzothiadiazole-4,7-bis(boronicacid pinacol ester) (21 mg, 0.054 mmol), $Pd(PPh_3)_4$ (3.2 mg, 0.003 mmol), Aliquat 336 (1 drop), aqueous potassium carbonate (2M, 1 ml), and toluene (2.5 ml) (30 mg, 37%).
T_g: 63.1 ^oC, T_m: 168.5 ^oC. ^1H NMR (CD_2Cl_2, 400 MHz, 298 K): δ 0.79-0.84 (m, 12H), 1.09-1.27 (m, 100H), 1.60 (broad, 4H), 2.38 (broad, 4H), 2.56 (broad, 4H), 3.76 (broad, 4H), 3.88 (broad, 4H), 6.39 (s, 4H), 6.72 (s, 2H), 7.37 (s, 2H), 7.53 (s, 2H). ^{13}C NMR (CD_2Cl_2, 100 MHz, 298 K): 14.70, 23.51, 24.82, 28.00, 29.96, 30.20, 30.32, 30.48, 30.54, 31.43, 32.47, 32.75, 37.55, 69.32, 105.06, 116.20, 127.77, 128.05, 130.05, 131.73, 131.92, 132.91, 142.01, 144.72, 145.48, 154.98, 158.62.

^{1}H and ^{13}C NMR spectra of the monomers and 3.1P1-3.1P4

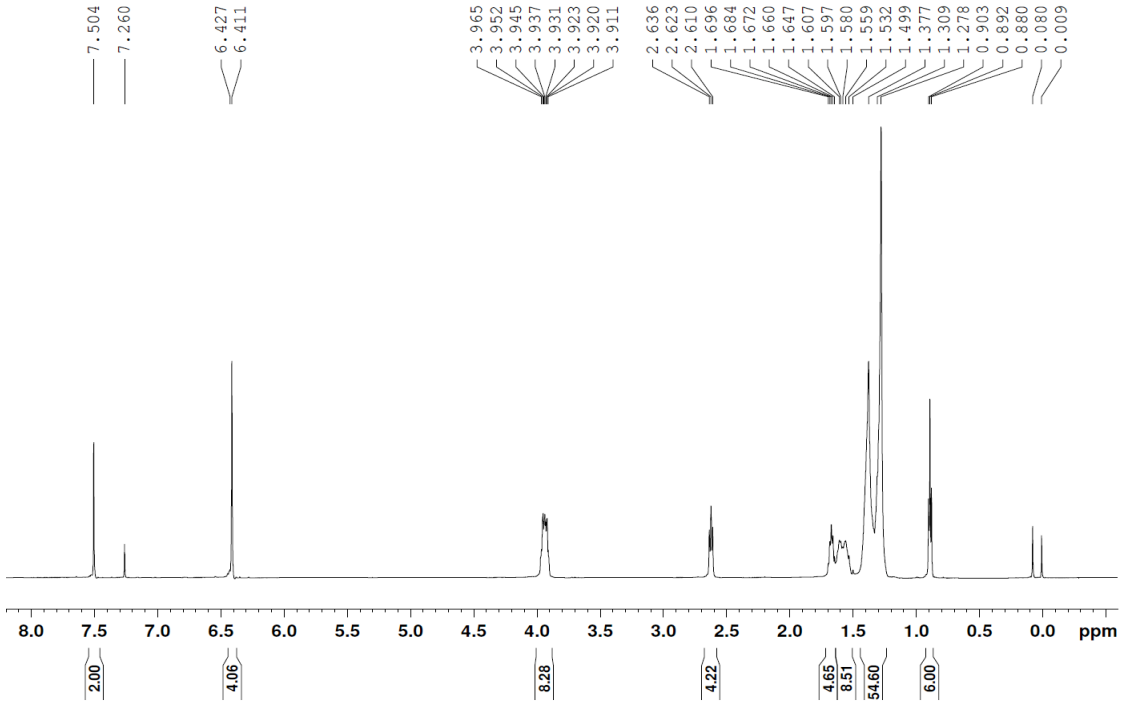

^{1}H NMR spectrum of **3M1**

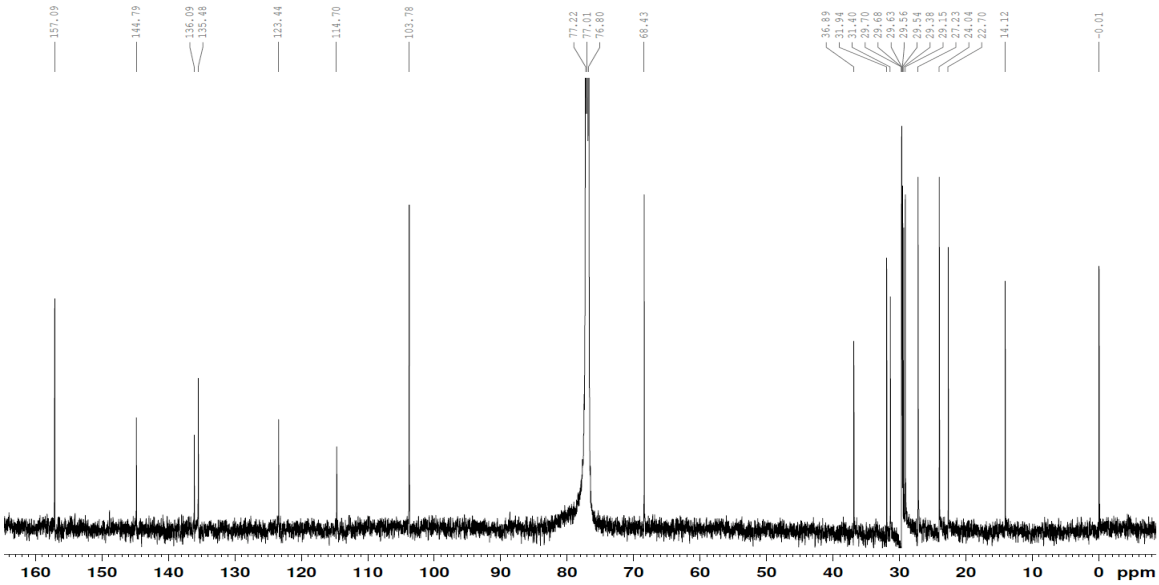

^{13}C NMR spectrum of **3M1**

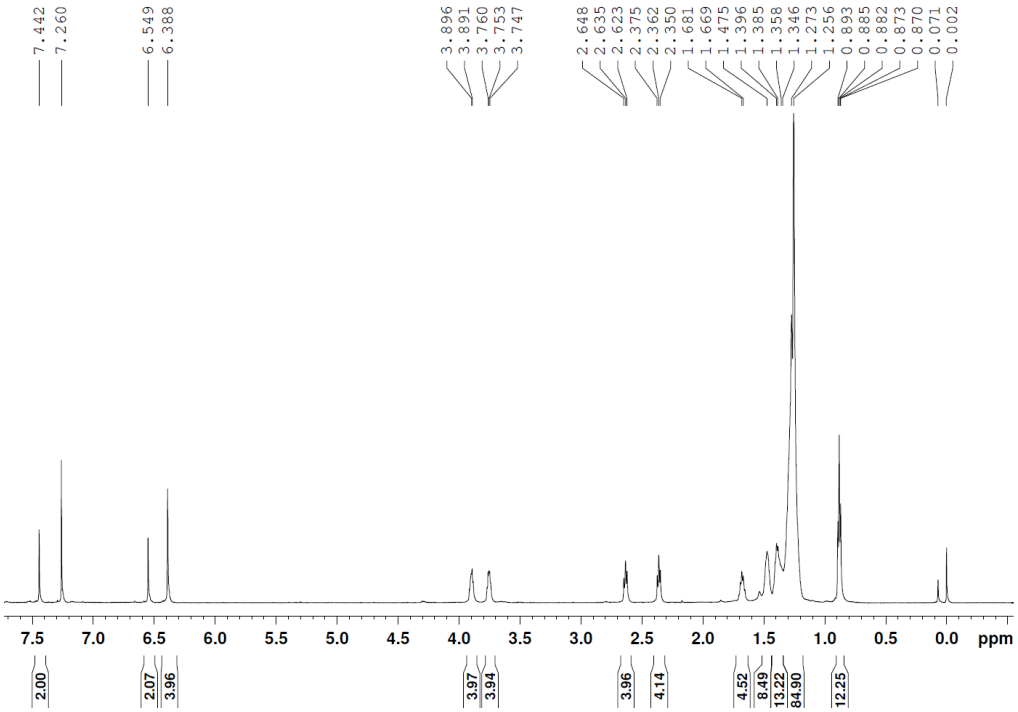

^{1}H NMR spectrum of **3M2**

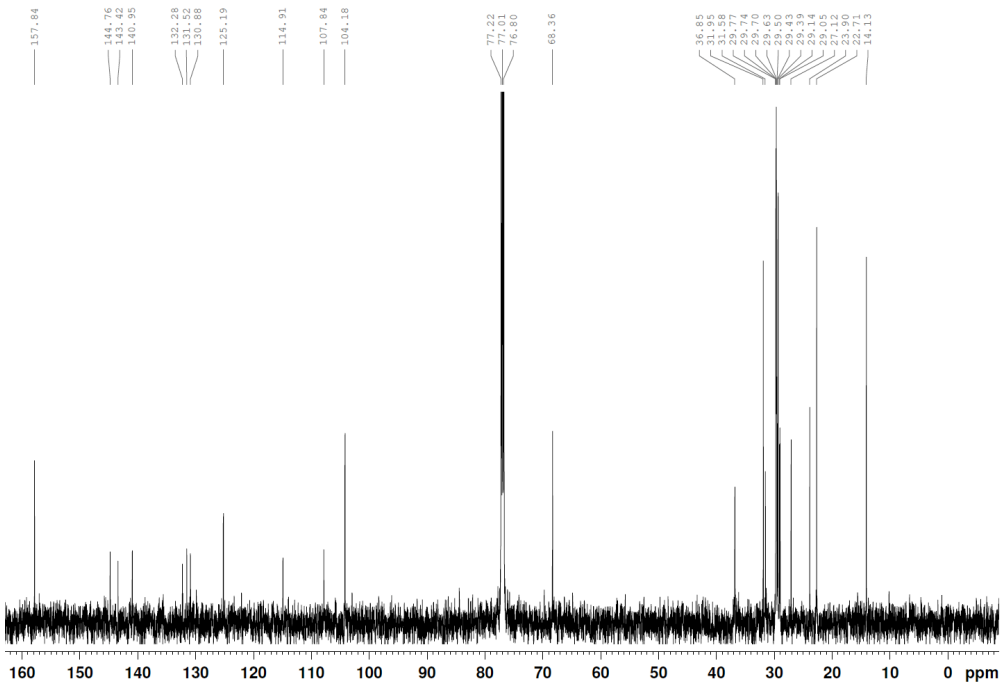

^{13}C NMR spectrum of **3M2**

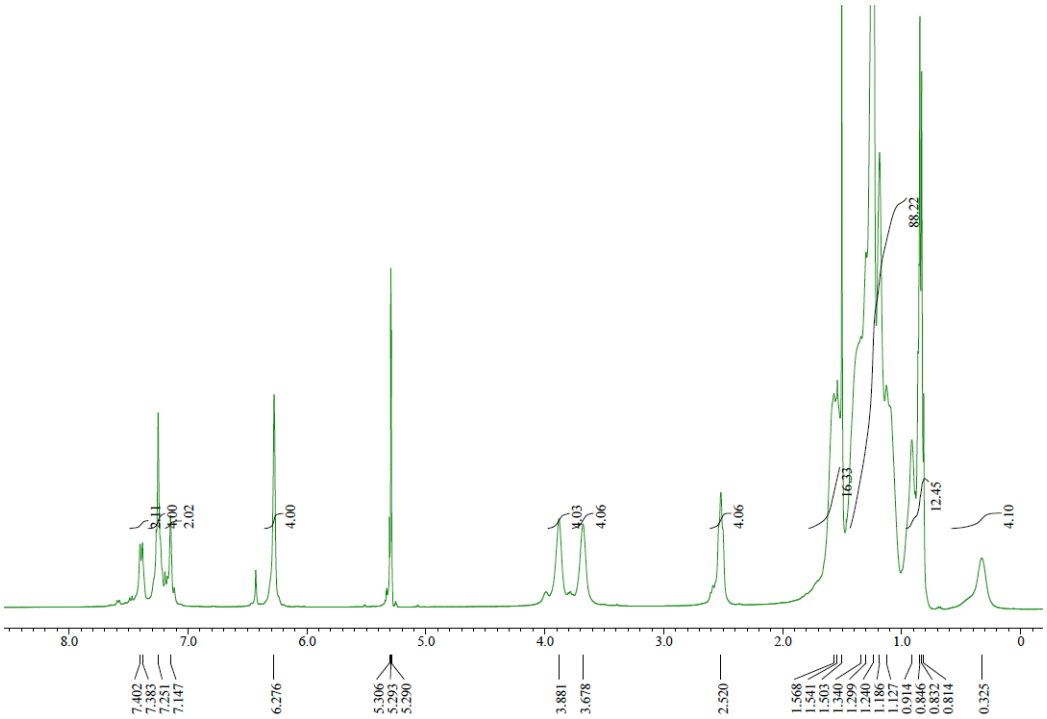

^{1}H NMR spectrum of **3.1P1**

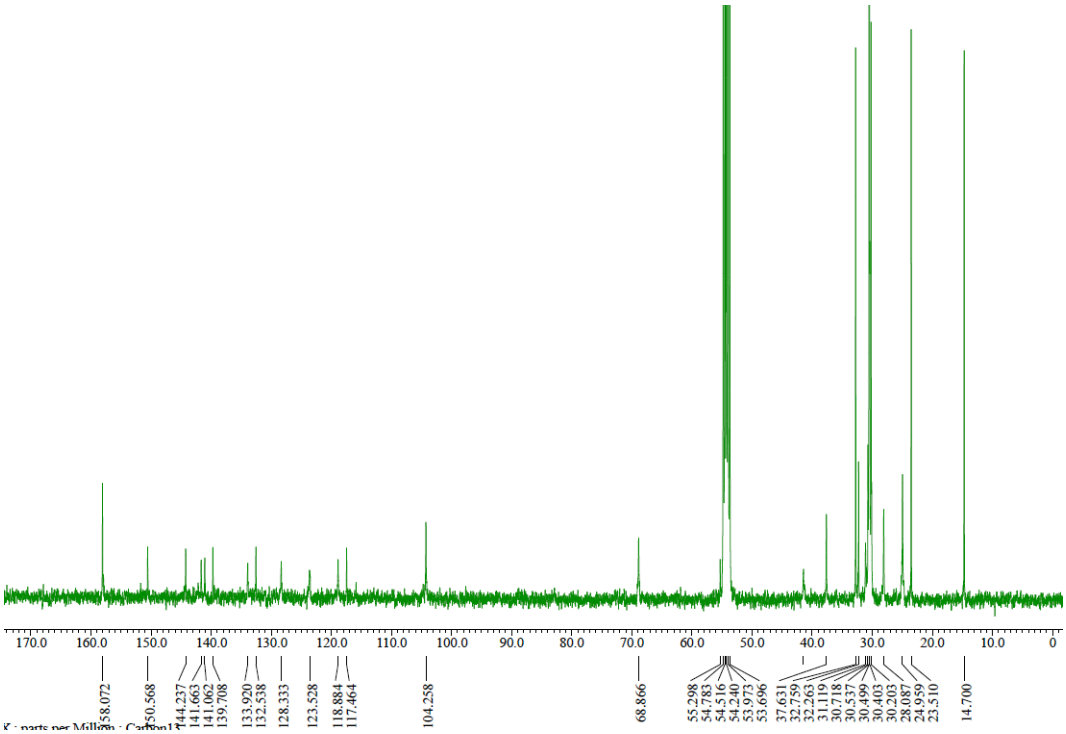

^{13}C NMR spectrum of **3.1P1**

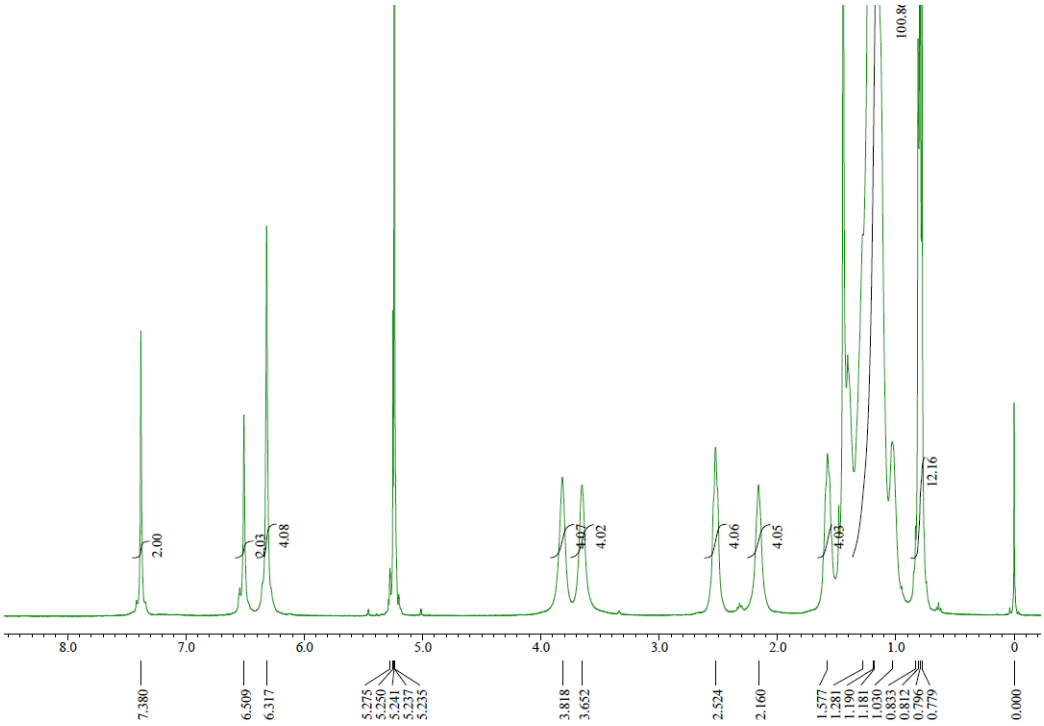

^{1}H NMR spectrum of **3.1P2**

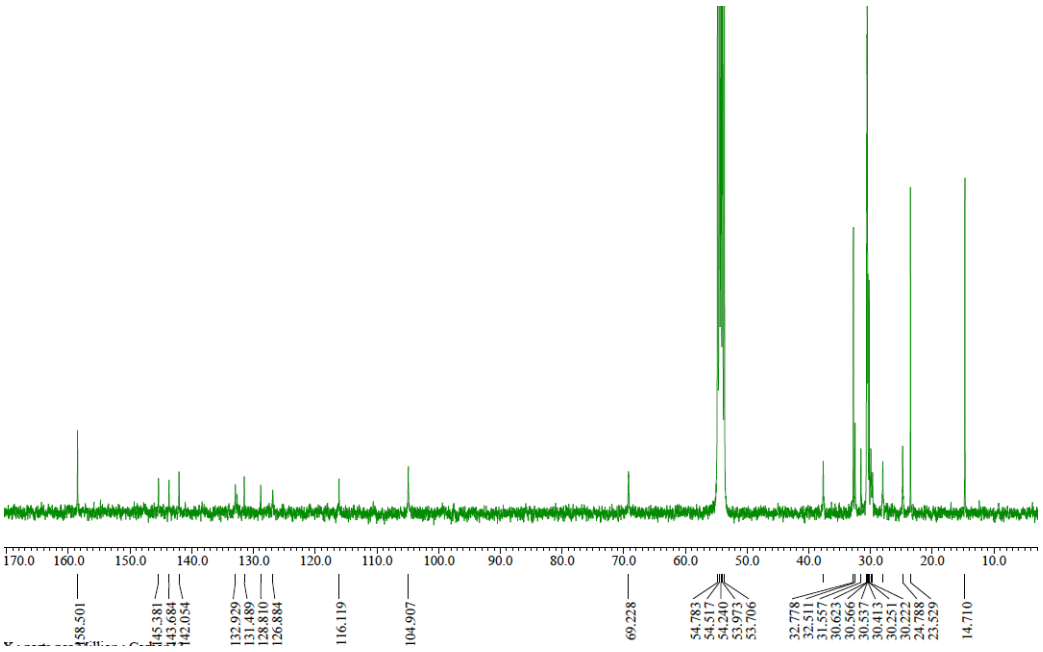

^{13}C NMR spectrum of **3.1P2**

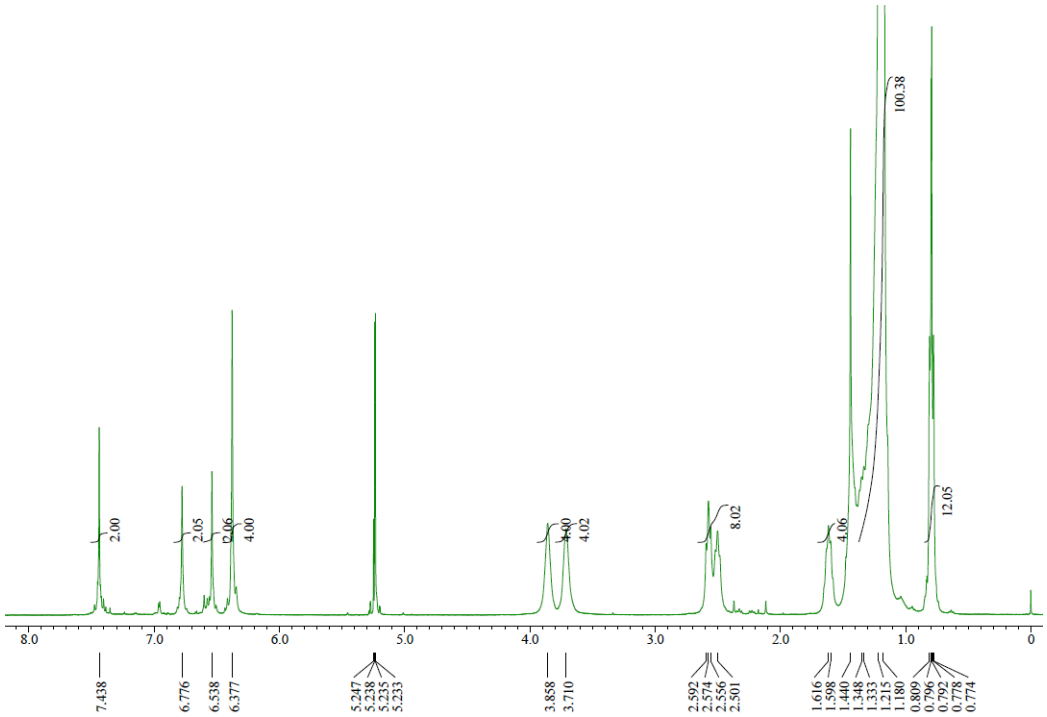

^{1}H NMR spectrum of **3.1P3**

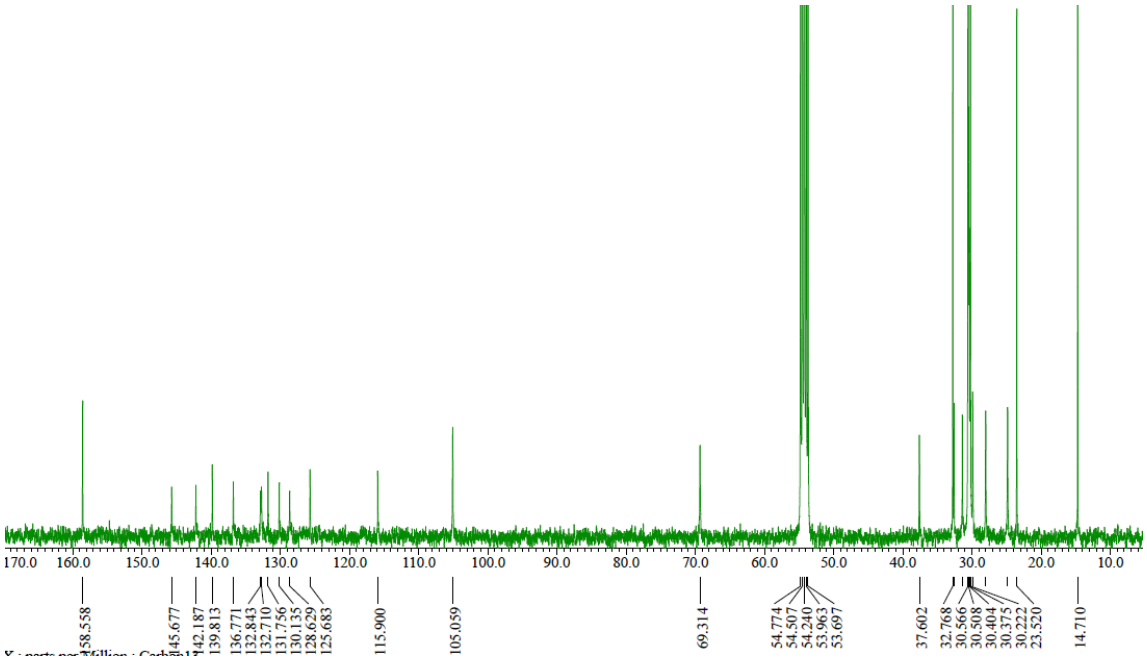

^{13}C NMR spectrum of **3.1P3**

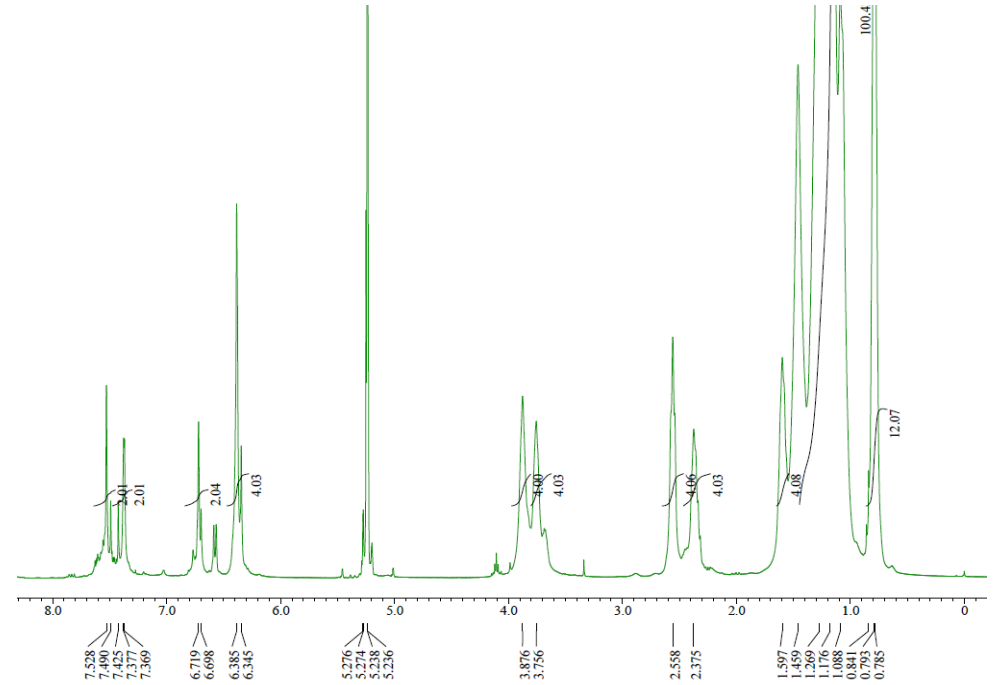

^{1}H NMR spectrum of **3.1P4**

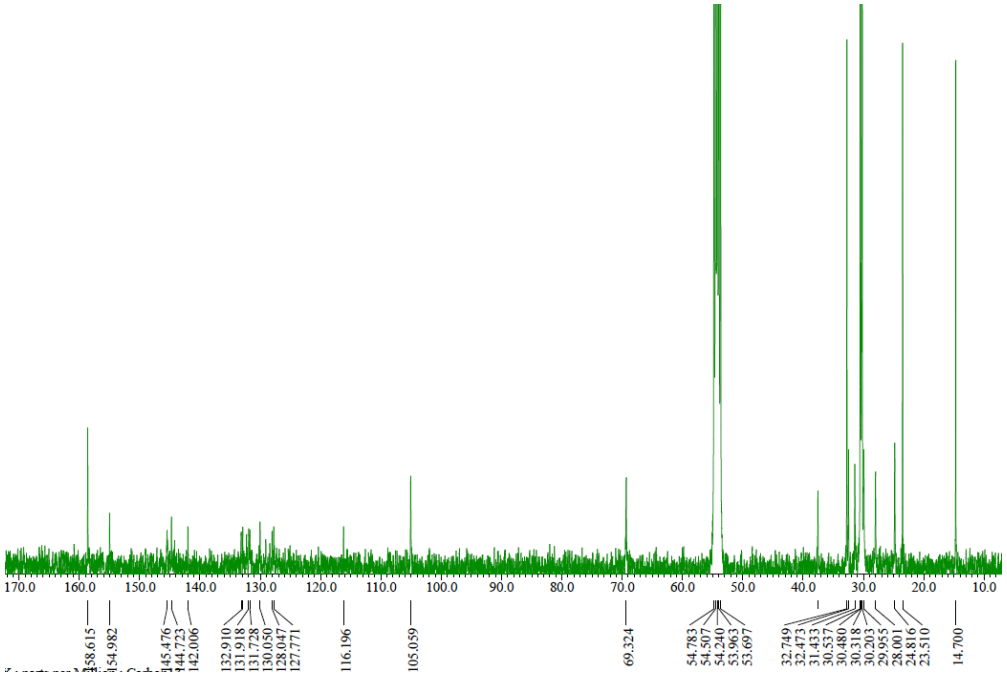

^{13}C NMR spectrum of **3.1P4**

REFERENCES

[1] For selected examples of highly emissive solid materials, see: a) A. Wakamiya, K. Mori, S. Yamaguchi, *Angew. Chem. Int. Ed.* **2007,** *46,* 4273; b) M. Shimizu, Y. Takeda, M. Higashi, T. Hiyama, *Angew. Chem. Int. Ed.* **2009**, *48*, 3653; c) M. Shimizu, T. Hiyama, *Chem. Asian J.* **2010**, *5*, 1516; d) O. Bolton, K. Lee, H. J. Kim, K. Y. Lin, J. Kim, *Nat. Chem.* **2011**, *3*, 205; e) T. Hinoue, M. Miyata, I. Hisaki, N. Tohnai, *Angew. Chem. Int. Ed.* **2012**, *51*, 155.

[2] For comprehensive review on light-emitting polymers, see, A. C. Grimsdale, K. L. Chan, R. E. Martin, P. G. Jokisz, A. B. Holmes, *Chem. Rev.* **2009**, *109*, 897.

[3] a) T. M. Swager, *Acc. Chem. Res.* **2008**, *41*, 1181; b) Z. Chen, J. Bouffard, S. E. Kooi, T. M. Swager, *Macromolecules* **2008**, *41*, 6672; c) J. Bouffard, T. M. Swager, *Macromolecules* **2008**, *41*, 5559.

[4] a) F. Caciall, J. S. Wilson, J. J. Michels, C. Daniel, C. Silva, R. H. Friend, N. Severin, P. Samorì, J. P. Rabe, M. J. O'Connell, P. N. Taylor, H. L. Anderson, *Nat. Mater.* **2002**, *1*, 160; b) S. Brovelli, G. Sforazzini, M. Serri, G. Winroth, K. Suzuki, F. Meinardi, H. L. Anderson, F. Cacialli, *Adv. Funct. Mater.* **2012**, *22*, 4284; c) M. J. Frampton, G. Sforazzini, S. Brovelli, G. Latini, E. Townsend, C. C. Williams, A. Charas, L. Zalewski, N. S. Kaka, M. Sirish, L. J. Parrott, J. S. Wilson, F. Cacialli, H. L. Anderson, *Adv. Funct. Mater*. **2008**, *18*, 3367.

[5] a) M. J. Frampton, H. L. Anderson, *Angew. Chem. Int. Ed.* **2007***, 46,* 1028; b) J. Terao, S. Tsuda, Y. Tanaka, K. Okoshi, T. Fujihara, Y. Tsuji, N. Kambe, *J. Am. Chem. Soc.* **2009**, *131*, 16004; c) C. H. Zhao, A. Wakamiya, S. Yamaguchi, *Macromolecules* **2007**, *40*, 3898; d) L. Chiavarone, M. D. Terlizzi, G. Scamarcio, F. Babudri, G. M. Farinola, F. Naso, *App. Phys. Lett.* **1999**, *75*, 2053.

[6] a) Y. Sagara, T, Kato, *Angew. Chem. Int. Ed*. **2011**, *50*, 9128; b) K. Tanabe, Y. Suzui, M. Hasegawa, T. Kato, *J. Am. Chem. Soc.* **2012**, *134*, 5652.

[7] a) S. S. Babu, J. Aimi, H. Ozawa. N. Shirahata, A. Saeki, S. Seki, A. Ajayaghosh, H. Möhwald, T. Nakanish, *Angew. Chem. Int. Ed*. **2012**, *51*, 3391; b) S. S. Babu, M. J. Hollamby, J. Aimi, H. Ozawa, A. Saeki, S. Seki, K. Kobayashi, K. Hagiwara, M. Yoshizawa, H. Möhwald, T. Nakanishi, *Nat. Commun.* **2013**, *4*, 1969.

[8] J. R. Lakowicz, *Principles of Fluorescence Spectroscopy*, *Third Edition.* Springer, **2006**.

[9] a) *Handbook of Conducting Polymers, Conjugated Polymers* (Eds.: T. A. Skotheim, J. R. Reynolds), CRC Press, Boca Raton, **2007**; b) *Introduction to Organic Electronic and Optoelectronic Materials and Devices* (Eds.: S.-S. Sun, L. R. Dalton), CRS Press, Boca Raton, **2008**.

[10] a) K. Sugiyasu, Y. Honsho, R. M. Harrison, A. Sato, T. Yasuda, S. Seki, M. Takeuchi, *J. Am. Chem. Soc.* **2010**, *132*, 14754; b) Y. Ouchi, K. Sugiyasu, S. Ogi, A. Sato, M. Takeuchi, *Chem. Asian J.* **2012**, *7*, 75; c) R. Shomura, K. Sugiyasu, T. Yasuda, A. Sato, M. Takeuchi, *Macromolecules* **2012**, *45*, 3759.

[11] a) S. M. E. Simpkins, B. M. Kariuki, L. R. Cox, *J. Organomet. Chem.* **2006**, *691*, 5517; b) L. de

Quadras, E. B. Bauer, W. Mohr, J. C. Bohling, T. B. Peters, J. M. Martín-Alvarez, F. Hampel, J. A. Gladysz, *J. Am. Chem. Soc.* **2007**, *129*, 8296.

[12] a) I. F. Perepichka, D. F. Perepichka, H. Meng, F. Wudl, *Adv. Mater.* **2005**, *17*, 2281; b) G. Barbarella, M. Melucci, G. Sotgiu, *Adv. Mater.* **2005**, *17*, 1581; c) A. Mishra, C.-Q. Ma, P. Bäuerle, *Chem. Rev.* **2009**, *109*, 1141.

[13] L. Lunazzi, A. Mazzanti, M. Minzoni, *J. Org. Chem.* **2005**, *70*, 10062.

[14] Our insulated polythiophene[10a] which has planar conjugated backbone is not emissive in the film state despite the sheathed structure, probably due to the efficient intrawire exciton transport.

[15]a) J. Cornil, D. Beljonne, J.-P. Calbert, J.-L. Brédas, *Adv. Mater.* **2001**, *13*, 1053; b) A. Salleo, R. J. Kline, D. M. DeLongchamp, M. L. Chabinyc, *Adv. Mater.* **2010**, *22*, 3812.

[16] The ρ value of MEH-PPV, which is a well-known emissive polymer, is reported to be 0.28.[5d]

[17] G. R. Strobl, *The Physics of Polymers: Concepts for Understanding Their Structures and Behavior*, Springer, **2007**.

[18] C. Ego, D. Marsitzky, S. Becker, J. Zhang, A. C. Grimsdale, K. Müllen, J. D. MacKenzie, C. Silva, R. H. Friend, *J. Am. Chem. Soc.* **2003**, *125*, 437.

[19] R. Abbel, C. Grenier, M. J. Pouderoijen, J. W. Stouwdam, P. E. L. G. Leclère, R. P. Sijbesma, E. W. Meijer, A. P. H. J. Schenning, *J. Am. Chem. Soc.* **2009**, *131*, 833.

[20] A. Adronov, J. M. J. Frechét, *Chem. Commun*. **2000**, 1701.

[21]N. T. Tsui, A. J. Paraskos, L. Torun, T. M. Swager, E. L. Thomas, *Macromolecules* **2006**, *39*, 3350.

[22]a) I. D. W. Samuel, G. A. Turnbull, *Chem. Rev*. **2007**, *107*, 1272; b) M. D. McGehee, A. J. Heeger, *Adv. Mater.* **2000**, *12*, 1655.

[23] X. Feng, W. Pisula, K. Müllen, *J. Am. Chem. Soc*. **2007**, *129*, 14116.

[24] U. Lüning, F. Fahrenkrug, M. Hagen, *Eur. J. Org. Chem.* **2001**, 2161.

[25] A. Jourdant, E. González-Zamora, J. Zhu, *J. Org. Chem.* **2002**, 67, 3163.

[26] Z. Chen, J. Bouffard, S. E. Kooi, T. M. Swager, *Macromolecules* **2008**, *41*, 6672.

[27] X. Guo, S. R. Puniredd, M. Baumgarten, W. Pisula, K. Müllen, *J. Am. Chem. Soc.* **2012**, *134*, 8404.

Chapter 4

Fluorescence Properties of Isolated Conjugated Polymer Blends

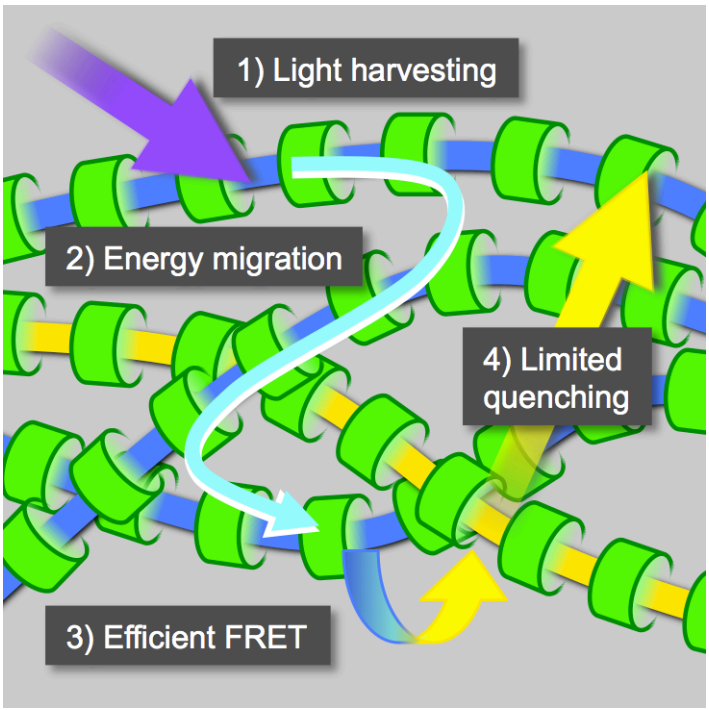

ABSTRACT: *Fluorescence properties of conjugated polymer blends were investigated using a combination of excitation energy donor and acceptor conjugated polymers encapsulated by identical cyclic sidechains. Wearing this 'uniform', the polymers did not segregate or phase-separate in the blends. As such, these polymers provide an effective ensemble for designing fluorescent polymeric materials.*

INTRODUCTION

Conjugated polymer (CP) blends have attracted much attention in the fabrication of organic electronic devices, as they allow for tuning of the photophysical, electronic, and mechanical properties of polymeric materials.1 Polymer blends can be briefly understood based on the free energy of mixing (ΔG_m) that determines whether a system undergoes phase-separation: $\Delta G_m = \Delta H_m - T\Delta S_m$, where ΔH_m and ΔS_m are the enthalpy and entropy of mixing, respectively. For polymer blends, the contribution of ΔS_m is very small as compared with that of low-molecular weight materials. Consequently, polymer blends, in most cases, result in phase separation ($\Delta G_m > 0$). The CP-based phase-separated structures are endowed with a variety of functions originating from the combination of the distinct polymeric domains, which offers many opportunities for the optimization of device performance.[1, 2] However, control over the phase-separated structures–a process that involves a complex interplay between kinetics and thermodynamics–is yet to be established,[3] and this intricate process has, to a certain extent, hampered CPs from further applications.[1] As such, blending processes are optimized for the occurrence of phase separation; alternatively, we wonder whether phase-separation is necessarily required. Polymer blends *without* phase-separation can be optically clear and thermodynamically stable. In addition, their photophysical properties are predictable as a function of the blending ratio and remain unchanged over time. Such CP-based materials will be useful for light-emitting applications such as sensors, lasers, and displays. To this end, ΔH_m, which is particularly significant in CP based blends, needs to be considered from a molecular design viewpoint.

Recently, a new type of CPs—so-called isolated CPs or insulated molecular wires–has attracted much attention.[4,5] Being interested in their unique structure-property relationships, we have designed and synthesized CPs of this kind based on a variety of conjugated backbones encapsulated by the same cyclic sidechains.[6] Owing to the absence of π–π staking, they are highly fluorescent even in the solid state. Remarkably, we found from AFM observations that these polymers were miscible. Such miscibility enabled facile mixing of fluorescence colors, which produced a white fluorescent polymeric film.[6] Although detailed photophysical studies on the polymer blends still remain to be conducted, we assert that their structural similarity and intrinsically weak inter-polymer interactions (i.e. the absence of π–π stacking) dictate the contribution of ΔH_m to be small compared to those in conventional CP blends. Intrigued by this unique structure-property relationship, we wanted to compare the photophysical properties of CP blends with and without phase separation. In this chapter, we studied fluorescence properties of isolated CP blends. Though isolated CPs are expected to be good fluorescent materials, their blended systems have scarcely been investigated.[5b,c] We show that the absence of phase-separation in the isolated CP blends is indeed advantageous for the creation of CP based fluorescent materials.

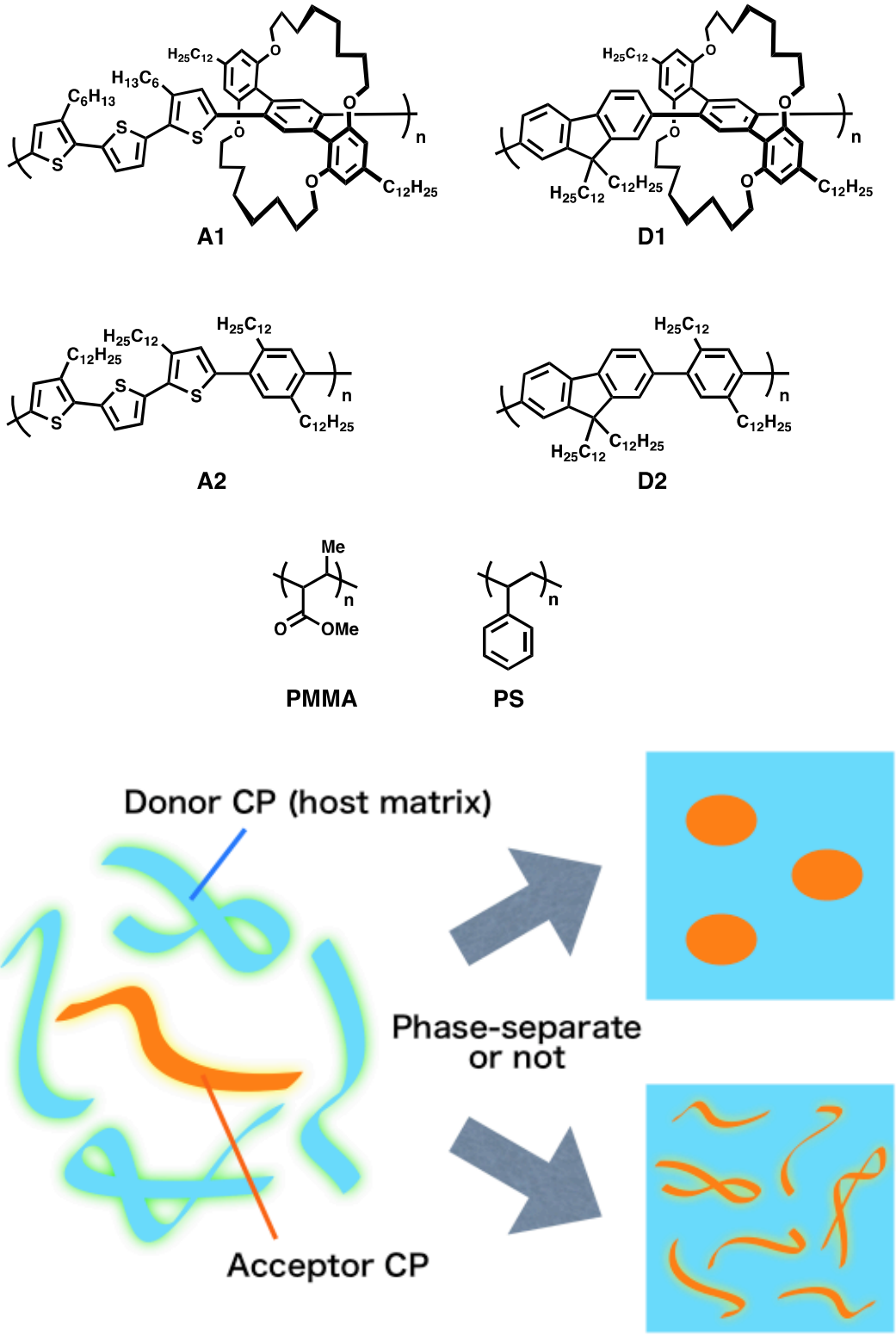

Chart 4-1. Structures of polymers used in this chapter and schematic illustration of the polymer blends with and without phase-separation.

***** In this chapter, we used **3.1P1** in Chapter 3 as **D1**.

In this chapter, we used thiophene- (**A1** and **A2**) and fluorene-based CPs (**D1*** and **D2**) (Chart 4-1) as a combination that promotes fluorescence resonance energy transfer (FRET). Isolated **A1** –a yellow fluorescent energy-accepting CP– was synthesized according to similar procedures in Chapter 3. **A2** is a reference polymer that has the same conjugated backbone as **A1** but is not sheathed. Poly(methyl methacrylate) (**PMMA**), polystyrene (**PS**), **D1**, and **D2**, were used as host polymer matrices for **A1** or **A2**. In the polymer blends, blue fluorescent isolated **D1** and naked **D2** act as energy-donating CPs for **A1** and **A2** owing to the overlap between the donor fluorescence and acceptor absorption (Figure 4-1).

RESULTS AND DISCUSSION

Photophysical Properties of A1. Figure 4-2 shows the absorption and fluorescence spectra of **A1** in diluted solution and pristine film. Because interpolymer electronic communication is prevented by the cyclic sidechains, **A1** shows virtually identical spectra in solution and film, displaying fluorescence quantum yields (Φ_F) of 0.36±0.01 and 0.15±0.01, respectively. As reported previously, [4-6] $\Phi_{F(film)}$s of isolated CPs are relatively high among fluorescent CPs but are not as high as Φ_f (solution)s; this indicates that exciton migration through long-range dipole-dipole interactions among the isolated CP chains is not completely suppressed in the film.

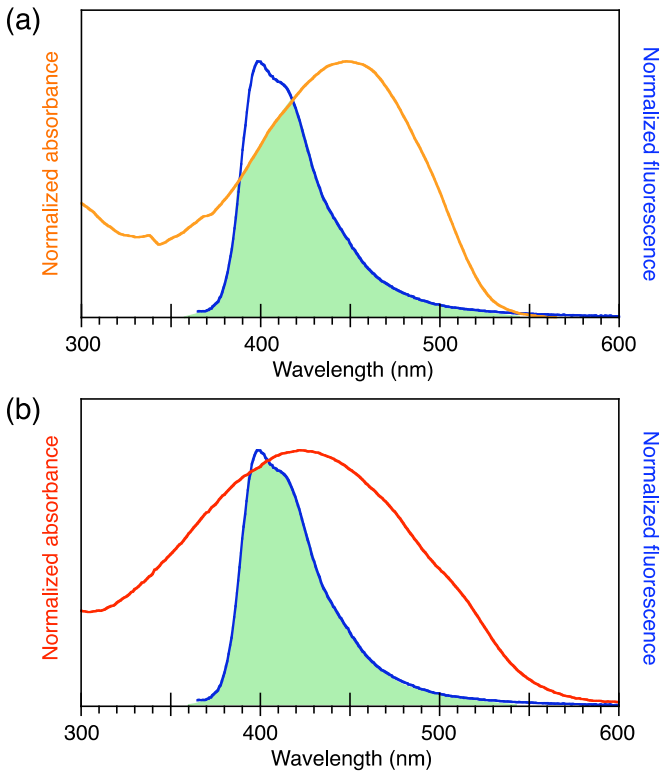

Figure 4-1. Spectral overlap between the emission of **D1** (blue line) and absorption of (a) **A1** and (b) **A2** in the film state.

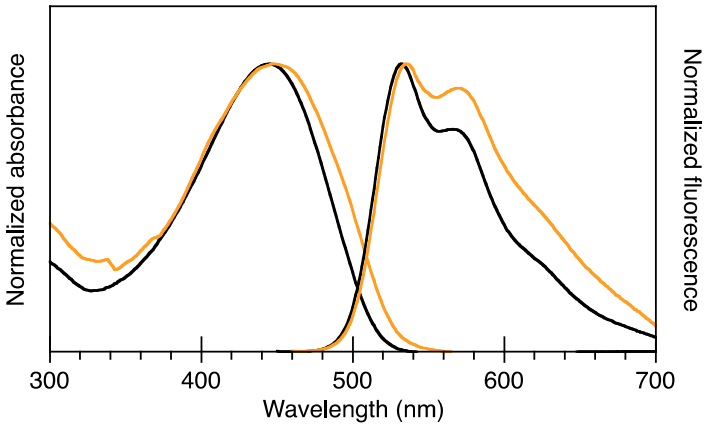

Figure 4-2. Absorption and fluorescence spectra of **A1** in solution (black, dichloromethane) and film form (orange). λ_{ex} = 445 and 447 nm for solution and film, respectively.

Solvent Effects. Notably, $\Phi_{F(solution)}$s of **A1** were independent of the solvent (Table 4-1 and Figure 4-3), indicating that Φ_f of **A1** is not significantly affected by the polarity of the matrix. Therefore, changes in Φ_f (matrix) of **A1** in the different polymer matrices (**PMMA**, **PS**, **D1**, or **D2**, see below) can be attributed not to the difference in the refractive indices of these polymer matrices but to the difference in the local concentration (i.e. phase-separation) of **A1** in the blends.

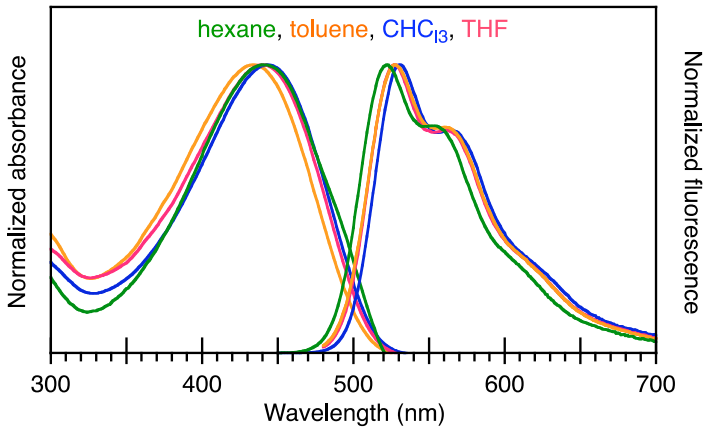

Figure 4-3. Absorption and fluorescence spectra of **A1** in different solvents.

Table 4-1. Fluorescence quantum yields (Φ_F)s of **A1** in different solvents.

A1 in different solvents	Fluorescence QY
Toluene	0.36
THF	0.37
DCM	0.35

Surface Morphologies of Polymer Blends. Polymer blends of **A1/D1**, **A1/PMMA**, **A1/PS**, and **A2/D1** systems were investigated by AFM (Figure 4-4). **A1** was not miscible with **PMMA** or **PS** even when the **A1** content was as low as 10% (wt/wt). In contrast, **A1** and **D1** appeared to be miscible as we did not observe any phase-separated morphology in the blended films, probably because both polymers are sheathed by the identical cyclic sidechains. In fact, unsheathed **A2** underwent phase separation with sheathed **D1**. This assertion will be further supported by the photophysical studies discussed below.

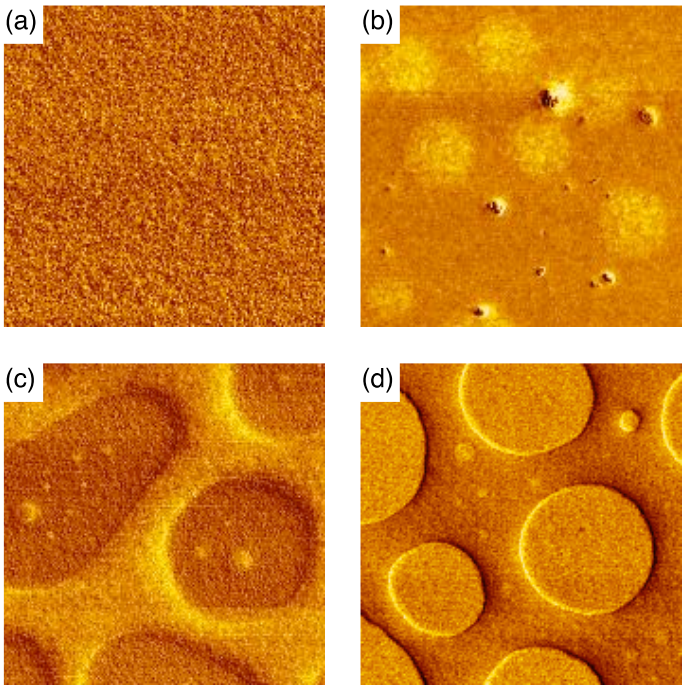

Figure 4-4. AFM phase images of polymer blends prepared from (a) **A1/D1**, (b) **A2/D1**, (c) **A1/PMMA**, and (d) **A1/PS**; 1:1 wt/wt%; 2 μm × 2 μm.

Matrices Effects on Fluorescence Maxima. Fluorescence spectra of sheathed **A1** and unsheathed **A2** were measured in different media as a function of concentration (Figure 4-5). The fluorescence maxima of both polymers were unchanged upon concentration in toluene solution (Figure 4-5, black marks). As can be expected from the result of Figure 4-2, the fluorescence spectra of **A1** were insensitive to concentration owing to its isolation even at very high concentrations. In contrast, the fluorescence maximum of **A2** in a **D1** matrix significantly changed upon increasing concentration (Figure 4-5, orange diamonds). The red shifted fluorescence observed under higher concentrations indicates that **A2** self-assembles and phase-separates in **D1** host matrix.

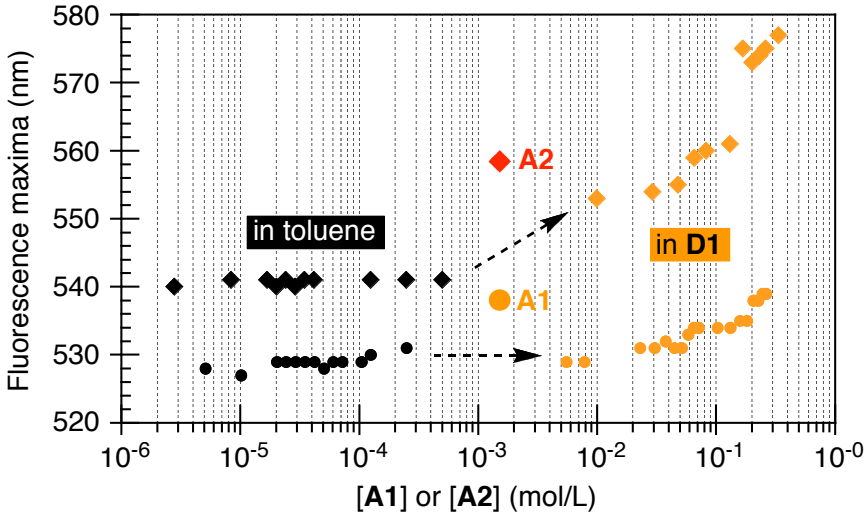

Figure 4-5. Plots of fluorescence maxima of **A1** (filled circle) and **A2** (filled diamonds) as a function of their concentrations measured in a toluene solution (black) and **D1** matrix (orange). λ_{ex} = 480 and 450 nm for **A1** and **A2**, respectively.

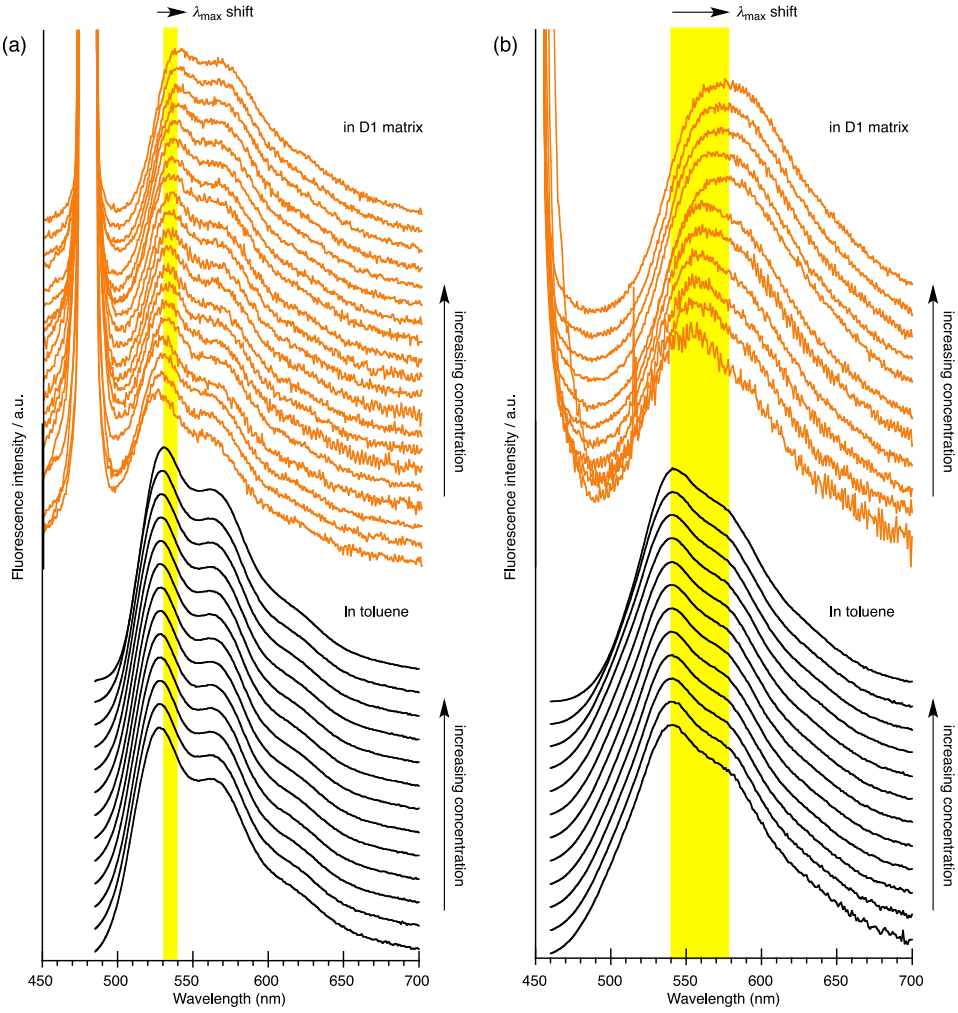

Figure 4-6. Fluorescence spectra, shown in a stacked mode, of (a) **A1** and (b) **A2** in toluene (black lines) and **D1** matrix (orange lines) measured as increasing their concentration. λ_{ex} = 480 and 450 nm for **A1** and **A2**.

Matrices Effects on Fluorescence QY of A1. Next, we evaluated Φ_f of **A1** in different media (Figure 4-7). In toluene, $\Phi_{F(solution)}$ was rapidly decreased upon increasing the **A1** concentration, which is thought to be due to a dynamic quenching process that accompanies collisional encounters between **A1** chains. When diluted in **PS** and **D2** matrices, **A1** showed relatively high Φ_f (matrix)s; however, the values abruptly decreased upon increasing the **A1** concentration. Lower Φ_f (matrix)s under concentrated conditions are consistent with Φ_f (film) of the pristine **A1** film; therefore, we conclude that phase-separation was induced above the concentration at which Φ_F discontinuously deteriorated. In **PMMA**, $\Phi_{F(matrix)}$ was low throughout the concentration range investigated. We infer that **A1** and **PMMA** are not miscible and phase-separate even at lower concentrations; in fact, **A1** was not soluble in esters such as ethyl acetate. In contrast to the above observations, $\Phi_{F(matrix)}$ of **A1** in the **D1** matrix was maintained at moderate values even at higher concentrations (Figure 4-7, orange circles). The gradual decrease in Φ_F is probably due to physical contacts between **A1** chains in the blend, which give rise to a sort of static quenching process. This result indicates that transition behaviors like phase-separation were not induced in the **A1**/**D1** blend.

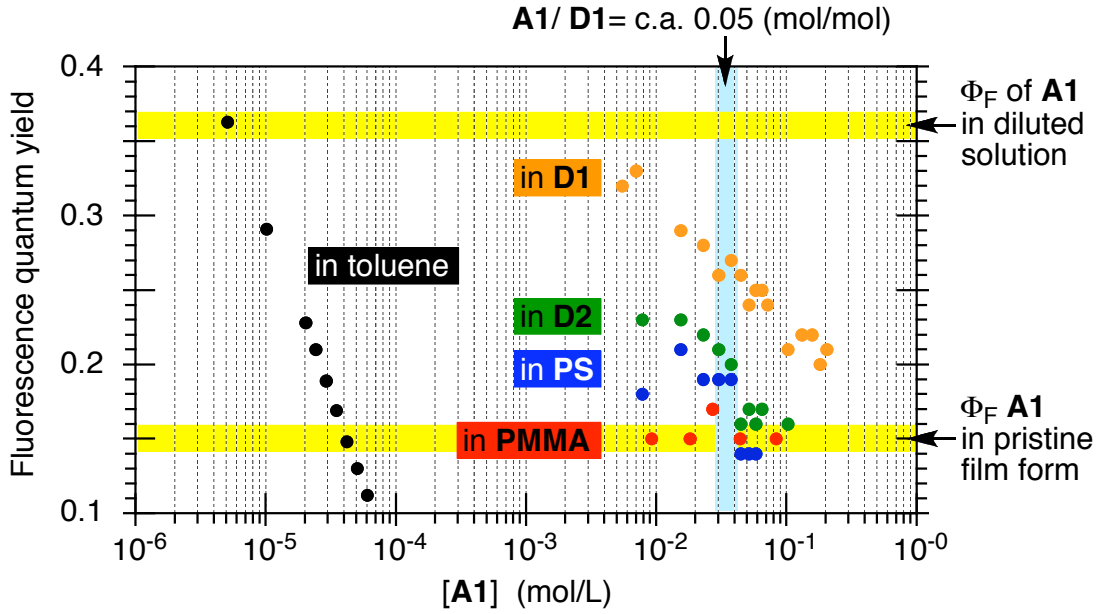

Figure 4-7. Plots of fluorescence quantum yields of **A1** measured in different matrices as a function of concentration: in toluene solution (black), and in **D1** (orange), **D2** (green), **PS** (blue), and **PMMA** matrices (red). λ_{ex} = 480 nm.

Lidzey and co-workers investigated a polymer blend that comprises CP and **PS** by using scanning near-field optical microscopy (SNOM)[3a] and found that in the PS-rich phase, interchain exciton diffusion between CPs is significantly suppressed by dilution. Similarly, we expect that interchain exciton diffusion among A1s can be prevented in **D1** because **A1** is not locally concentrated (no phase-separation). Therefore, **A1** can have a better Φ_f in the **D1** matrix than in the pristine film and other host matrices.

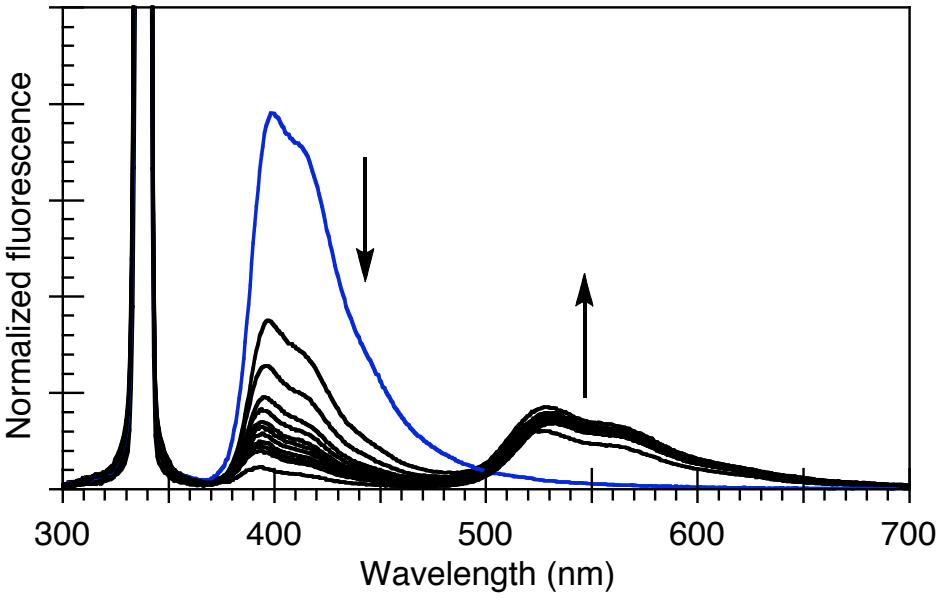

Figure 4-8. Fluorescence spectra of **A1**/**D1** blended films measured with increasing the **A1** ratio.). λ_{ex} = 338 nm.

FRET Studies of A1/D1 Blend. Because the absorption of **A1** overlaps well with the fluorescence of **D1** (Figure 4-1), FRET can occur from **D1** to **A1** in their polymer blends. Absorption and fluorescence spectra of **A1**/**D1** blends with different molar ratios are shown in Figure 4-8. Note that **D1** was selectively excited under the measurement conditions (λ_{ex} = 338 nm). With the addition of the **A1** acceptor, the fluorescence of the **D1** donor was significantly quenched while the fluorescence of **A1** appeared. The excitation spectrum (λ_{moni} = 580 nm) of the blend suggested a contribution of the excited **D1** to **A1** fluorescence. (Figure 4-9) In addition, the fluorescence lifetime of **D1** decreased with the addition of **A1**, evidencing the energy transfer (Figure 4-10).

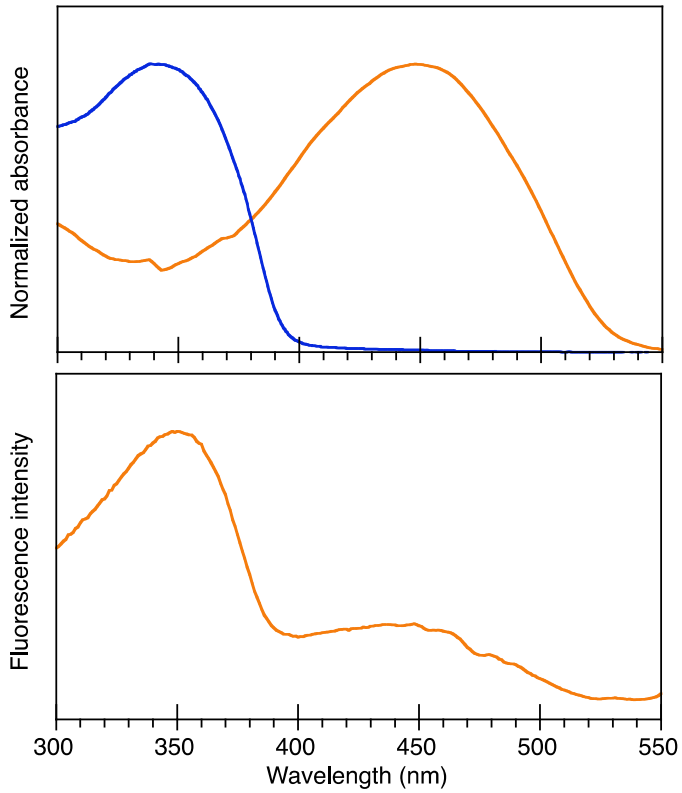

Figure 4-9. (a) Absorption spectra of **A1** (orange) and **D1** (blue) in their film forms. (b) Excitation spectrum of the **A1**/**D1** blend (15%, wt/wt) monitored at 580 nm, which indicates the contribution of absorption by **D1** to the fluorescence of **A1**.

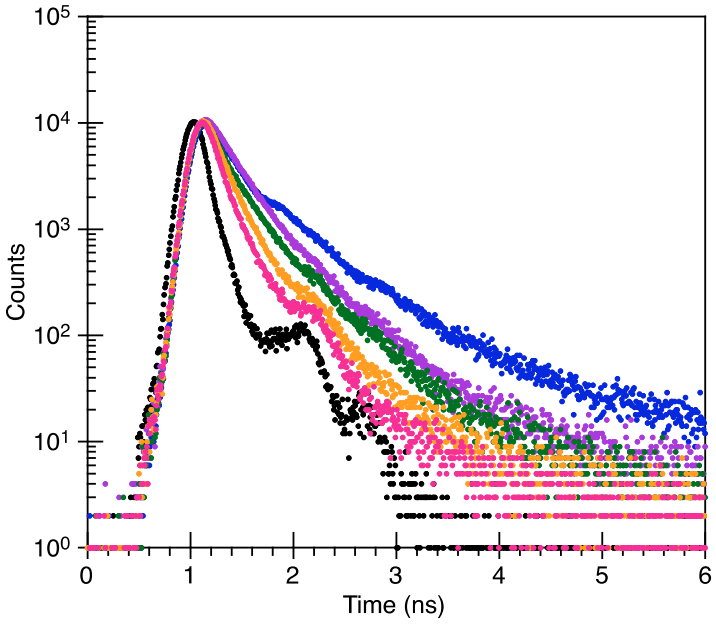

Figure 4-10. Fluorescence lifetime decay of **A1**/**D1** blend at different ratios: outer (blue) to inner (red), 0, 1, 3, 5, 15% of **A1** was blended into **D1**: black: IRF, λ_{ex} = 375 nm, λ_{moni} = 420 nm. These results indicate the excited energy transfer from **D1** to **A1** in the blended films.

Since the fluorescence spectra of **A1** and **D1** are well resolved and able to be integrated individually, the number of photons emitted from each polymer can be determined (Figure 4-11). This number was then divided by the number of photons absorbed by **D1** and is plotted in Figure 4-12. The values for **D1** correspond to Φ_F D, and changes in Φ_F D yield FRET efficiency (ϕFRET = 1– Φ_f D/ Φ_f D_0, Figure 4-12, green line). On the other hand, we defined the values for **A1** as the fluorescence efficiencies of **A1** (Φ_F A). Here, Φ_F A can be described as ϕ FRET Φ_F A(in **D1**), and as discussed above, Φ_F A(in **D1**) is larger than Φ_F A(film). Consequently, as indicated by the yellow bar and orange line in Figure 4-12, the blended systems showed better fluorescence efficiency than isolated CP film when ϕFRET was high (**A1**/**D1** > 0.02).

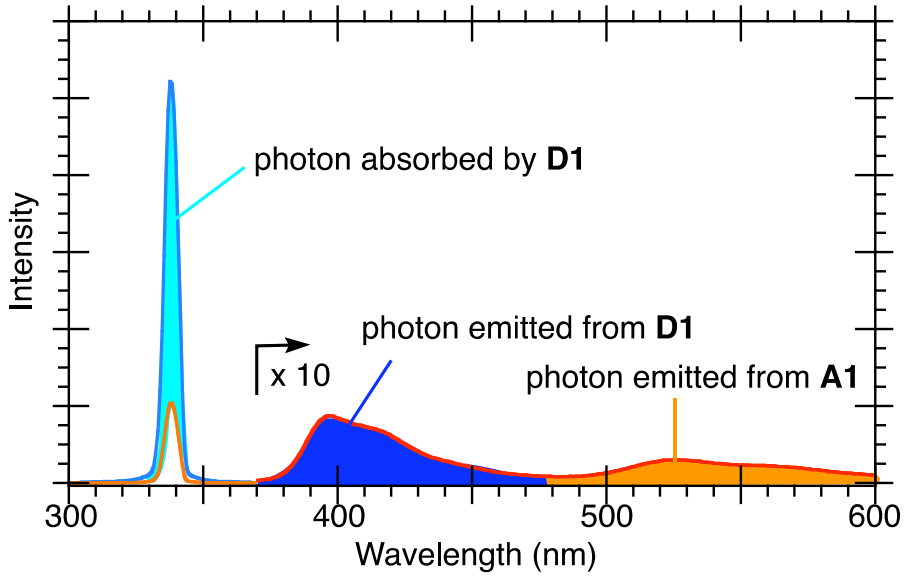

Figure 4-11. Fluorescence spectra of **A1**/**D1** blended films ([**D1**] = 1 mol%) excited at 338 nm. The values calculated based on this measurement are plotted in **Figure 4-12**.

We note that such a photophysical scheme–sensitization via FRET and suppression of quenching by 'dilution' effects in a donor host–can be readily realized with small molecules because their large entropy of mixing allows for facile blending of a donor/acceptor ensemble.[7] Some of these systems have found application in efficient organic light-emitting devices.[8] In this chapter, we have succeeded in realizing the same scheme using CPs through preventing dissimilar conjugated backbones from phase separation by molecular design.

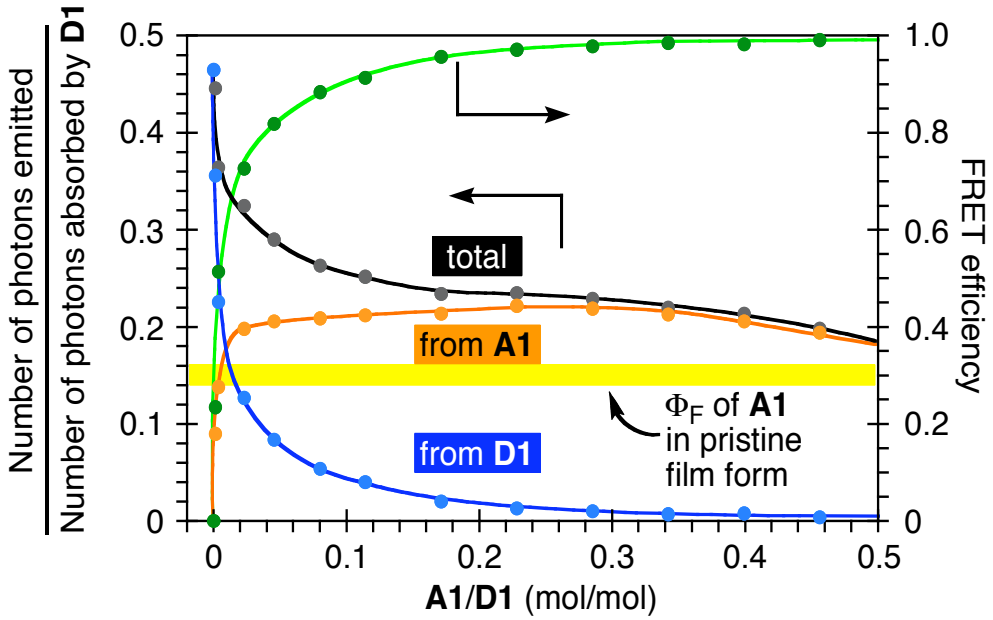

Figure 4-12. Plots of the fluorescence (left y-axis) and FRET (right y-axis) efficiencies of the **A1**/**D1**. The x-axis, mol/mol ratio, is in terms of monomer units. Color lines act as eye-guilds, while the yellow bar indicates the Φ_F of **A1** in the pristine film. λ_{ex} = 338 nm.

CONCLUSION

In this chapter, on the basis of the microscopic and spectroscopic studies, we have shown that isolated CPs encapsulated by the identical cyclic sidechains make an effective host-guest ensemble for designing fluorescent polymeric materials. The fluorescence scheme established in the blend is as follows: (1) light-harvesting by **D1** with large absorption; (2) energy migration among **D1** units; (3) FRET from **D1** to **A1**; (4) suppression of the quenching process of **A1** by the dilution effect; and (5) preservation of the fluorescence color of **A1** owing to the encapsulation. We believe this material design concept demonstrates a new potential of isolated CPs and will find various applications in sensors, lasers, and displays.

EXPERIMENTAL SECTION

The polymer **A1** was synthesized by following the procedure of **3.1P3** as mentioned in Chapter 3.

Characterization of Polymer A1: ^{1}H NMR (CD_2Cl_2, 400 MHz, TMS, 298 K, see below): δ 0.83-0.87 (m, 12H), 1.25-1.40 (m, 76H), 1.66-1.69 (m, 4H), 2.57 (t, J = 7.6 Hz, 4H), 2.64 (t, J = 7.6 Hz, 4H), 3.77 (m, 4H), 3.92 (m, 4H), 6.44 (s, 4H), 6.61 (s, 2H), 6.84 (s, 2H), 7.50 (s, 2H). ^{13}C NMR (CD_2Cl_2, 100 MHz, TMS, 298 K, see below): δ 13.90, 22.65, 22.68, 24.01, 27.17, 29.04, 29.18, 29.36, 29.41, 29.51, 29.66, 29.71, 30.49, 31.73, 31.92, 36.74, 68.49, 104.22, 115.04, 124.86, 129.31, 130.91, 131.86, 132.00, 141.36, 157.72. M_n = 19.6K, M_w = 36.5K against polystyrene standard.

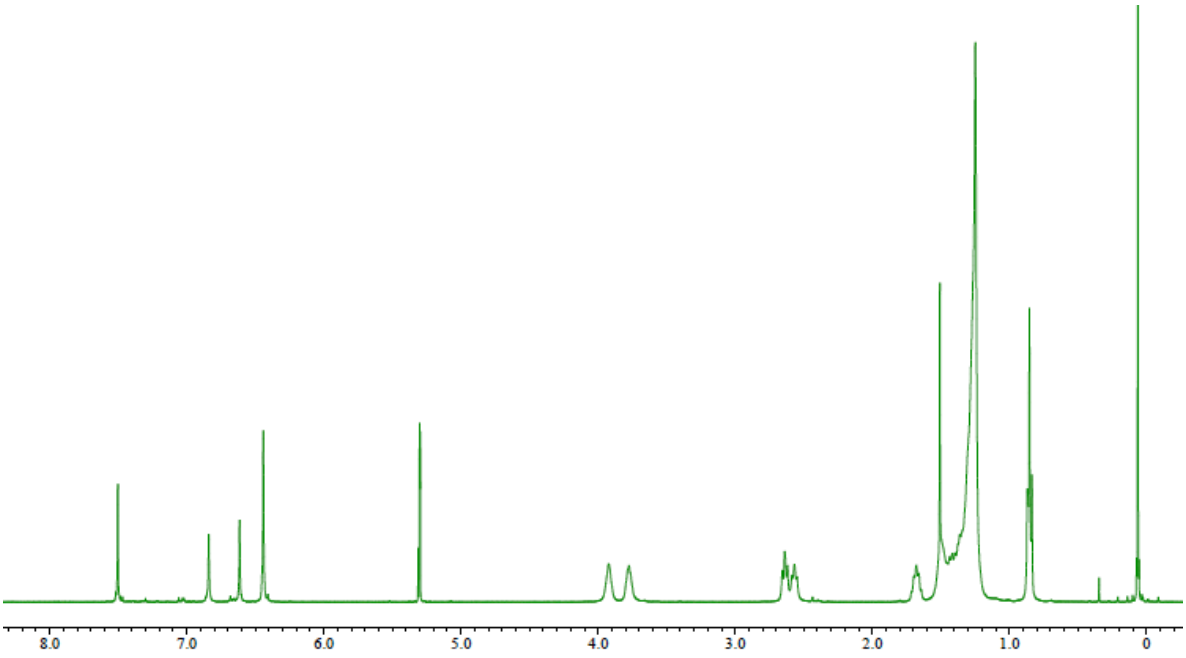

^{1}H NMR spectrum of **A1**

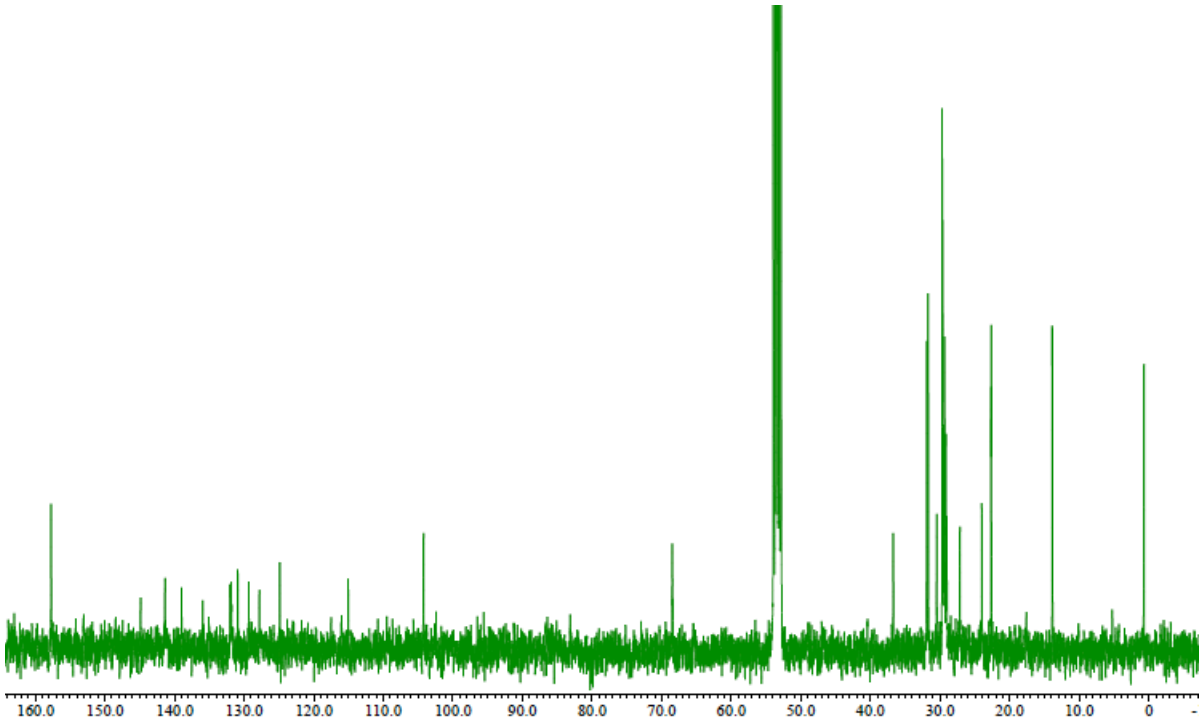

^{13}C NMR spectrum of **A1**

REFERENCES

[1] C. R. McNeil, N. C. Greenham, *Adv. Mater*. **2009**, *21*, 3840, and references are cited therein. The CPs-based blends are useful for photovoltaics and electroluminescence, and only references of the latter, which are relevant to the present study, are cited in ref. 2.

[2] a) M. Berggren, O. Inganäs, G. Gustafsson, J. Rasmusson, M. R. Andersson, T. Hjertberg, O. Wennerström, *Nature* **1994**, *372*, 444; b) E. J. W. List, S. Tasch, C. Hochfilzer, G. Leising, P.Schlichting, U. Rohr, Y. Geerts, U. Scherf, K. Müllen, *Opt. Mater.***1998**, *9*, 183; c) M. M. Alam, C. J. Tonzola, S. A. Jenekhe, *Macromolecules* **2003**, *36*, 6577; d) N. Ananthakrishnan, G. Padmanaban, S. Ramakrishnan, J. R. Reynolds, *Macromolecules* **2005**, *38*, 7660; e) P.-I Shih, Y.-H Tseng, F.-I Wu, A. K. Dixit, C.-F. Shu, *Adv. Funct. Mater*. **2006**, *16*, 1582.

[3] a) A. Cadby, R. Dean, A. M. Fox, R. A. L. Jones, D. G. Lidzey, *Nano Lett*. **2005**, *5*, 2232; b) J. Chappell, D. G. Lidzey, P. C. Jukes, A. M. Higgins, R. L. Thompson, S. O'Connor, I. Grizzi, R. Fletcher, J. O'Brien, M. Geoghegan, R. A. L. Jones, *Nature Mater*. **2003**, *2*, 616-621; c) J. E. Slota, E. Elmalem, G. Tu, B. Watts, J. Fang, P. M. Oberhumer, R. H. Friend, W. T. S. Huck, *Macromolecules* **2012**, *45*, 1468.

[4] a) M. J. Frampton, H. L. Anderson, *Angew. Chem. Int. Ed.* **2007**, *46*, 1028; b) T. M. Swager, *Acc. Chem. Res.* **2008**, *41*, 1181; c) J. Terao, *Polym. Chem*. **2011**, *2*, 2444; d) D. J. Cardin, *Adv. Mater*. **2002**, *14*, 553.

[5] Recent selected examples of isolated CPs, see: a) F. Cacialli, J. S. Wilson, J. J. Michels, C. Daniel, C. Silva, R. H. Friend, N. Severin, P. Samorì, J. P. Rabe, M. J. O'Connell, P. N. Taylor, H. L. Anderson, *Nat. Mater*. **2002**, *1*, 160; b) S. Brovelli, G. Sforazzini, M. Serri, G.Winroth, K. Suzuki, F. Meinardi, H. L. Anderson, F. Cacialli, *Adv. Funct. Mater*. **2012**, *22*, 4284; c) F. D. Stasio, P. Korniychuk, S. Brovelli, P. Uznanski, S. O. McDonnell, G. Winroth, H. L. Anderson, A. Tracz, F. Cacialli, *Adv. Mater.* **2011**, *23*, 1855; d) M. J. Frampton, G. Sforazzini, S. Brovelli, G. Latini, E. Townsend, C. C. Williams, A. Charas, L. Zalewski, N. S. Kaka, M. Sirish, L. J. Parrott, J. S.Wilson, F. Cacialli, H. L. Anderson, *Adv. Funct. Mater*. **2008**, *18*, 3367; e) J. Terao, S. Tsuda, Y. Tanaka, K. Okoshi, T. Fujihara, Y. Tsuji, N. Kambe, *J. Am. Chem. Soc.* **2009**, *131*, 16004; f) K. Sugiyasu, Y. Honsho, R. M. Harrison, A. Sato, T. Yasuda, S. Seki, M. Takeuchi, *J. Am. Chem. Soc*. **2010**, *132*, 14754; g) R. Shomura, K. Sugiyasu, T. Yasuda, A. Sato, M. Takeuchi, *Macromolecules* **2012**, *45*, 3759; h) C. Pan, K. Sugiyasu, J. Aimi, A. Sato, M. Takeuchi, *Angew. Chem. Int. Ed*. DOI: 10.1002/anie.201402813R2.

[6] C. Pan, K. Sugiyasu, Y. Wakayama, A. Sato, M. Takeuchi, *Angew. Chem. Int. Ed.* **2013**, *52*, 10775.

[7] Recent examples, see, a) S. Yang, J. You, J. Lan, G. Gao, *J. Am. Chem. Soc.* **2012**, *134*, 11868; b) D. Genovese, S. Bonacchi, R. Juris, M. Montalti, L. Prodi, E. Rampazzo, N. Zaccheroni, *Angew. Chem. Int. Ed.* **2013**, *52*, 5965.

[8] a) C. W. Tang, S. A. VanSlyke, C. H. Chen, *J. Appl. Phys.* **1989**, *65*, 3610; b) H. Nakanotani, M.

Saito, H. Nakamura, C. Adachi, *Adv. Funct. Mater.* **2010**, *20*, 1610.

Chapter 5

Encapsulated Phenylene-terthiophene Copolymers: A Case of the Alkyl Side-chain Effects

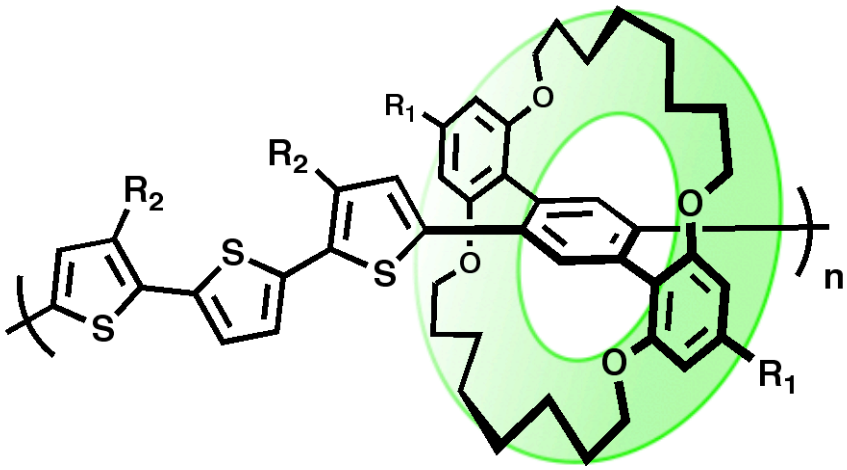

ABSTRACT: *We synthesized a series of IMWs with the same conjugated backbone, in which the length, number and positions of alky side-chains are different. By changing the length, number, and positions of alky side-chain, the glass transition temperatures of the IMWs can be tuned without any significant change of the photophysical properties. The AFM observations of the blended IMWs showed homogenous flat surfaces without forming any phase separation, thus we can conclude that the miscibility of our IMWs should be mainly attributed to the self-threaded cyclic sidechains.*

INTRODUCTION

With the first discovery of electroluminescence of CPs in 1990,[1] many different types of CPs have been widely studied for various optoelectronic devices including polymer light-emitting devices (PLED),[2] organic thin film transistors (OFET),[3] organic solar cells (OSC),[4] and organic lasers.[5] The combination of the optical and electronic properties of π-conjugated polymers with the attractive processability of polymers can advance the progress of the next generation flexible and printed electronics.[6] However, owing to the strong inter-polymer interactions and rigid polymer backbones, the CPs are generally insoluble and non-melting with relatively poor mechanical properties compared to conventional thermoplastic polymers.[7] Progress in developing processing techniques for CPs has opened the door to fabricate CPs to specific shapes for the applications in organic electronics.[8]

Introducing solubilizing groups (i.e. alky sidechains) to the conjugated backbones is a versatile strategy to make the CPs soluble in common organic solvents; therefore CPs can be easily processed by using solution-process technique.[8] Recently, several advanced techniques have been developed to fabricate CPs nanopatterns or nanofiber.[9] For example, nanoimprinting method can be used to confine the CPs to form one-dimensional nanochannel arrays.[9] Electrostatic spinning permits processing CPs to form fibers with sub-micrometer diameter.[10] Those processing techniques need the polymers to be soluble in common organic solvents and relatively soft.[11] The attachment of alky sidechains can benefit the conjugated polymers from enhancing the solubility to softening the CPs, thus the investigation of alky sidechain effect on the properties of CPs is highly important.[8]

In Chapter 3, we have already designed and synthesized a series of IMWs based on a variety of conjugated backbones encapsulated by the same cyclic sidechains.[12] All the polymers studied in Chapter 3 have four dodecyl alkyl sidechains, thus the different optoelectronic properties of the IMWs were determined by the π-conjugated backbone. We found that all the IMWs in Chapter 3 have relatively low glass transition temperature, thus we can easily process the polymers at low temperature. We mainly attribute the thermoplasticity properties of those IMWs to the weak inter-polymer interactions (i.e. the absence of π–π stacking), however, the attached alky sidechains should also play an important role in determining the thermal properties of this type of CPs. In this chapter, we synthesized a series of IMWs with the same π-conjugated backbone (Chart 5-1), in which the length, number, and positions of alky side-chains are altered. We studied the photophysical properties, surface morphology of polymer blends, thermal properties, and nanoimprinting of the IMWs (**5.1P1-5.1P4**) in detail with the comparison to the reference polymer **5.1P5** without cyclic side-chains.

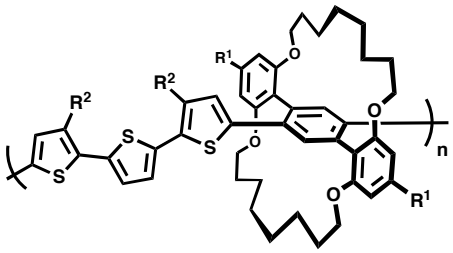

5.1P1 ~ 5.1P4

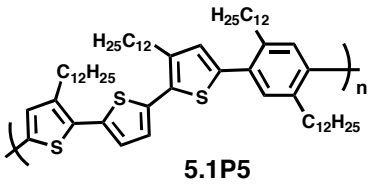

5.1P5

uninsulated reference polymer

R_2 \ R_1	H	$C_{12}H_{25}$
H		5.1P3
C_6H_{13}		5.1P2
$C_{12}H_{25}$	5.1P4	5.1P1

Comparison of alkyl side-chains regarding:

Number **5.1P1** ⟷ **5.1P3** and **5.1P4**

Length **5.1P1** ⟷ **5.1P2** ⟷ **5.1P3**

Position **5.1P3** ⟷ **5.1P4**

Chart 5-1. Chemical structures of the polymers studied in this chapter.

RESULTS AND DISCUSSION

Synthesis and Characterization of the Monomers. Monomers **5.1** and **5.2** have been synthesized in Chapter 3 and Chapter 4, respectively (for clear discussion, we changed the name of the polymers in this chapter). **5.3** were prepared by following the same procedures of **5.1** and **5.2**.[12] The solubility of **5.7H** was poor in the common organic solvents; it is difficult to synthesize **5.4** directly from **5.7H**, therefore the synthesis of **5.4** was carried out using the newly developed synthetic route as illustrated in Scheme 5-1. Compound **5.8** was obtained through Suzuki coupling by using Buchwald conditions from **5.5** as starting material.[13] The ring closing metathesis reaction (RCM) of **5.8** to **5.9** was not perfect as the conversion of **5.5** to **5.6**. The ^{1}H NMR spectrum of compound **5.8** indicated a mixture was formed after the RCM. Several attempts to optimize the RCM reaction conditions for synthesizing **5.9** were not successful. We then directly used the crude product to synthesize **5.4** through hydrogenation reaction by using our previous developed reaction condition. After we confirmed that all the double bond has been converted, several spots were observed on TLC plate. Monomer **5.4** was obtained after chromatography.

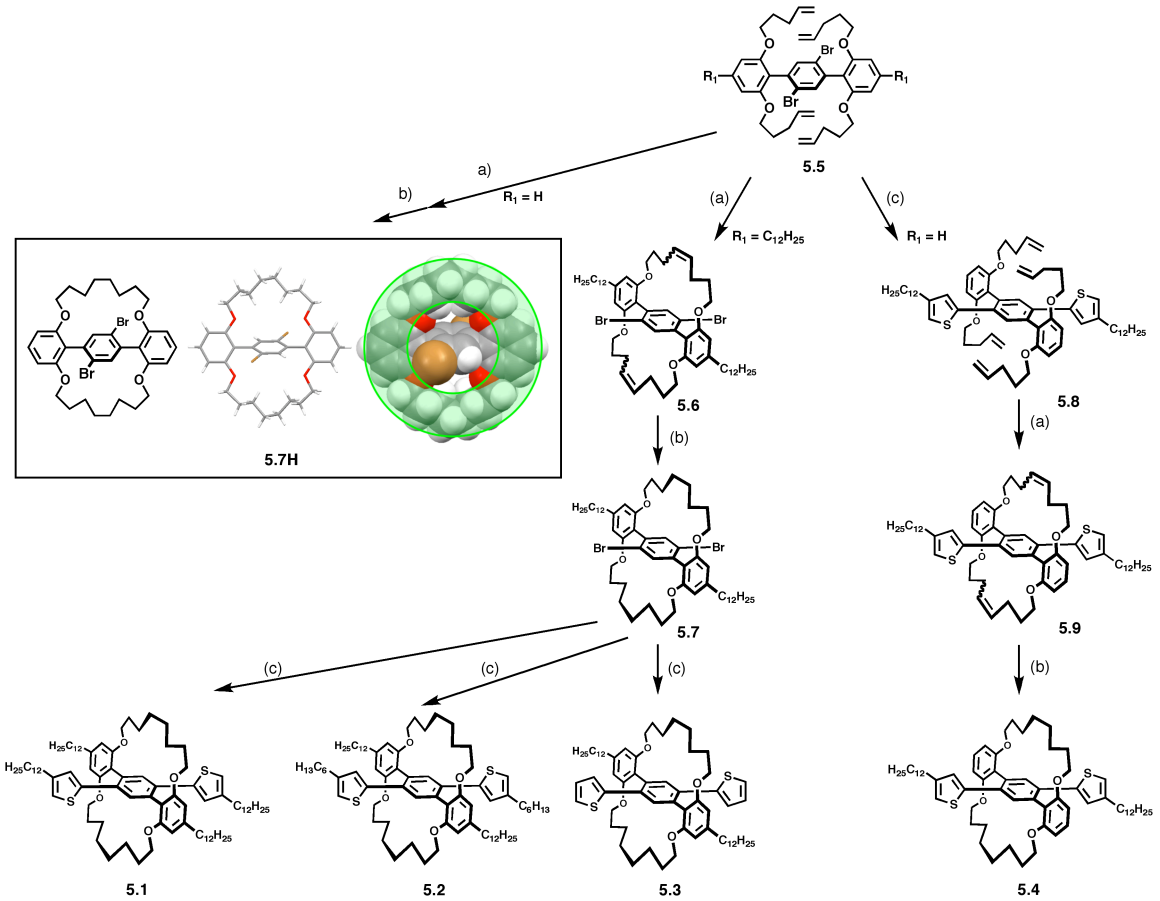

Scheme 5-1. Synthetic scheme of the monomers **5.1~5.4**; (a) second generation Grubbs catalyst, DCM, reflux; (b) Wilkinson's catalyst, THF, *t*-BuOH, H_2, 40 ^oC; (c) $Pd_2(dba)_3$, s-phos, K_3PO_4, toluene, 100 ^oC.

Synthesis and Characterization of IMWs. All the polymers were obtained by using the same procedures as described in chapter 3 with nearly quantitative yield (Scheme 5-2). All the polymers were characterized by ^1H NMR, ^{13}C NMR, and MALDI-TOF MS, the detailed procedures were described in the experimental section.

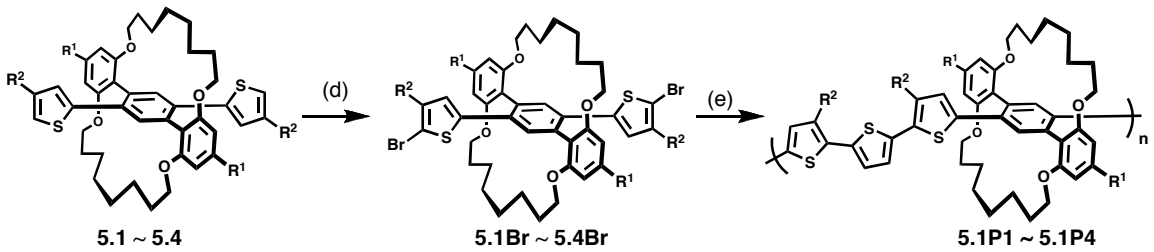

Scheme 5-2. Synthetic scheme of the polymers **5.1P1-5.1P4:** (d) NBS, THF, r.t., 2h; (e) 2,5-Bis(trimethylstannyl)thiophene, $Pd_2(dba)_3$, $P(o\text{-}tol)_3$, toluene.

The GPC profiles of all the polymers are shown in Figure 5-1. All the polymers have relatively high number average molecular weight (M_n) and narrow molecular weight distribution (PDI). The data are summarized in Table 5-1.

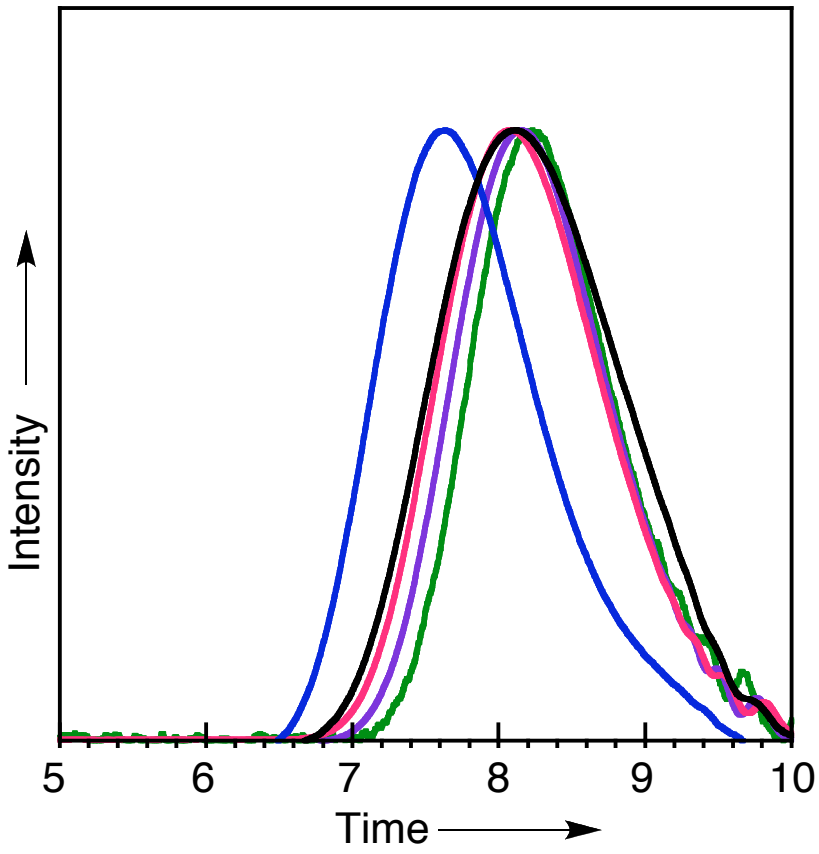

Figure 5-1. GPC profiles of **5.1P1** (green), **5.1P2** (purple), **5.1P3** (red), **5.1P4** (blue), and **5.1P5** (black).

Photophysical Properties. To explore the photophysical properties of the IMWs (**5.1P1-5.1P4**), the UV-vis absorption spectra, fluorescence spectra, and Φ_Fs of the samples were measured both in solution (DCM) and thin film state. We first compared the absorption spectra of the polymers in solution as shown in Figure 5-2a, the absorption maxima of IMWs (**5.1P1-5.1P4**) were red shifted to longer wavelength with respect to that of the reference uninsulated polymer **5.1P5**. As evidenced by Figure 3-2a, the absorption spectra of **5.1P1**, **5.1P2**, and **5.1P4** are identical, whereas **5.1P3** is red shifted to longer wavelength owing to the absence of dodecyl in the terthiophene segment. However, the fluorescence spectra of **5.1P1-5.1P5** are almost identical as depicted in Figure 5-2b.

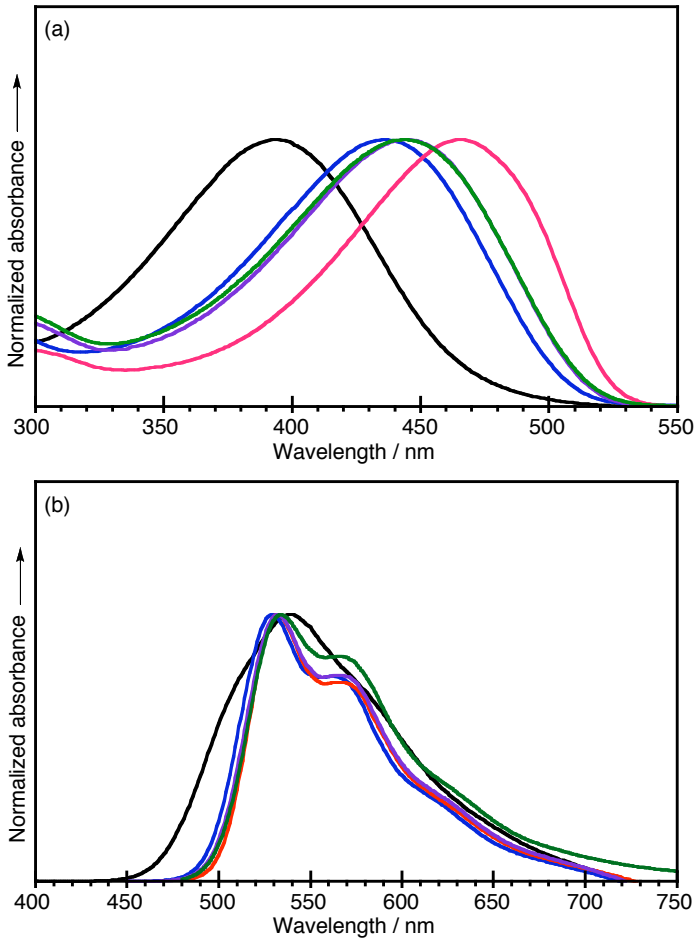

Figure 5-2. Normalized absorption and fluorescence spectra of **5.1P1** (green), **5.1P2** (purple), **5.1P3** (red), **5.1P4** (blue), and **5.1P5** (black) in solution (DCM). The fluorescence spectra were excited at the absorption maxima for all the polymers.

Table 5-1. Photophysical data of **5.1P1-5.1P5.**

Compd.		λ_{abs} [nm]	λ_{em} [nm]	Φ	M_n[a] (kg/mol)	PDI[a]
5.1P1[d]	sol.	443	534	0.33	21.2	1.8
	film	443	539	0.18		
5.1P2	sol.	444	532	0.36	19.6	1.9
	film	438	536	0.16		
5.1P3	sol.	464	532	0.44	22	1.8
	film	463	550	0.09		
5.1P4	sol.	437	529	0.34	37	2.1
	film	451	540	0.19		
5.1P5	sol.	395	539	0.34	20	2.2
	film	422	589	0.19		

[a] The M_n and PDI were determined by GPC by using polystyrene as a standard; [b] The fluorescence spectra were excited at the absorption maxima for all the polymers; [c] Absolute quantum yields (Φ) determined with a calibrated sphere system; [d] This data of **5.1P1** is the same as **3.1P1** in **Table 3-2** of Chapter 3.

The absorption and fluorescence maxima for **5.1P1-5.1P4** are little affected upon film preparation because of the weak inter-polymer interactions between the polymer backbones of IMWs; however, those of the **5.1P5** are obviously red shifted to longer wavelength from solution (DCM) to thin film state due to the strong π–π stacking. After removing the alkychains on R^2 position, the polymer **5.1P3** exhibits an absorption maximum at 464 nm at DCM, which is about 20 nm red shift compared to **5.1P1** (443 nm), **5.1P2** (444 nm), and **5.1P4** (437 nm) without the alkychains on R^2 position. We attribute this difference of around 20 nm to the more extended conjugation length of **5.1P3** as compared to other derivatives. This result indicates that the incorporation of alkychains to position R^2 can twist the terthiophene segments, thus reducing the effective conjugation of CPs. The Φ of all the copolymers are identical with around 0.33 in DCM and around 0.18 in film state, however, we observed that the Φ of **5.1P3** in film state is relative low due to the formation of more planar backbone in the condensed state. This is also in consistent with the red shift of the fluorescence maxima from solution to film state (($\lambda_{abs.}$: 532 nm → 550 nm). We found that the absorption and fluorescence maxima in DCM are similar to those of **5.1 P1** and **5.1 P2,** but around 10 nm red shifted in films state. We attribute this red shift to the closer packing of the conjugated backbones after removing the alkychain on R^1 position. From the results we obtained, we can conclude that (1) the length of the alkychain on R^2 position has little affect of the optical properties of IMWs with fixing the alkychain on R^1 position; (2) The existence of alkychain on R^1 position influences the packing structure of CPs in film state whereas has little effect in solution; (3) The existence of alkychain on R^2 position influences the optical properties of our IMWs in solution and film state due to the twist effect of the alkychain.

Surface Morphologies of Polymer Blends. As investigated in Chapters 3-4, we have proved that when the CPs backbone was wrapped with same cyclic side-chains, phase separation can be prevented; We ascribed characteristics to the limited interpolymer interactions and structural similarity. Herein, the morphologies of **5.1P1-5.1P4** blends have been investigated by using atomic force microscopy (AFM). Figure 5-3 shows the AFM phase images of the blended films prepared on mica. The homogenous smooth images for all the polymer blends provides the evidence for the absence of phase separations. This indicates a good miscibility of the polymer blends regardless of the difference of alkyl side-chains.

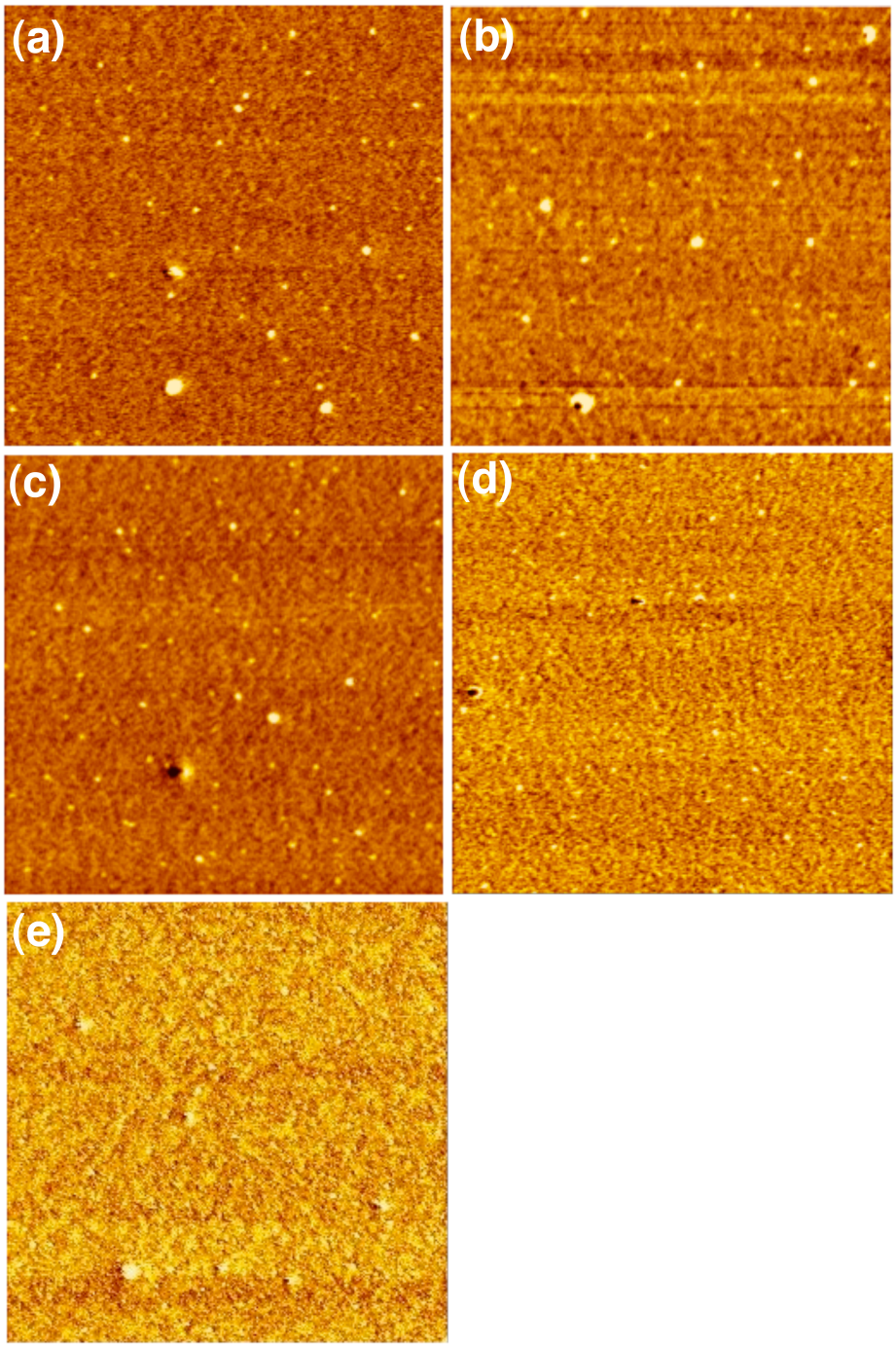

Figure 3-3. AFM phase images of **5.1P1/5.1P2** (a), **5.1P1/5.1P3** (b), **5.1P1/5.1P4** (c), **5.1P2/5.1P3** (d), and **5.1P3/5.1P4** (e) blends (wt / wt, 1:1), 2μm x 2μm.

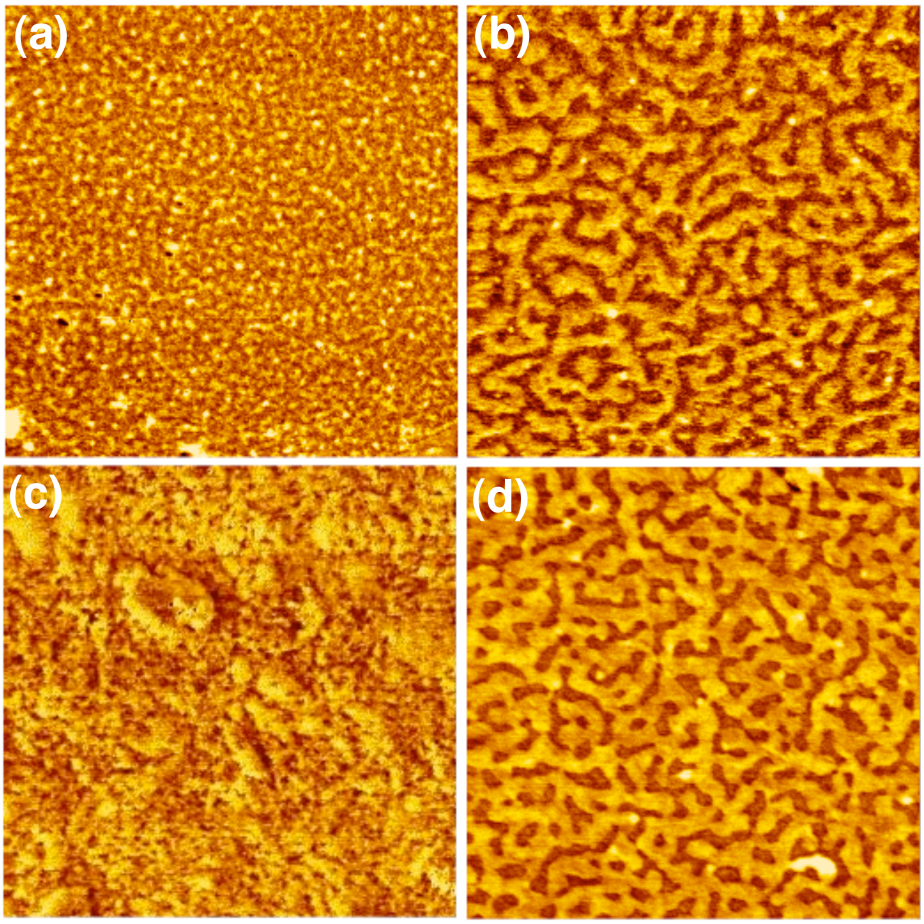

Figure 5-4. AFM phase images of **5.1P3/5.1P5** (a), **5.1P2/5.1P5** (b), **5.1P1/5.1P5** (c), and **5.1P4/5.1P5** (d) blends (wt / wt, 1:1), 2μm x 2μm.

In contrast, when we mixed the IMWs **5.1P1-5.1P4** with the uninsulated **5.1P5**, obvious phase separations were observed as shown in Figure 5-4. Considering the same conjugated backbone of those polymers, we assert that the cyclic side-chains should play a key role in determining the miscibility of those polymers.

Thermal Properties. To investigate the thermal behavior of the IMWs (**5.1P1-5.1P4**), we carried out the DSC measurements and the results are shown in Figure 5-5. All the polymers show amorphous feature as confirmed by the absence of peaks of melting points in the heating process of the third cycle. From **5.1P1** to **5.1P3**, the alkyl chain of R^1 (Chart 5-1) is fixed; the glass transition temperature (T_g) is increasing as shortening the length of the alkyl chain of R2 from dodecyl and hexyl to only proton, this result indicated that the length of alkyl chain can influence the T_g of IMWs. **5.1P3** and **5.1P4** have same number of alkyl side-chains (two dodecyl alkychains) with different positions (R^1 and R^2), however, the T_g of **5.1P4** (54.3 ^oC) is slightly lower than that of **5.1P3** (63.1 ^oC). The comparison of **5.1P1** and **5.1P3** revealed that the T_g of IMWs could be greatly reduced by increasing the numbers of alkyl side-chains.

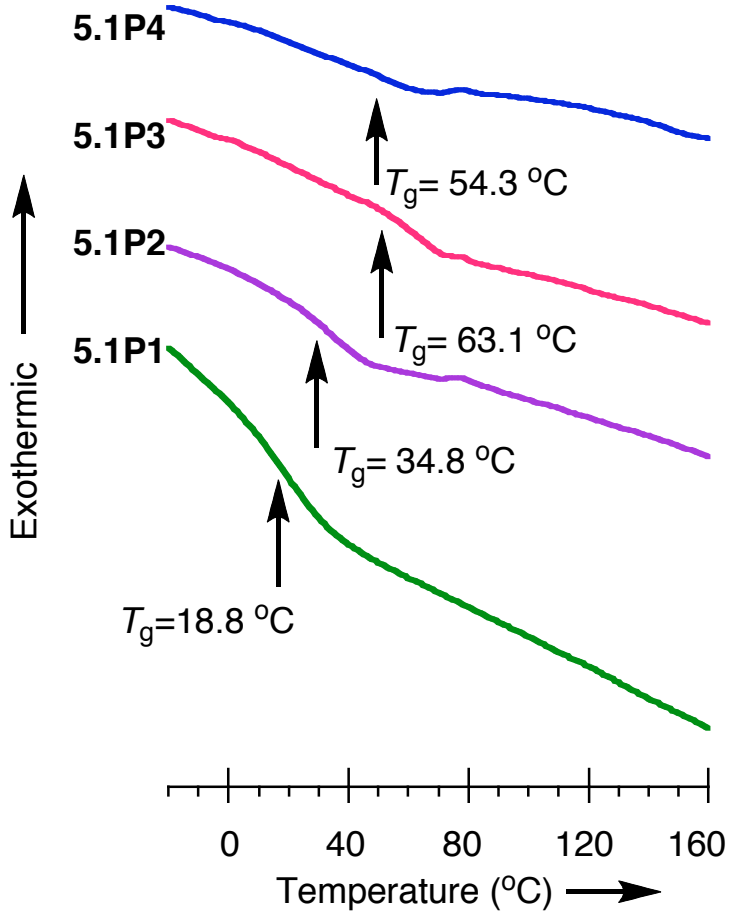

Figure 5-4. DSC profiles of **5.1P1** (green), **5.1P2** (purple), **5.1P3** (red), **5.1P4** (blue).

Nanoimprinting Experiments of 5.1P2.[14] Based on the investigation of the thermal properties of this series of IMWs in detail, we attempt to process this type of IMWs by using nanoimprinting technology with designed silicon molds (Figure 5-5). Films were firstly prepared by spincoating a chlorobenzene solution of **5.1P2** on precleaned silicon wafer and then heated to specific temperature (above T_g), and then a silicon mold was placed against the **5.1P2** film. The mold was finally removed after the temperature was cooled down to room temperature. The detailed nanoimprinting process is shown in Figure 5-5.

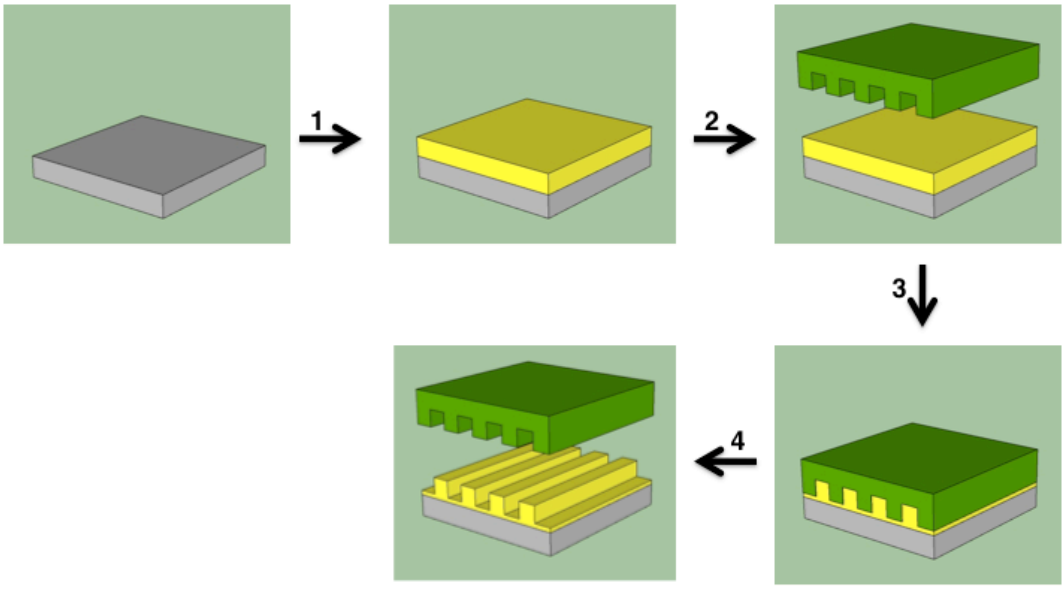

Figure 5-5. Schematic presentation of the nanoimprinting process: 1) anti-sticking treatment of the mold, 2) spin-coating the polymer solution, 3) elevating the temperature, 4) demolding after cooling down to room temperature.

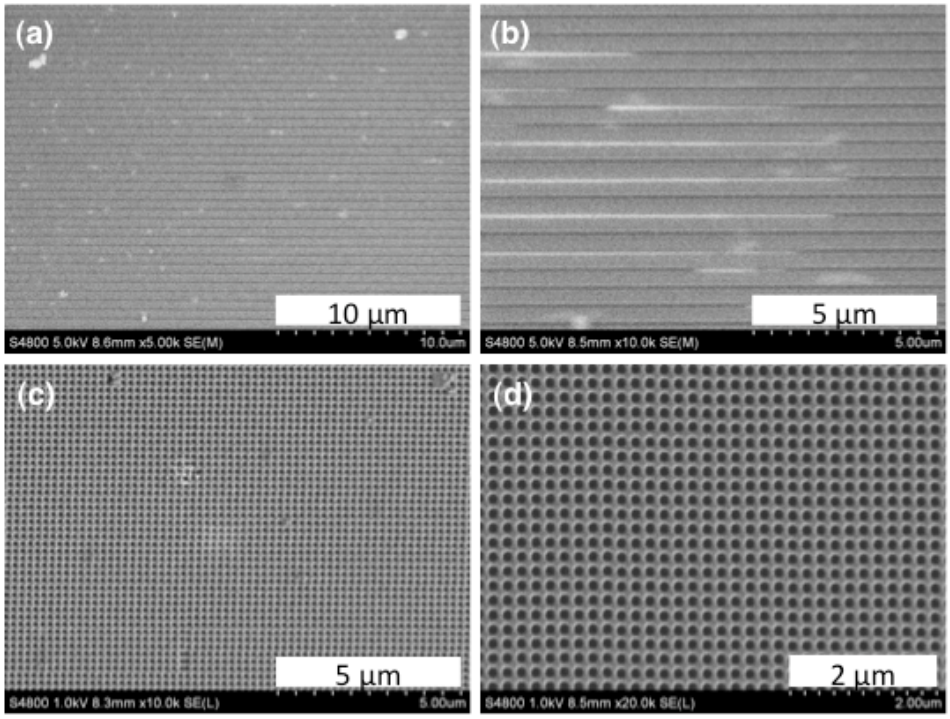

Figure 5-6. SEM images of **5.1P2** patterns fabricated by line and space mold (a, b) and pillar mold (c and d). The condition for line and space pattern: pressure: 2000 N, temperature: 100 ^{o}C, pressing time: 30 min; for pillar pattern: pressure: 2000 N, temperature: 150 ^{o}C, pressing time: 30 min, under air condition.

We conducted the scanning electron microscopy (SEM) to visualize the quality of the nanoimprinting experiments as shown in Figure 5-6. Figure 5-6a-b shows the results of the patterned film by using the line and space silicon mold, the polymers are well shaped to form line structure. Figure 5-6c-d show the results of polymer pattern by using a mold with pillar structure; the formed uniform honeycomb structure indicates the good processability of polymer **5.1P2**. Such type of structures has potential application in organic lasers. [15]

CONCLUSION

In this chapter, we have investigated that the alkychain effects on the optical properties, surface morphologies of polymer blends, and thermal properties of a series of IMWs. We found that the number and positions of alkychains have effects on the optical properties of our IMWs, however, the length of alkychains have little effects. The length and number of alkychains alter the glass transition temperatures of the IMWs. The length, number, and position of alkychains on IMWs have little effects of the surface morphologies of the polymer blends, which is contrast to the results when blending the IMWs with uninsulated polymer that showing obvious phase separation.

EXPERIMENTAL SECTION

Compounds **5.1** and **5.1Br** are the same compounds of **3.6** and **3M2** respectively as studied in Chapter 3. Polymer **5.1P1** is the same polymer of **3.1P1** as studied in Chapter 3. Polymer **5.1P2** is the same polymer of **A1** as studied in Chapter 4.The polymer **5.1P3** was synthesized by following the procedure as mentioned in Chapter 3.

Characterization of Polymer 5.1P3: ^{1}H NMR (CD_2Cl_2, 400 MHz, TMS, 298 K, see below): δ 0.84-0.87 (m, 6H), 1.25-1.36 (m, 60H), 1.67-1.69 (m, 4H), 2.65 (t, J = 7.2 Hz, 4H), 3.78 (m, 4H), 3.91 (m, 4H), 6.44 (s, 4H), 6.74 (d, J = 3.6, 2H), 6.84-6.86 (m, 4H), 7.51 (s, 2H). ^{13}C NMR (CD_2Cl_2, 400 MHz, TMS, 298 K, see below): δ 13.87, 22.68, 23.97, 27.09, 28.99, 29.27, 29.37, 29.50, 29.66, 29.70, 29.72, 31.61, 31.91, 36.68, 68.47, 104.24, 114.77, 123.02, 123.32, 125.35, 131.11, 132.00, 135.65, 136.09, 142.91, 144.99, 157.76.

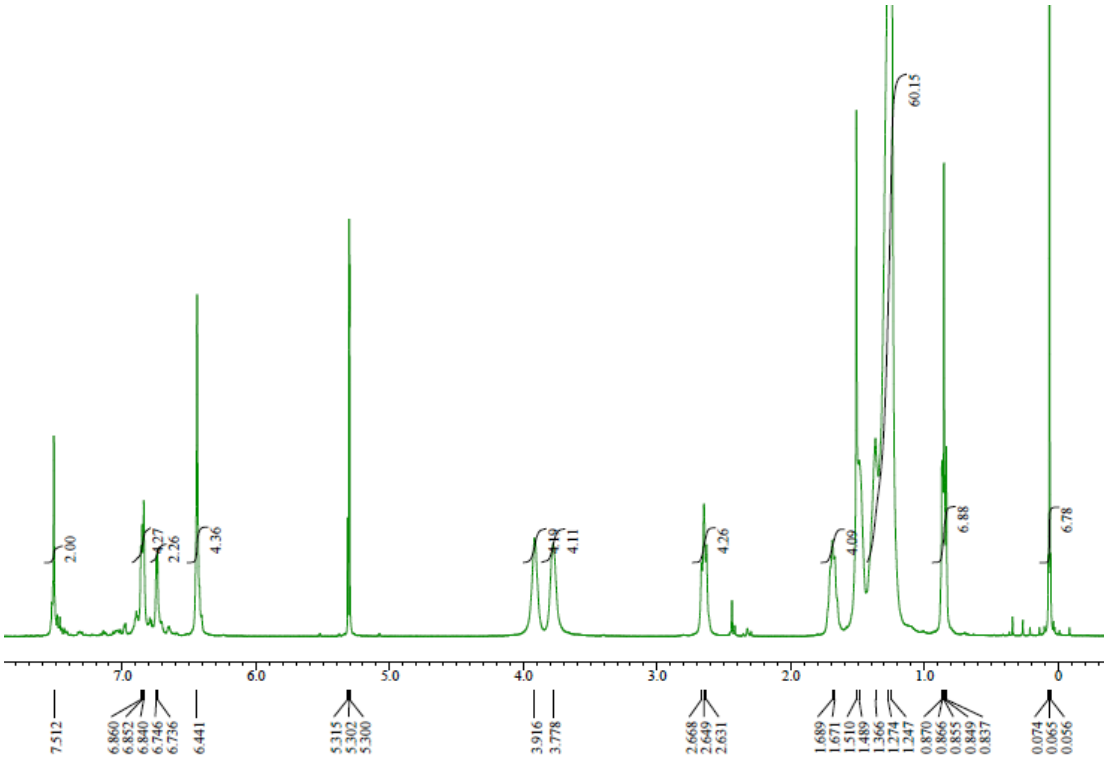

^{1}H NMR spectrum of **5.1P3**

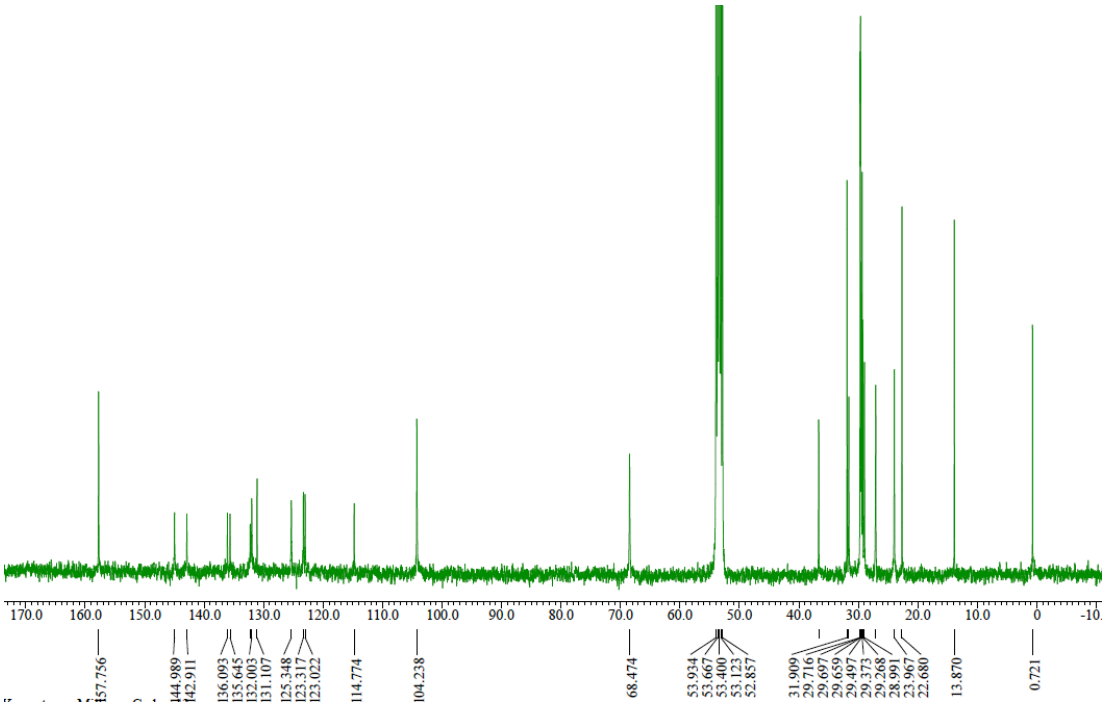

^{13}C NMR spectrum of **5.1P3**

Characterization of Polymer 5.1P4: ^{1}H NMR (CD_2Cl_2, 400 MHz, TMS, 298 K, see below): δ 0.84-0.88 (m, 6H), 1.04 (m, 8H), 1.24 (m, 40H), 1.47 (m, 16H), 2.69 (m, 4H), 3.80-3.84 (m, 8H), 6.65-6.77 (m, 8H), 7.28-7.32 (m, 2H), 7.54 (s, 2H). ^{13}C NMR (CD_2Cl_2, 400 MHz, TMS, 298 K, see below): δ 13.86, 22.67, 26.57, 29.34, 29.44, 29.53, 29.60, 29.63, 29.69, 30.53, 31.91, 71.91, 112.26, 124.98, 125.53, 129.64, 131.80, 132.04.

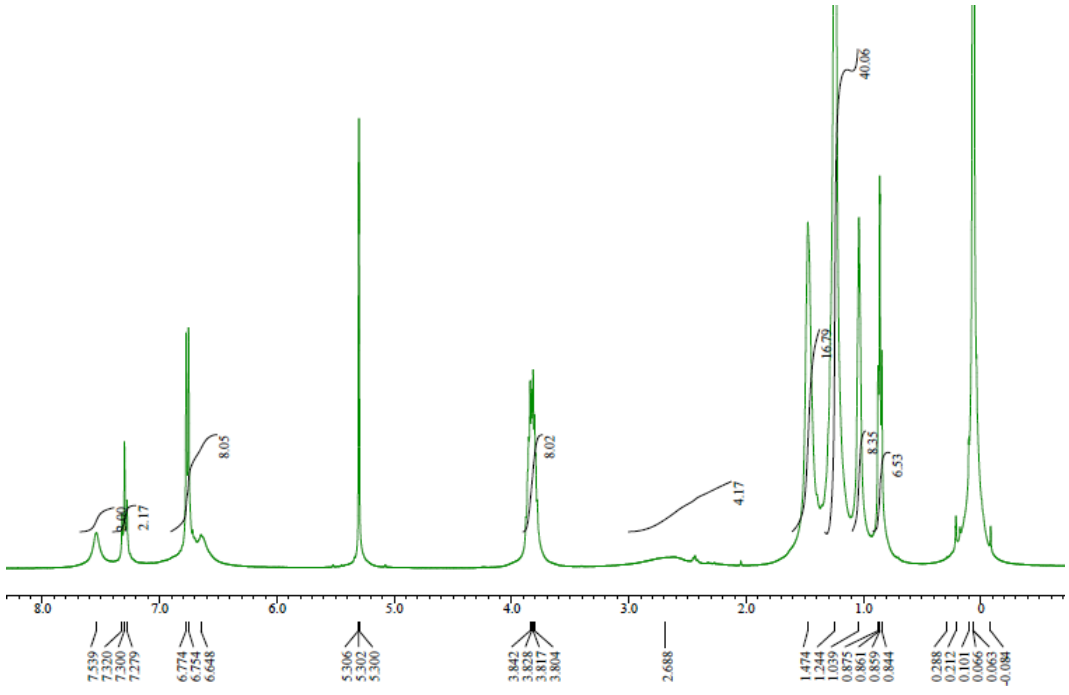

^{1}H NMR spectrum of **5.1P4**

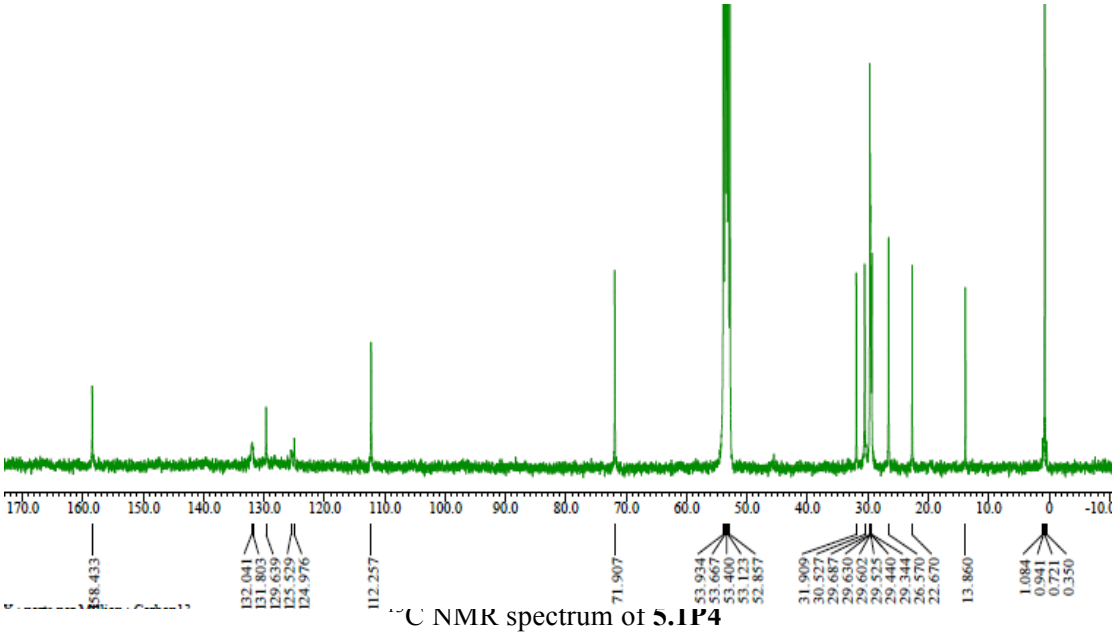

^{13}C NMR spectrum of **5.1P4**

Characterization of Polymer 5.1P5: ^{1}H NMR (CD_2Cl_2, 400 MHz, TMS, 298 K, see below): δ 0.83-0.87 (m, 12H), 1.23-1.43 (m, 72H), 1.70 (m, 4H), 1.72 (m, 4H), 2.77-2.85 (m, 8H), 6.93 (s, 2H), 7.12 (s, 2H), 7.32 (s, 2H). ^{13}C NMR (CD_2Cl_2, 400 MHz, TMS, 298 K, see below): δ 13.87, 22.68, 29.36, 29.46, 29.56, 29.60, 29.67, 29.71, 30.71, 31.63, 31.92, 33.13, 125.78, 129.66, 130.31, 131.97, 133.01, 135.82, 135.82, 138.51, 139.81, 140.61.

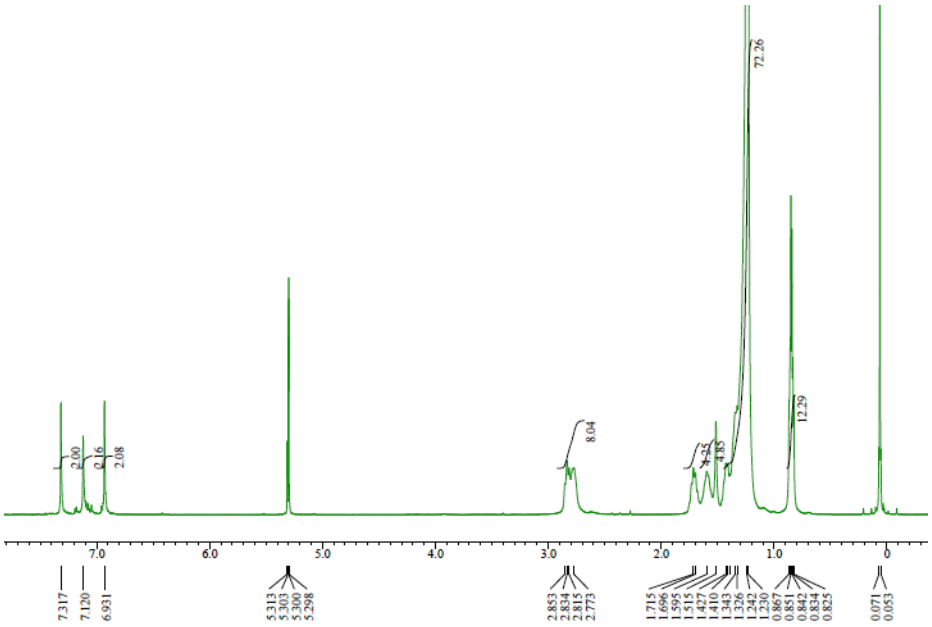

^{1}H NMR spectrum of **5.1P5**

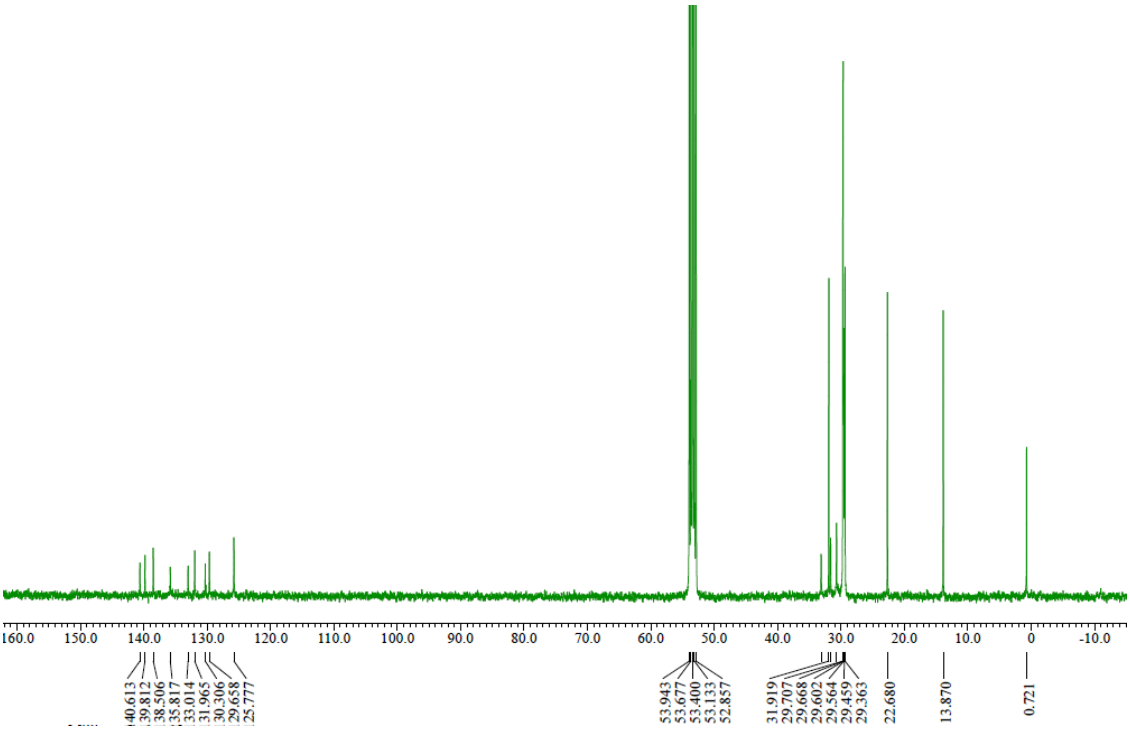

^{13}C NMR spectrum of **5.1P5**

REFERENCES

[1] J. H. Burroughes, D. D. C. Bradley, A. R. Brown, R. N. Marks, K. Mackay, R. H. Friend, P. L. Burn, A. B. Holmes, *Nature* **1990**, *347*, 539.

[2] J. J. M. Halls, C. A. Walsh, N. C. Greenham, E. A. Marseglia, R. H. Friend, S. C. Moratti and A. B. Holmes, *Nature*, **1995**, *376*, 498.

[3] a) L. L. Chua, J. Zaumseil, J. -F. Chang, E. C. W. Ou, P. K. H. Ho, H. Sirringhaus, R. H. Friend, *Nature*, **2005**, *434*, 194; b) H. Pan, Y. Li, Y. Wu, P. Liu, B. S. Ong, S. Zhu, G. Xu, *J. Am. Chem. Soc.*, **2007**, *129*, 4112.

[4] H. Hoppe, D. A. M. Egbe, D. Muhlbacher, N. S. Sariciftci, *J. Mater. Chem.* **2004**, *14*, 3462.

[5] G. Heliotis, D. D. C. Bradley, G. A. Turnbull, I. D. W. Samuel, *Appl. Phys. Lett.* **2002**, *81*, 415.

[6] A. C. Arias, J. D. MacKenzie, I. McCullough, J. Rivnay, A. Salleo, *Chem. Rev.* **2010**, *110*, 3

[7] Y. -J. Jin, J. -E. Bae, K.-S. Cho, W.-E. Lee, D.-Y. Hwang, G. Kwak, *Adv. Funct. Mater.* **2014**, *24*, 1928.

[8] J. Mei, Z. Bao, *Chem. Mater.* **2014**, *26*, 604.

[9] Z. Zheng, K. –H. Yim, M. S. M. Saifullah, M. E. Welland, R. H. Friend, J. –S. Kim, W. T. S. Huck, *Nano Lett.* **2007**, *7*, 987.

[10] F. D. Benedetto, A. Camposeo, S. Pagliara, E. Mele, L. Persano, R. Stabile, R. Cingolani, D. Pisignano, *Nat. Nanotechnol.* **2008**, *3*, 614.

[11] L. J. Guo, *Adv. Mater.* **2007**, 19, 495.

[12] C. Pan, K. Sugiyasu, Y. Wakayama, A. Sato, M. Takeuchi, *Angew. Chem. Int. Ed.* **2013**, *52*, 10775.

[13] S. D. Walker, T. E. Barder, J. R. Martinelli, S. L. Buchwald, *Angew. Chem. Int. Ed.* **2004**, *43*, 1871.

[14] Z. Hu, G. Baralia, V. Bayot, J. -F. Gohy, A. M. Jonas, *Nano Lett*. **2005**, *5*, 1738.

[15] I. D. W. Samuel, G. A. Turnbull, *Chem. Rev.* **2007**, *107*, 1272.

Conclusion

This thesis has described a series of three-dimensionally designed conjugated polymers (CPs) that showed unique optoelectronic properties.

In Chapter 1, a new type of CPs (referred as IMWs) – 'picket fence polythiophene' – has been realized through catalyst transfer polycondensation (CTP). The CTP method afforded the CPs with well–defined structure and narrow molecular weight distribution. The terphenyl picket fence can not only isolate the conjugated backbone, but also fix the CPs backbone to be planar, thus producing the CPs with extended conjugation length compared to the conventional poly (3-hexylthiophene) (**P3HT**).

In Chapter 2, motivated by the successful formation of IMWs through CTP featuring a chain-growth nature. Poly(3-hexylthiophene)–*block*–poly(3–'fenced'thiophene)s with different block ratios have been prepared through CTP. Such a sophisticated structure constructed a microphase separated thin films comprising a naked block and isolated block ensemble.

In Chapters 3–5, we have demonstrated a series of CPs appended with a three-dimensional architecture (cyclic sidechain). The obtained polymers can highly emissive even in the film state. The polymers are even miscible with each other to create various emission colors by polymer blending. Owing to the unique structures, the polymers are also thermoformable and can be easily processed (Chapter 3). We found that the blended IMWs films can have even enhanced photoluminescence efficiency, which was investigated in detail in Chapter 4. The three-dimensionally designed architecture was found to be the key point to the thermo-plasticity and miscibility whereas the alky sidechains have little effects on the miscibility of these IMWs, though the glass transition temperatures could be tuned by changing the length, position, and number of alkyside chains (Chapter 5).

Major achievements of this thesis are as follows:

List of Publications

(1) Chengjun Pan, Kazunori Sugiyasu, Yutaka Wakayama, Akira Sato, and Masayuki Takeuchi, Thermoplastic Fluorescent Conjugated Polymers: Benefits of Preventing π–π Stacking,
Angew. Chem. Int. Ed. **2013**, *52*, 10775–10779.

(2) Chengjun Pan, Kazunori Sugiyasu, Junko Aimi, Akira Sato, and Masayuki Takeuchi, Picket-Fence Polythiophene and its Diblock Copolymers that Afford Microphase Separations Comprising a Stacked and Isolated Polythiophene Ensemble,
Angew. Chem. Int. Ed. **2014**, in press. (DOI: 10.1002/anie.201402813)
(**Highlighted on the frontispiece**)

(3) Chengjun Pan, Kazunori Sugiyasu, and Masayuki Takeuchi, Blending conjugated polymers without phase separation for fluorescent colour tuning of polymeric materials through FRET,
Chem. *Commun*. **2014**, in press. (DOI:10.1039/c4cc03594a)

Selected Presentations at International Conferences

(1) C. Pan, K. Sugiyasu, M. Takeuchi, Synthesis and Characterization of Conjugated Polymers Threaded through Their Own Macrocyclic Sidechains, *International Workshop on Soft Interface Sciences*, Nov. 21–22, **2012**, Tsukuba.
(**Best Poster Award**)

(2) C. Pan, K. Sugiyasu, Y. Wakayama, M. Takeuchi, A Versatile Core Skeleton for Highly Emissive Conjugated Polymers in the Solid-State, *NIMS Conference 2013*, July 01–03, **2013**, Tsukuba.
(**Best Poster Award**)

Acknowledgment

At first, I would like to express my deepest respect and gratitude to my thesis supervisor Professor Masayuki Takeuchi for his continuous support, education, and encouragement throughout my PhD study period. I would also like to thank Dr. Kazunori Sugiyasu for his amazing advices for my research projects and I really enjoyed working with him.

I would like to thank Prof. Takao Aoyagi, Prof. Tetsushi Taguchi, and Prof. Yohei Yamamoto for reviewing my PhD thesis.

Many thanks to the collaborators, Dr. Junko Aimi, Dr. Yutaka Wakayama, and Dr. Seungjun Oh for their precious cooperation on the properties investigations of our IMWs.

I am grateful to Dr. Takashi Nakanishi, Dr. Sadaki Samitsu, Dr. Soichiro Ogi, Dr. Martin J. Hollamby, and Dr. Atsuro Takai for their valuable discussions on my research projects. Thank Dr. Xianglan Li, Mr. Akira Sato, and Mrs. Mami Inoue for measurements support.

Thank all the group members in organic materials group at National Institute for Materials Science (NIMS) for fruitful discussions on my research projects.

Finally, I would like to appreciate the great support from my family and friends.

Tsukuba, Japan
June, 2014

Chengjun Pan

Department of Materials Science and Engineering
Graduate School of Pure and Applied Sciences
University of Tsukuba